THE EFFECT OF MODEL SEAGRASS ON WAVE RUNUP: A LABORATORY INVESTIGATION

BY

ALLISON BRIDGES AND JAMES T. KIRBY

RESEARCH REPORT NO. CACR-08-03
MAY 2008

CENTER FOR APPLIED COASTAL RESEARCH

Ocean Engineering Laboratory
University of Delaware
Newark, Delaware 19716

ACKNOWLEDGEMENT

This project was funded by the Delaware Sea Grant Program, Project Number SG2001-04 R/OE-30.

TABLE OF CONTENTS

LIST OF FIGURES

LIST OF TABLES

ABSTRACT

The detrimental impacts of wave forces upon submerged aquatic vegetation (SAV) have been well researched while the effect of these plants on hydrodynamic forces more recently become more aggressively studied. A model eelgrass bed was employed to study the effect of SAV on wave runup along a ramp in a laboratory flume.

Two regular wave conditions revealed similar variance patterns in the time and frequency domains. Time series analysis revealed a steady decrease in water surface elevation variance with the smallest variance along the runup wire. Spectral analysis also showed a steadily decreasing wave energy variance as the waves approached the beach with the smallest variance at the runup wire. Both analyses revealed the ability of the model plants to hinder runup and rundown to within a smaller range than without plants in the flume. Additionally, a weaker variance occurred along the runup wire with plants in the flume versus without.

Four irregular wave cases revealed the influence of peak wave period and spectral width on water surface elevation in the time and frequency domains. With a peak period of 1 s, minimal wave breaking occurred and steady water surface elevation and wave energy variances developed. With a 2 s peak period, smoother breaking occurred slightly further offshore and rundown was restricted to within a smaller range under influence of the plants. Also, an increase in water surface elevation and wave energy variances resulted at and along the ramp. Similarly, cases with a 1.5 s peak period exhibited similar patterns to the 2 s peak period case. An increase in the spectral width parameter (3.3 to

30) revealed a sharper peak at the prominent peak frequency as well as an additional peak at the first harmonic.

Chapter 1

INTRODUCTION

1.1 Opening

A delicate balance exists between fluid dynamics and submerged aquatic vegetation (SAV). While the detrimental impacts of wave and current forces upon SAV have been well researched and documented, the significance of these plants to reduce current flow and dampen wave energy has more recently become an important field of study. By creating lower energy conditions, these plants help maintain a healthy productive environment. This is well regarded as a major benefit of these wetlands vegetation. The sustainability of SAV is largely due to their ability to adapt to hydrodynamic forces. In nature, large groups of plants wave in an organized manner with the direction of water particle velocity. While field studies provide insight, in order to develop a better understanding of the relationship between SAV and hydrodynamics, laboratory research provides a more controlled environment. The laboratory allows creation of specific conditions and isolation of individual parameters. The use of model plants, as opposed to live, creates a more regulated environment as long as the model plants accurately mimic their natural counterpart.

This study utilizes laboratory experiments to investigate the effects of model flexible SAV on wave runup under both regular and irregular wave conditions. Time series analysis provides insight into the behavior of the waveform while spectral analysis determines the distribution of wave energy over the frequency domain.

1.2 Outline

Chapter 2 discusses the motivation for this research and reviews results from previous studies. Chapter 3 discusses development of the model eelgrass bed while Chapter 4 outlines the preparation for the laboratory experiments. Chapter 5 presents time series and spectral analyses and Chapter 6 summarizes the findings. A list of references follows Chapter 5. Appendix A contains pictures taken during field investigations and Appendix B contains pictures taken during laboratory experiments.

Chapter 2

BACKGROUND

2.1 Wetlands and Seagrass

Wetlands have experienced tremendous losses due to human-induced changes in the coastal environment. In the United States, in the late 1960s, public awareness of the environmental benefits of wetlands began to increase. Areas once labeled “wasted” land soon became an important aspect of federal policy.

The National Environmental Protection Act of 1969 required an annual Environmental Quality Report denoting the status and condition of major natural environmental classes such as wetlands. A package of wetland reforms, Protecting America’s Wetlands: A Fair, Flexible, and Effective Approach, created on August 24, 1993, set the goal of “no net loss” of wetlands. Since initiation of the “no net loss” goal, wetland area has begun to stabilize.

With the onset of increasing public awareness and federal policy implementation, the general function and resource value of wetlands became more extensively researched and documented. Research shows wetlands preserve biodiversity by providing habitat to an assortment of species, provide erosion and flood control, stabilize flow, recharge underground aquifers, and filter water, i.e. denitrification.

Within the unique wetland environment are specialized aquatic vegetation adapted for growing within the hydric soil of this inundated or saturated environment. Studies have concluded submerged aquatic vegetation sustainability is extremely sensitive

to light availability, water clarity, hydrodynamic forcings, boat traffic, and mechanical harvesting impacts (Stewart et al., 1997; Fonseca et al., 1998; Chesapeake Bay Program, 2000; Koch et al., 2003).

Studies also provide evidence of a feedback mechanism between SAV sustainability and hydrodynamics. An example cycle begins with a dense SAV bed. The dense bed decreases current velocity, dampens wave energy, and allows sediment deposition. This creates an environment more conducive to plant reproduction. Due to the increased density of the bed, and resulting decrease in current velocity and wave energy, the inundation of organic matter reaches a point that the high phytotoxin levels cause the plants to die back. As the bed density becomes reduced, current velocity and wave energy increase. This increased flow reduces the organic matter and phytotoxins. Eventually, the plants are able to begin to reproduce again, due to increased light availability, and establish a dense bed.

Due to human interference, factors that inhibit the ability of SAV to thrive have become more abundant which decreases the ability of SAV to recover. Notably, SAV beds are depleted quickly but recovery is a very slow process (Fonseca et al., 1998). The loss of seagrass has extreme detrimental biological and environmental implications. Seagrasses supply food, shelter, and protection to an assortment of aquatic organisms to create an excellent breeding ground, incubation area, and nursery or permanent residence. At the same time, SAV acts as a sediment trap with its extensive root and rhizome system and baffles current and wave energy with its canopy of stems and shoots (Fonseca et al., 1998). An SAV bed can reduce current velocity, attenuate waves, and change the height of the water column. Researchers have noted currents in SAV beds to be 2 – 10 times slower than in adjacent unvegetated areas (Chesapeake Bay Program, 2000).

2.2 Past Studies

Different techniques have been implemented to better understand the dynamic relationship between fluid dynamics and flexible vegetation. A value of Manning's n, a function of U X R, where U is the average flow velocity and R is the hydraulic radius, has been roughly determined for a variety of vegetative channel linings through both field and laboratory tests. Kouwen et al. (1969) improved upon the friction factor n by introduction of a relative roughness parameter y/k, where y is the water depth and k is the deflected height of the vegetation. This deflected height refers to the location of the roughness tips from the bed during the majority of time. The resulting formula describing flow retardance in vegetated channels

$$\frac{U}{u_*} = C_1 + C_2 \ln\left(\frac{y}{k}\right) \tag{2.1}$$

incorporates vegetation characteristics, where C_1 is a function of vegetation bed density and C_2 is a function of individual vegetation stiffness. Kouwen and Unny (1973) expanded upon these results by showing flexible plastic roughness elements behave hydraulically similar to the natural vegetation they model. Kouwen and Li (1980) examined the deflected roughness height between erect, waving, and prone motions.

As flow velocity increases, the vertical plants bend and become more streamlined. The area perpendicular to the flow (projected area) decreases which results in a decrease in drag. Similarly, as a wave passes over the vertical plants, the plants bend in the direction of the horizontal particle velocity. Gaylord et al. (1984) determined the optimal size of flexible plants, such as seagrass, is limited by mechanical factors, such as drag, not biological factors alone, such as sunlight availability. Denny et al. (1997) suggest the ability

of flexible vegetation, such as seagrass, to reorient itself with the flow may benefit larger plants but be detrimental to smaller plants. Reorientation, most effective for plants longer than the diameter of the wave-driven water orbit, allows the plant to bend slightly but not to a degree severe enough to cause breakage before the water motion reverses (Gaylord and Denny, 1997).

A major complication encountered in modeling flexible roughness elements is incorporation of a damping coefficient due to this ability to reorient with the flow. Dalrymple et al. (1984) modeled a cluster of rigid vertical cylinders as a region of localized energy dissipation with drag constant over depth. They found a shadow region of wave damping developed onshore of the cylinders in the direction of the oblique wave. Gaylord and Denny (1997) and Denny et al. (1997) investigated a simple numerical model based on vertically oriented cantilever beams. The model incorporated forces, including drag, virtual buoyancy, and a restoring force, on a point mass at the end of a kelp stipe, however, it lacked a vertically directed force balance.

Kobayashi et al. (1993) developed an analytical solution to the vertically two-dimensional problem of waves propagating over submerged vegetation by introducing a damping coefficient. This calibrated drag coefficient varied greatly for the different wave cases of the artificial seaweed experiment (Asano et al., 1988). Asano et al. (1992) incorporated the swaying motion of the flexible element, including the vegetation size and proximity of surrounding elements, into the constant drag model. By including the plant motion, the drag coefficient value was found to be approximately 0.5. This value proves much better agreement to the experimental data than the 0.1 value determined by Kobayashi et al. (1993).

Wang and Torum (1994) developed a theoretical model based on limited experimental data. They found the damping coefficient increased with increasing wave period until reaching an asymptotic value based on plant density. Dubi and Torum (1996) expanded this study by using both theoretical and experimental means to determine the damping rate. They found the drag coefficient increased as the wave period increased for short period waves, reached a maximum, and then decreased gradually with longer period waves. They also determined the damping coefficient was governed by water depth and plant population density. Field and laboratory studies reveal a positive correlation between wave attenuation by flexible vegetation and the percentage of water column the plants occupy (Chesapeake Bay Program, 2000).

Dean (1978) found the dense root system of aquatic vegetation creates strong durable plants. Since these plants decrease bottom shear stress, deposition of sediment rather than erosion may result. Also, these plants have the ability to decrease wave energy, or wave height, and, ultimately, wave steepness. By changing breaking wave conditions, accretional rather than erosional conditions may develop along the shoreline. Lovas and Torum (2000) show, similar to live vegetation, model kelp reduces wave breaking as an effect of wave damping. Notably, wave attenuation begins in deeper water and less runup occurs on the beach when the kelp is present.

Chapter 3

MODEL DEVELOPMENT

3.1 Field Visits

To develop a better understanding of the plants and environment I intended to model, I joined Dr. Evamaria Koch and associates to Chincoteague Bay. We visited Wildcat Marsh in southeastern Chincoteague Bay and Mills and Tizzard Islands along southwestern Chincoteague Bay. Figure 3.1, taken from Google Maps, shows these areas.

The Chincoteague Bay is a coastal barrier island or lagoon system located at the southeastern edge of the Delmarva Peninsula near the mouth of the Chesapeake Bay. Wave exposure in the Chincoteague Bay is relatively low as compared to the rest of the Chesapeake Bay. However, Koch et al. (2003) points out, within Chincoteague Bay, extensive dense eelgrass beds thrive on the eastern shore while sparse, isolated beds are present on the western side.

According to the Maryland Department of Natural Resources (DNR), of the bay grass species found in the high-salinity areas of Chesapeake Bay, eelgrass, *Zostera marina*, is one of the most abundant and persistent. Figure 3.2 shows a picture of an eelgrass plant from the DNR website. An eelgrass plant consists of a single shoot arising from a rhizome node. The underground creeping rhizome, and roots which grow from its nodes, bind the sediment and stabilize the shoot. A tubular sheath surrounds 3 – 5 ribbon-like leaves which sprout from this single shoot. New leaves sprout in an alternating pattern as the shoot grows for protection.

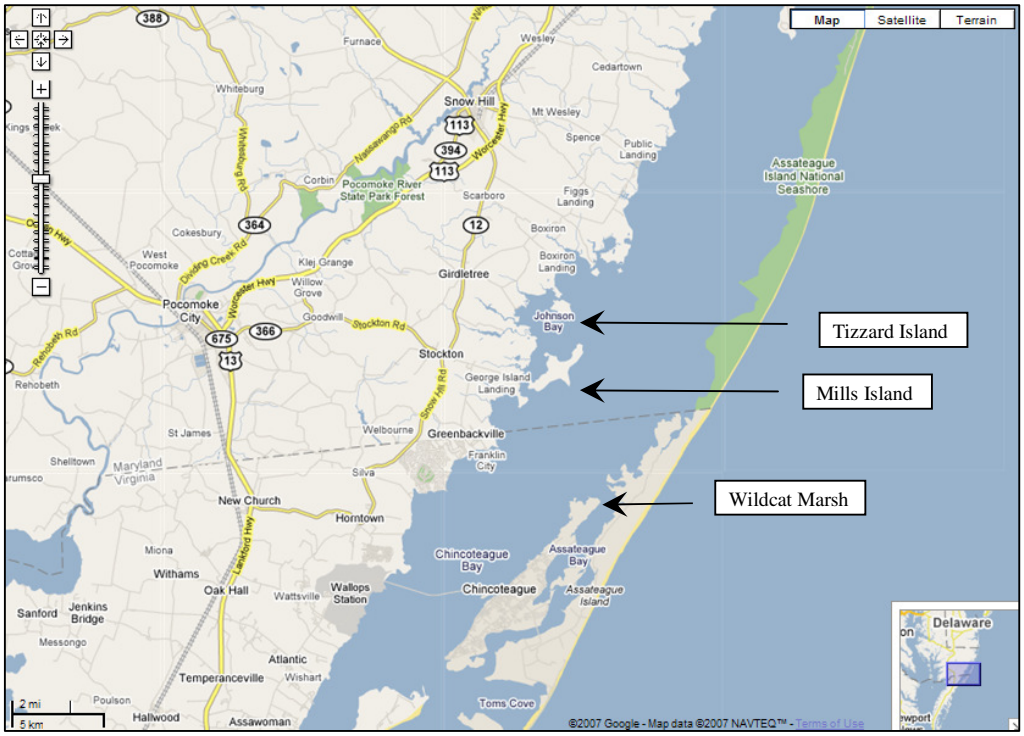

Figure 3.1 Map of Chincoteague Bay Area

Figure 3.2 Picture of Natural Eelgrass Plant

Initial observation of an eelgrass bed revealed organized oscillatory swaying of the plants with wave interaction. Closer inspection revealed the flexibility of each individual plant to become prone in both directions. Basic fluorocene dye tests performed within these beds showed the effect of the plant waving on the flow. When released near the bottom, the dye moved back and forth with the plant swaying but remained concentrated near the bottom. The dye dispersed very slowly toward the surface and horizontally. Dye released within a sparsely populated area within the bed also remained near the bottom but quicker vertical dispersion occurred here than within a more densely populated portion of the bed. Appendix A contains pictures taken during these field investigations.

3.2 Model Eelgrass Bed

During these visits I collected samples of *Zostera marina* from multiple sites. Attempts to measure flexural properties of live eelgrass by machine failed due to the sensitivity of the plant membrane and the inability to retain water within the plant during measurement. Based on field observation and basic flexural rigidity tests, I decided to model an eelgrass plant with Mylar strips.

A model eelgrass plant consisted of a 7.5 cm tall basal stem with 4 – 7 mm wide 0.1016 mm thick blades (Figure 3.3). The length of the blades were, in order facing the oncoming waves – 21.5 cm, 16.5 cm, 18.5 cm, and 29.5 cm. Individual model plants were glued into 0.5 cm deep holes drilled in 2 cm thick 2.5 m X 58 cm Plexiglas sheets. The silicone glue attachment allowed the plants movement as in natural substrate. The canopy consisted of a regular matrix configuration to reduce shelter effects by surrounding plants. The matrix was comprised of alternating rows of 18 and 19 plants with 1.4 cm spacing (twice the blade width) between the plants and rows. The Plexiglas sheet was attached to the sidewalls and bottom of the ramp with silicone and water-resistant tape (Figure 3.4).

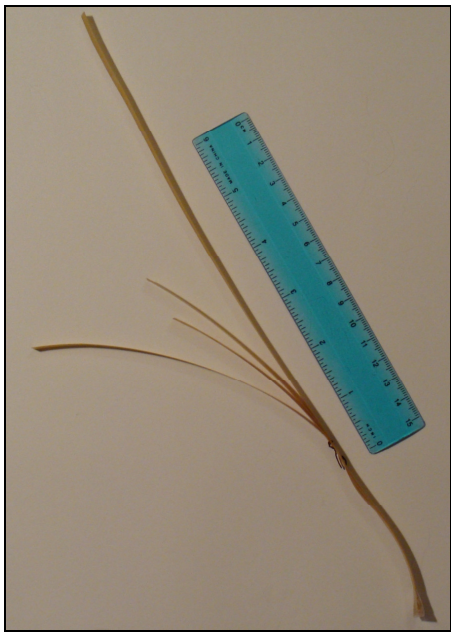

Figure 3.3 Picture of Model Eelgrass Plant

Figure 3.4 Picture of Model Eelgrass Bed in Flume Facing Wave Maker

Chapter 4

LABORATORY EXPERIMENTS

4.1 Experimental Setup

4.1.1 Flume Preparation

Laboratory experiments were conducted at the Center for Applied Coastal Research at the University of Delaware. The facility houses a 30 m long, 0.6 m wide, and 1.0 m deep two-dimensional wave flume. The hydraulically-driven piston-type wave maker generated waves for the experimental cases. Within the limitations of paddle motion, the wave maker has the capability to create both regular and irregular waves. A user-defined input voltage signal time series determines the rate and magnitude of paddle displacement. Since the correlation between paddle displacement and resulting wave height was not determined prior to the experiments, direct observation served as verification of resulting wave parameters. Notably, the wave maker does not have the ability to absorb reflected waves.

Beginning 9.1 m from the wave maker paddle neutral position, a series of bottom slopes was installed to produce depth-limited breaking waves (Figure 4.1). The first ramp, with an initial slope of 1:15, extended between 9.1 m and 10.4 m from the wave maker paddle neutral position. The second ramp, with a 1:35 slope, extended 10.7 m from the first ramp. The third ramp, serving as the beach, extended 1.2 m from the second ramp with a slope of 1:5.

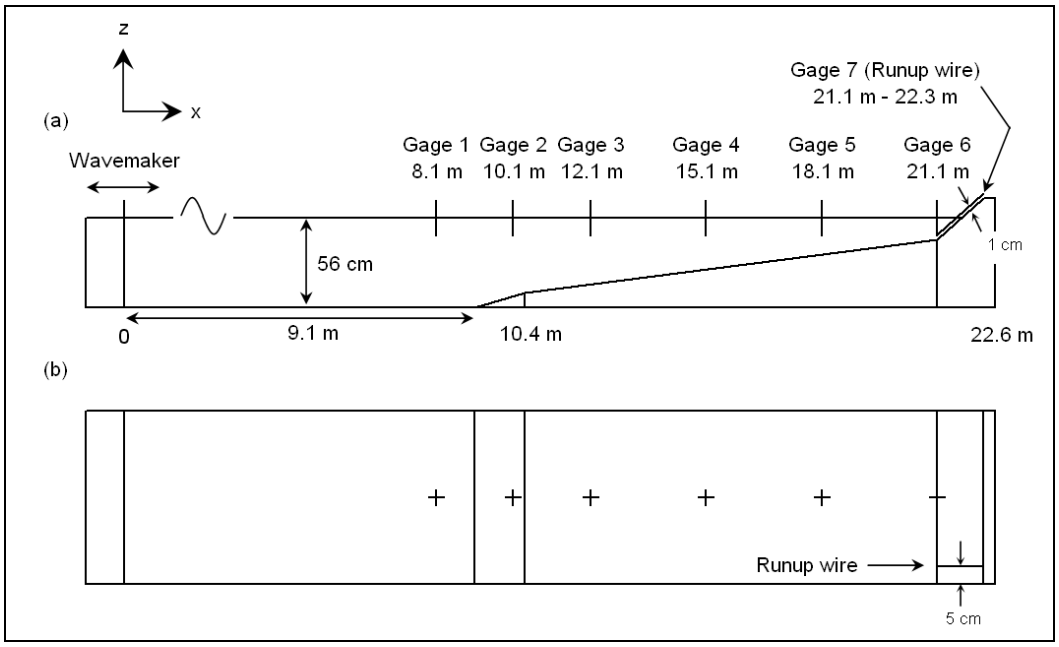

Figure 4.1 Flume Setup (a) Plan View (b) View From Above

4.1.2 Waves

Regular wave trial runs were conducted to determine an approximate relationship between input voltage magnitude and resulting wave height. Input of these sinusoidal voltage time series helped determine the time necessary to obtain a steady regular wave condition. Comparisons of regular wave patterns up to 60 minutes indicated steady regular wave motion developed after 10 minutes.

An irregular wave voltage time series was created based on a Texel, Marsen, Arsloe (TMA) spectrum. The spectrum was produced via a Matlab program dependent on user inputs of significant wave height, peak frequency, and the spectral width parameter (γ). While these parameters determine the shape of the energy spectrum, wave height and period magnitudes are not established a priori. An infinite number of voltage time series can be produced based on the same criteria.

4.1.3 Data Acquisition Equipment

The following laboratory experiments incorporated a total of 7 capacitance gages with a sampling frequency of 50 Hz. Figure 4.1 outlines the experimental layout of the flume. Six capacitance gages were placed along the center of the flume to measure the water surface fluctuation over time. Gages 1 through 6 were placed 8.1 m, 10.1 m, 12.1 m, 15.1 m, 18.1 m, and 21.1 m from the wave maker paddle neutral position. These gages were aligned manually to face directly into the oncoming waves. The calibration procedure accounted for any alignment inaccuracy. A seventh capacitance gage stretched from the top of the 2nd ramp to the top of the beach (3rd ramp) to record runup along the beach. This gage was installed 5 cm from the flume sidewall, parallel to the bottom. The gage was strategically placed 1 cm from the bottom to record the maximum runup without encountering viscous effects. An intricate calibration procedure ensured accurate results.

The capacitance gage calibration procedure consisted of obtaining a voltage reading while varying the water depth in the flume in 1 cm increments. The calibration procedure began with the still water level positioned in the middle of the runup wire (56 cm from the horizontal bottom of the flume). The six gages were adjusted vertically so the water level was positioned in the center of the gage wires and the voltage of each of the seven gages was zeroed. A voltage reading was recorded at each 1 cm interval as the water depth was increased from 56 cm to 68 cm (upper limit of the runup wire), decreased to 46 cm (lower limit of the runup wire), and returned to 56 cm.

For the 6 capacitance gages along the center of the flume, the calibration procedure ultimately produces a calibration coefficient relating the linear relationship between the water surface elevation and gage voltage. A 3rd order regression curve fit to

the runup wire (gage 7) calibration data related water surface elevation and voltage for this gage.

4.2 Experimental Procedure

After determining accurate operation of the wave maker and gages, trial runs determined acceptable regular and irregular wave parameters. The resulting waves needed to capture the majority of the runup wire but not overtop the beach. Table 4.1 outlines the parameters of each experimental case. Note, the spectral width parameter is represented by γ. In order to densely populate the frequency spectra, the length of record corresponding to each case captured 800 waves.

For each case, the wave maker received the same input voltage time series for the without and with plants runs. Prior to each run, the gages recorded the still water level (56 cm depth) for 30 s. The average value was removed from the gage output prior to processing. Data acquisition for the regular wave conditions began 10 minutes after initiation of the waves. Figure 4.2 shows the TMA spectrum corresponding to each irregular wave case and Figure 4.3 shows the input voltage signal time series for each of these cases. Appendix B contains pictures taken during these laboratory experiments.

Table 4.1 Experimental Cases

Experimental Runs		T_p (s)	H_s (cm)	γ
Regular Wave Cases	**Case 1**	1	-	-
	Case 2	1.5	-	-
Irregular Wave Cases	**Case 3**	1	6	3.3
	Case 4	1.5	6	3.3
	Case 5	1.5	6	30
	Case 6	2	3	3.3

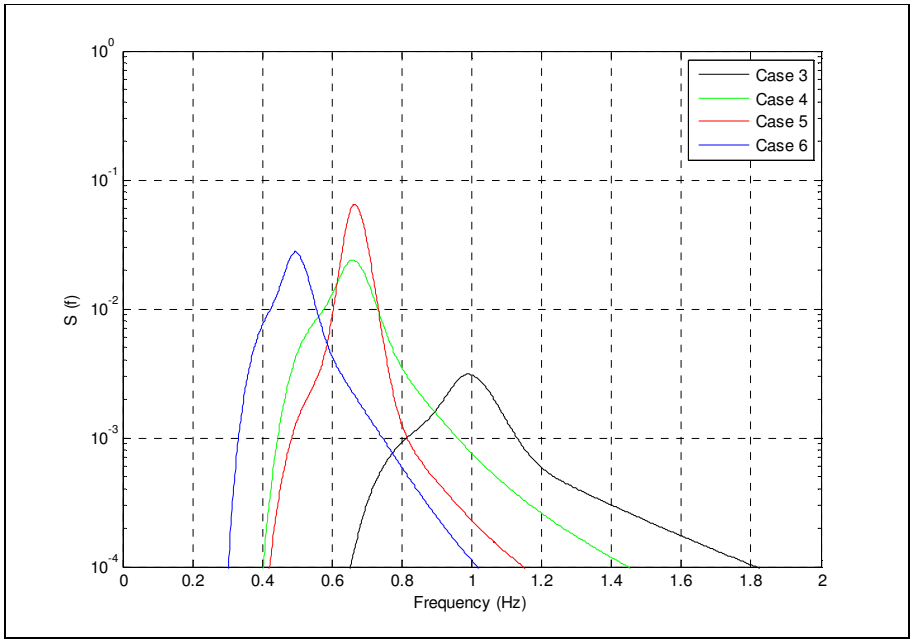

Figure 4.2 TMA Spectra for Irregular Wave Cases

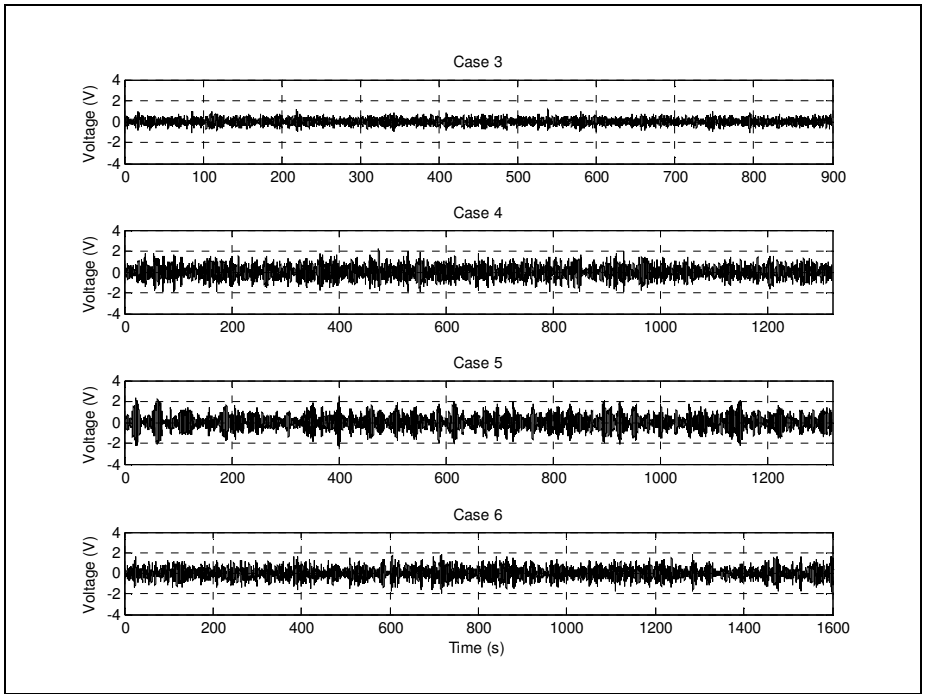

Figure 4.3 Time Series of Irregular Wave Cases

Chapter 5

DATA ANALYSIS

5.1 Time Series Analysis

Analysis of multiple segments of gage output (water surface elevation) revealed general trends in wave height and period during each run. Included are sections of water surface elevation time series indicative of the findings. The mean water level at each gage reveals the accumulation of water at that location while the variance and skewness of each gage's output signal provides insight into the behavior of the waveform during its shoaling process. For a simple regular linearly shoaling wave, it is expected that the variance of the water surface elevation decreases slightly as the wave approaches breaking while the skewness of the signal increases toward and then decreases following breaking.

5.1.1 Regular Wave Cases

Case 1

As seen from the time series figures (Figures 5.1 – 5.3), the waveform proceeded with similar dimensions in the without and with plants runs of case 1 (T_p = 1 s), until gage 7. The 1 s period was retained throughout both runs. At gage 1, the wave measured approximately 14 cm from peak to trough with a slightly taller crest than trough. The waveform became steeper as it shoaled up ramps 1 and 2 and began spilling near gage 5. Notably, the plants oscillated with the passing waves but remained bent toward the oncoming waves. Analysis of the water surface elevation time series at each gage reveals a steadily decreasing signal variance and a signal skewness that peaked at gage 4 (Table 5.1 and Figure 5.4).

The runup/rundown patterns during both runs retain the 1 s period but are quite muddled. The runup typically proceeded up the ramp slowly but was abruptly returned up the ramp during rundown. For the without plants run, the increasing mean water level at gages 6 and 7 indicates an accumulation of water landward of the breaking wave. Without influence of the plants, after breaking, the wave excursion varied between approximately 2.5 cm above and 3 cm below still water level along the runup wire (Table 5.1 and Figure 5.3). For the with plants run, the slightly negative mean water level at gage 7 indicates the runup generally remained below still water level (between approximately still water and 2 cm below still water level). As evidenced by Figure 5.3, the plants generally hindered runup above still water level.

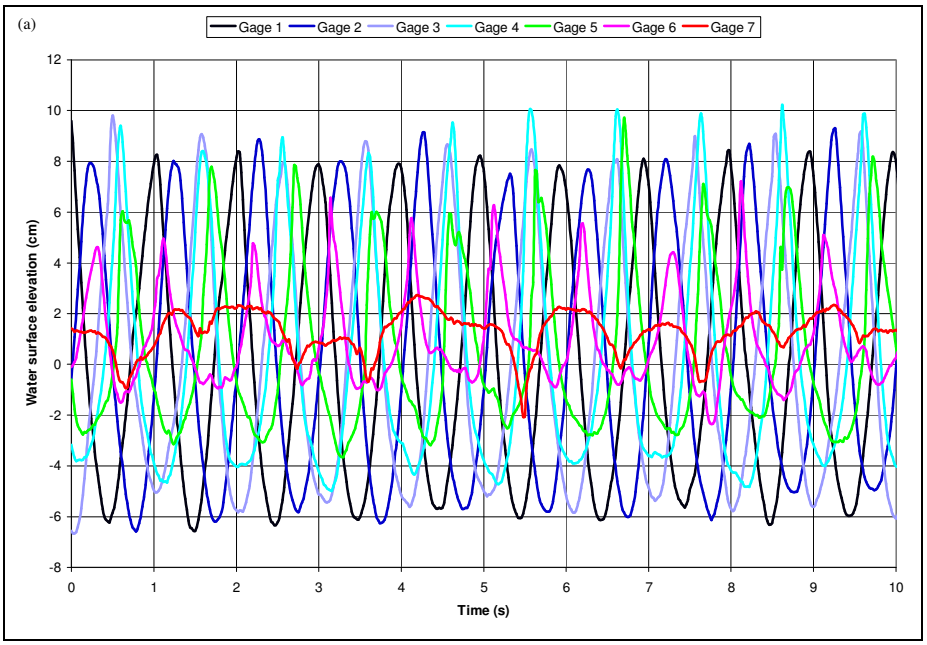

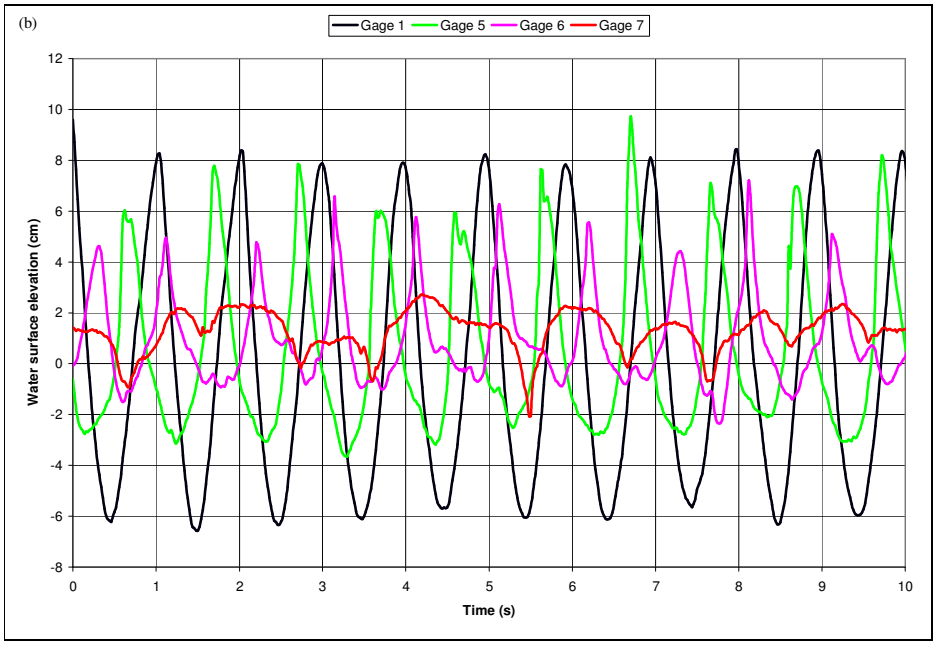

Figure 5.1 Case 1 Without Plants Run Water Surface Elevation Time Series (a) All gages (b) Gages 1, 5, 6, and 7

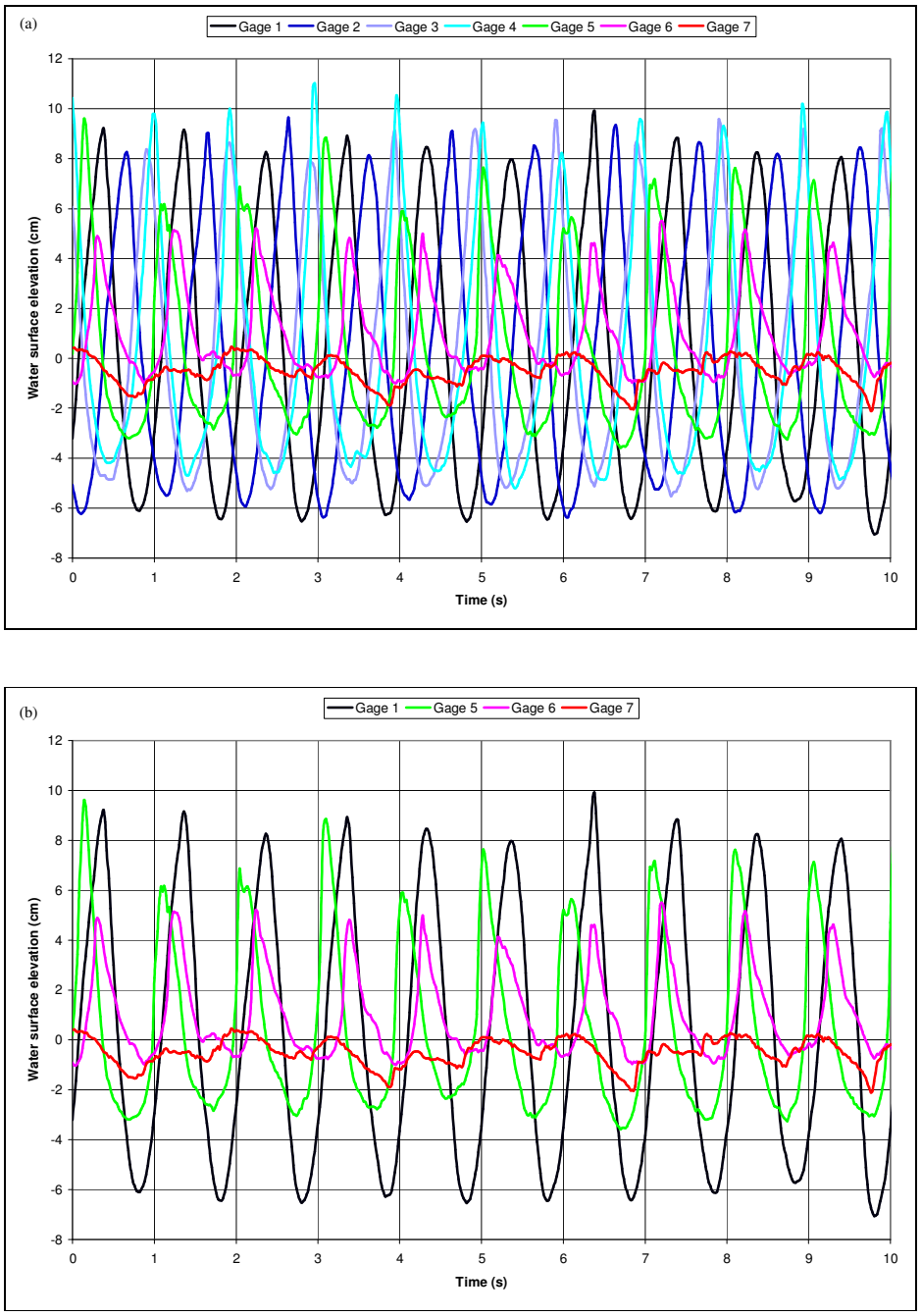

Figure 5.2 Case 1 With Plants Run Water Surface Elevation Time Series (a) All gages (b) Gages 1, 5, 6, and 7

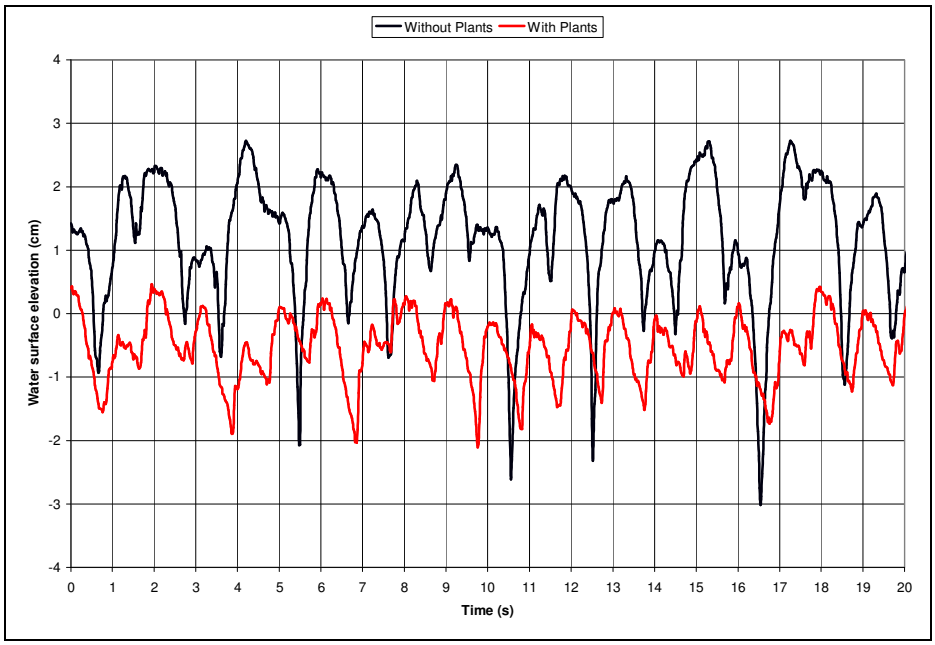

Figure 5.3 Case 1 Without and With Plants Runs Water Surface Elevation Time Series Gage 7

Table 5.1 Case 1 Runs Water Surface Elevation Time Series Mean, Variance, and Skewness (a) Without Plants (b) With Plants

(a)	**Gage 1**	**Gage 2**	**Gage 3**	**Gage 4**	**Gage 5**	**Gage 6**	**Gage 7**
Mean	0.133	0.205	0.122	0.116	0.383	0.964	1.243
Variance	25.284	24.542	22.130	18.846	10.997	3.245	0.819
Skewness	32.245	35.771	43.805	62.218	30.661	6.132	-0.492
(b)	**Gage 1**	**Gage 2**	**Gage 3**	**Gage 4**	**Gage 5**	**Gage 6**	**Gage 7**
Mean	0.247	0.229	0.144	0.272	0.330	0.981	-0.446
Variance	26.255	23.972	20.589	20.850	11.023	3.130	0.169
Skewness	33.862	37.729	39.961	68.321	30.356	5.714	-0.022

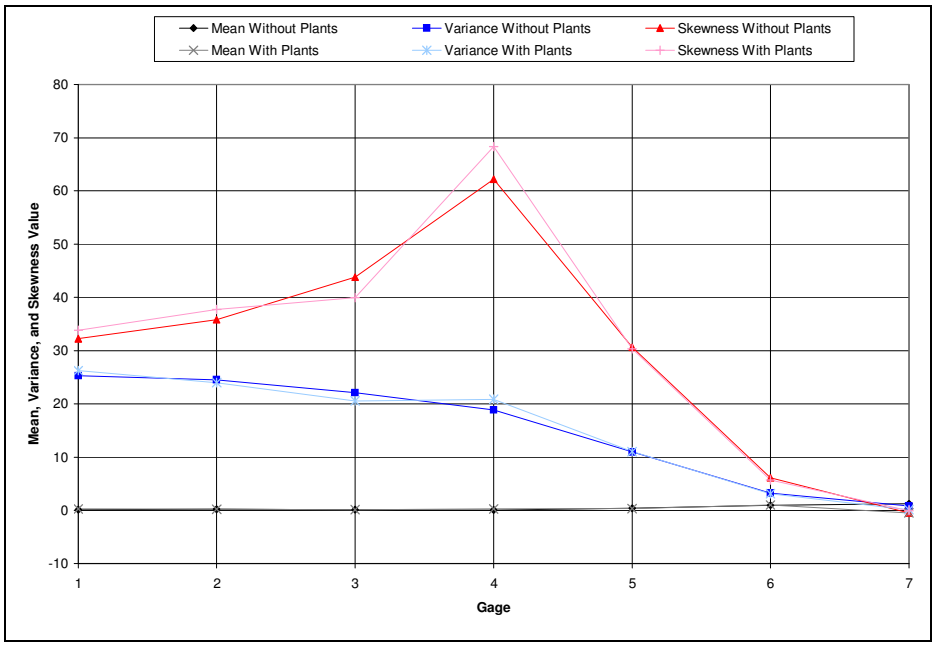

Figure 5.4 Case 1 Without and With Plants Runs Water Surface Elevation Time Series Mean, Variance, and Skewness All Gages

Case 2

For case 2 (T_p = 1.5 s), the time series figures (Figures 5.5 – 5.7) indicate a waveform with similar dimensions and a consistent 1.5 s period propagated during the without and with plants runs. The wave measured approximately 12 cm from peak to trough at gage 1 with an approximate 8 cm tall crest. At gage 2, the crest height increased slightly, as indicated by the peak in water surface elevation skewness in Table 5.2 and Figure 5.8. The wave continued to shoal as it propagated up ramp 2 with an approximate 10 cm wave height at gage 5. The waves were seen to begin spilling between gages 5 and 6 and finally break along the runup wire. Notably, wave breaking was seen to begin slightly further offshore with plants in the flume than without. The plants oscillated with the oncoming waves by bending toward the oncoming wave during rundown and then backwards as the wave proceeded up the ramp.

Figure 5.7 shows a very similar runup/rundown pattern between the without and with plants runs. Both patterns generally retained the 1.5 s period of the initial waveform. Without influence of the plants, wave runup reached approximately 3 cm above still water level along the ramp while the rundown varied between still water level and 3 cm below still water level. With plants in the flume, the runup only reached approximately 2 cm above still water level and the rundown only reached approximately 2 cm below still water level. The figures indicate the plants restricted wave runup and rundown to within a more limited, regular pattern than without plants in the flume.

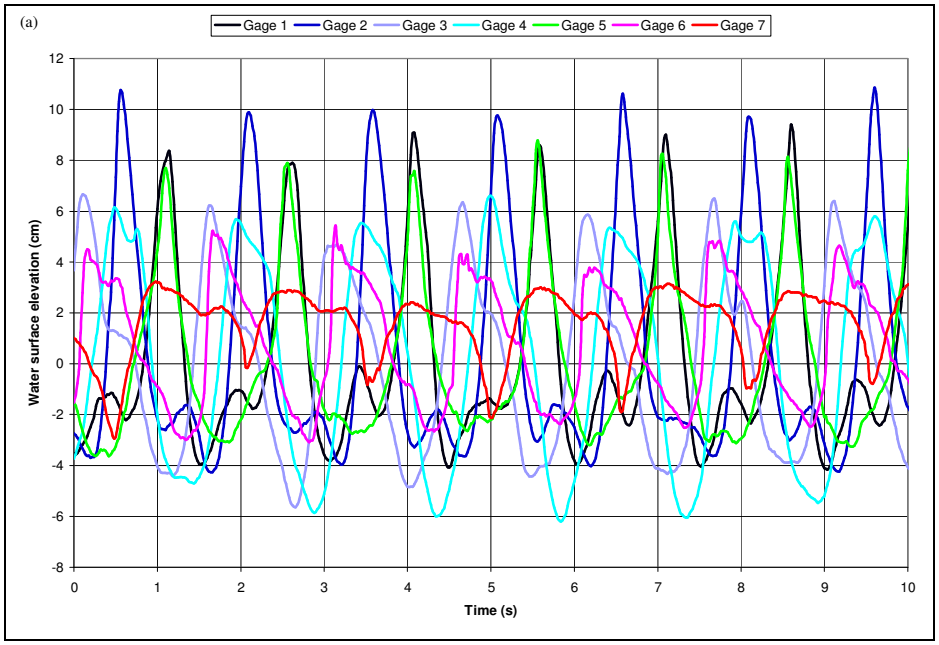

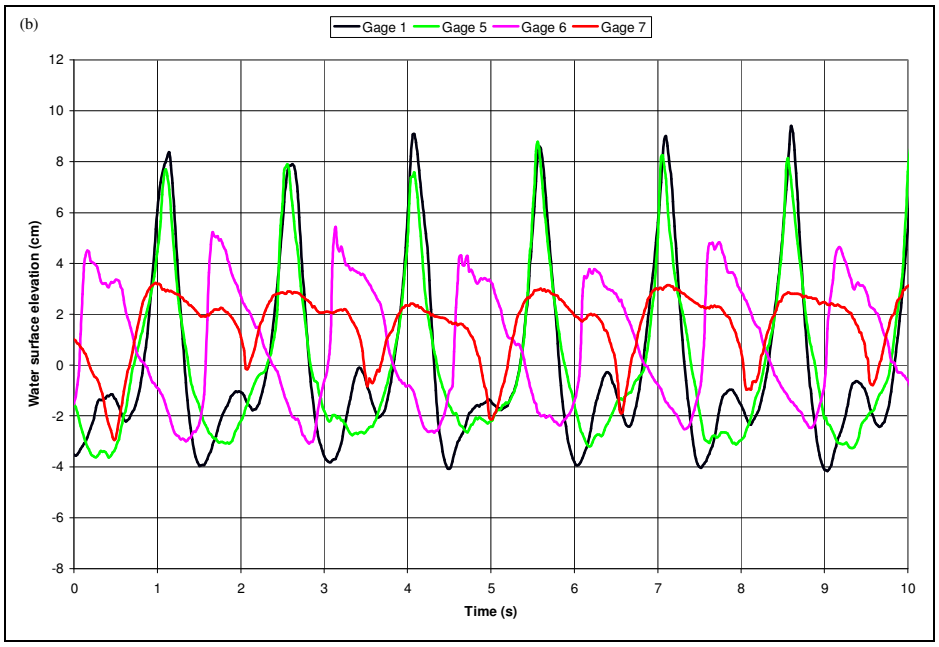

Figure 5.5 Case 2 Without Plants Run Water Surface Elevation Time Series (a) All gages (b) Gages 1, 5, 6, and 7

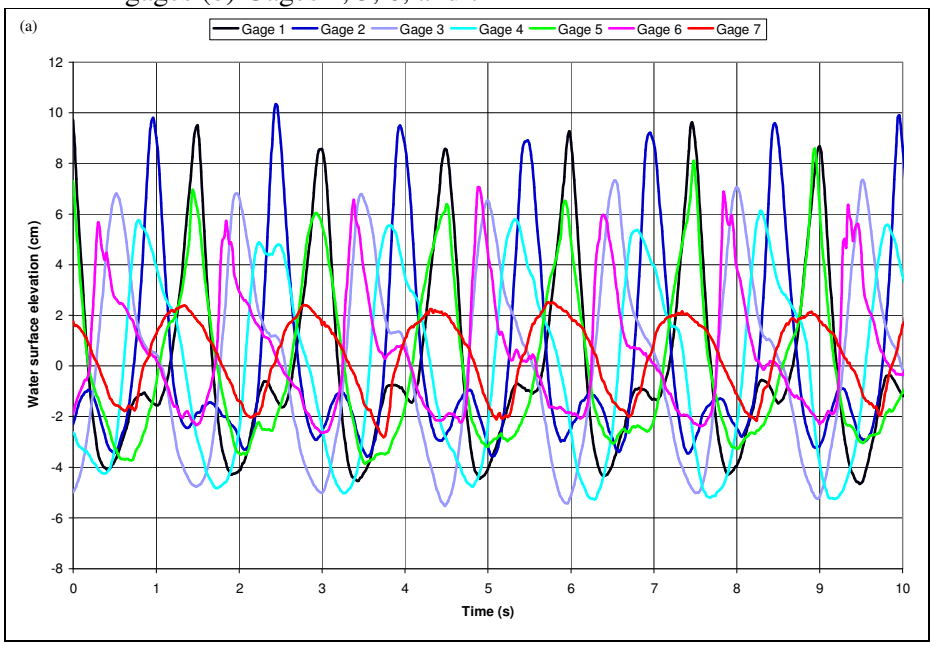

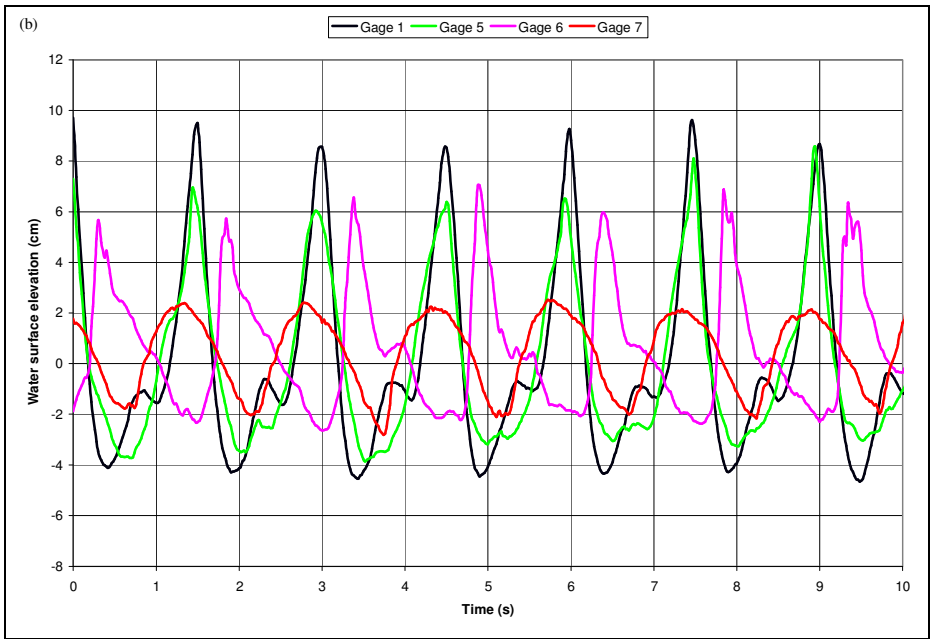

Figure 5.6 Case 2 With Plants Run Water Surface Elevation Time Series (a) All gages (b) Gages 1, 5, 6, and 7

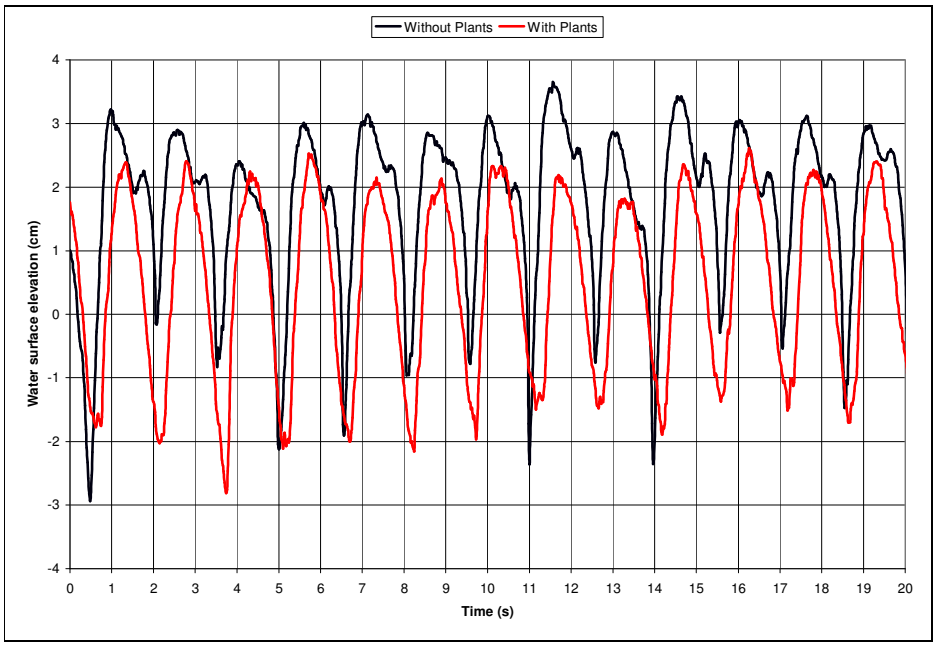

Figure 5.7 Case 2 Without and With Plants Runs Water Surface Elevation Time Series Gage 7

Table 5.2 Case 2 Runs Water Surface Elevation Time Series Mean, Variance, and Skewness (a) Without Plants (b) With Plants

(a)	**Gage 1**	**Gage 2**	**Gage 3**	**Gage 4**	**Gage 5**	**Gage 6**	**Gage 7**
Mean	0.140	0.227	0.009	0.111	0.100	0.724	1.726
Variance	13.374	18.529	12.137	16.568	9.687	5.924	1.568
Skewness	51.628	93.179	6.831	3.296	32.371	1.273	-2.563
(b)	**Gage 1**	**Gage 2**	**Gage 3**	**Gage 4**	**Gage 5**	**Gage 6**	**Gage 7**
Mean	0.180	0.190	0.107	0.060	0.141	0.484	0.403
Variance	15.100	14.646	13.712	13.487	10.351	5.207	2.082
Skewness	38.788	70.265	15.986	4.151	27.553	8.051	-1.392

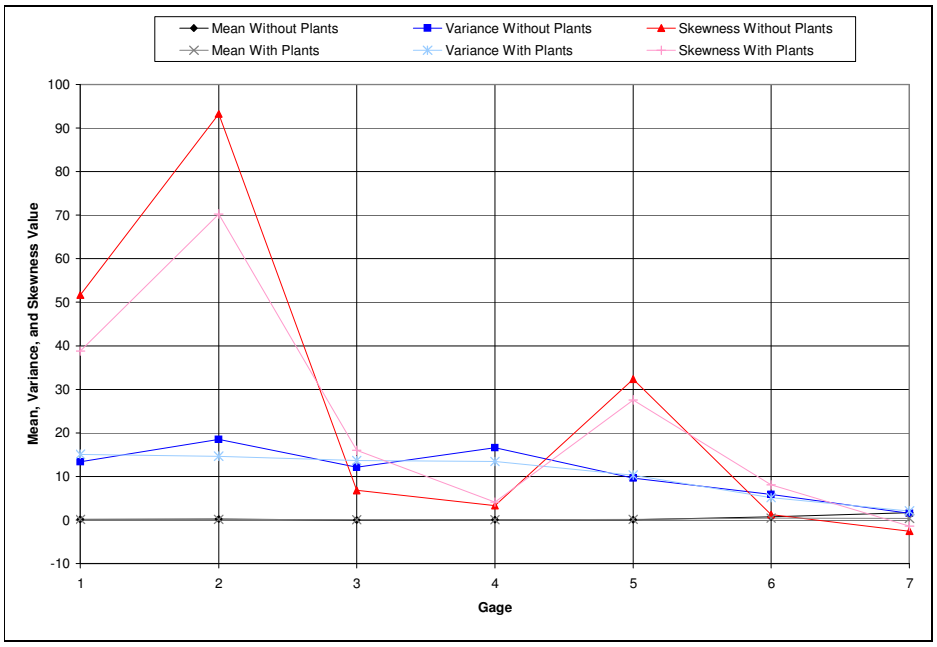

Figure 5.8 Case 2 Without and With Plants Runs Water Surface Elevation Time Series Mean, Variance, and Skewness All Gages

5.1.2 Irregular Wave Cases

Case 3

Minimal wave breaking occurred during both the without and with plants runs of case 3 (T_p = 1 s and γ = 3.3), as indicated by the constant variance and skewness of each gage's output signal (Table 5.3 and Figure 5.11). The plants oscillated with the passing waves but did not bend backwards. During both runs, the waves typically proceeded up the ramp slowly but were abruptly returned up the ramp during rundown. The negative mean water level at gage 7 during both the without and with plants runs indicates the runup/rundown pattern typically remained below still water level. Without plants in the flume, the wave excursion along the ramp centered about approximately 1.6 cm below still water level. With influence of the plants, this excursion centered about approximately 2.5 cm below still water level. Notably, the runup was generally proportional to and similar in extent to the wave height at gage 6 during both runs (Figures 5.9 and 5.10).

Table 5.3 Case 3 Runs Water Surface Elevation Time Series Mean, Variance, and Skewness (a) Without Plants (b) With Plants

(a)	**Gage 1**	**Gage 2**	**Gage 3**	**Gage 4**	**Gage 5**	**Gage 6**	**Gage 7**
Mean	-0.006	0.014	-0.016	-0.014	-0.004	-0.005	-1.659
Variance	0.522	0.502	0.468	0.441	0.430	0.445	0.302
Skewness	0.016	0.016	0.028	0.006	0.026	0.074	-0.035
(b)	**Gage 1**	**Gage 2**	**Gage 3**	**Gage 4**	**Gage 5**	**Gage 6**	**Gage 7**
Mean	0.007	-0.004	-0.002	0.006	-0.005	0.005	-2.467
Variance	0.478	0.465	0.431	0.404	0.374	0.374	0.152
Skewness	0.032	0.004	0.045	0.013	0.036	0.048	-0.034

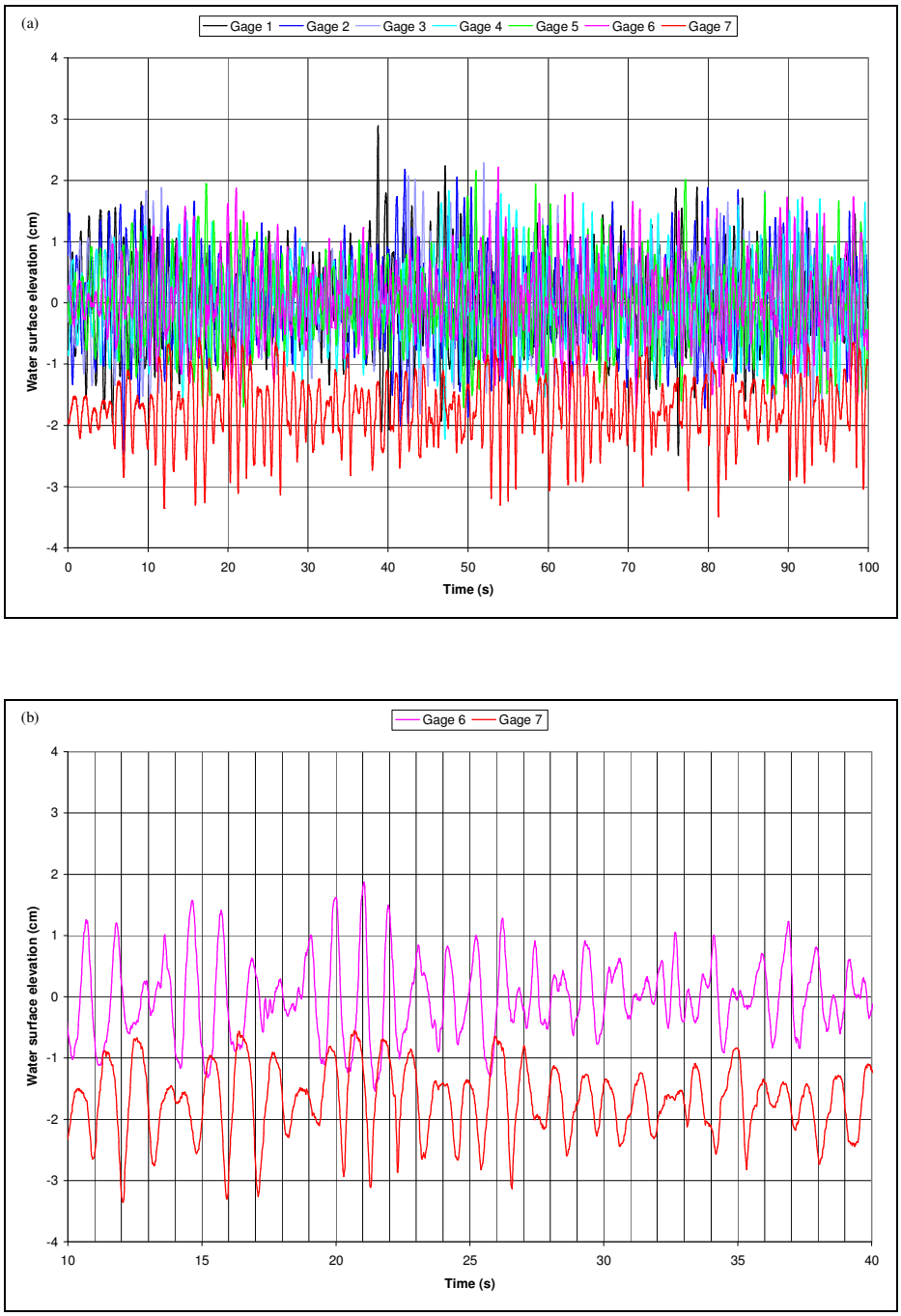

Figure 5.9 Case 3 Without Plants Run Water Surface Elevation Time Series (a) All gages (b) Gages 6 and 7

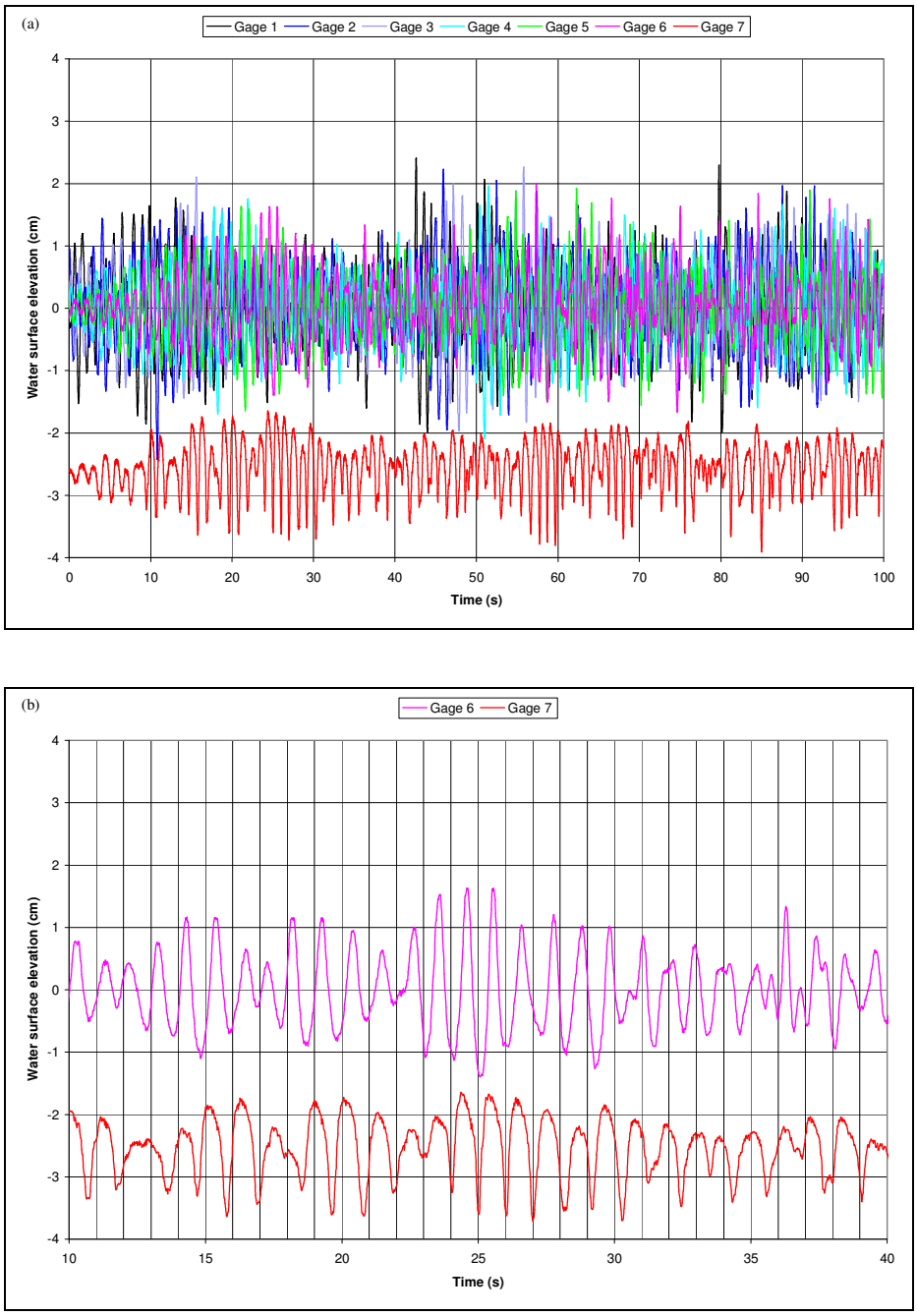

Figure 5.10 Case 3 With Plants Run Water Surface Elevation Time Series (a) All gages (b) Gages 6 and 7

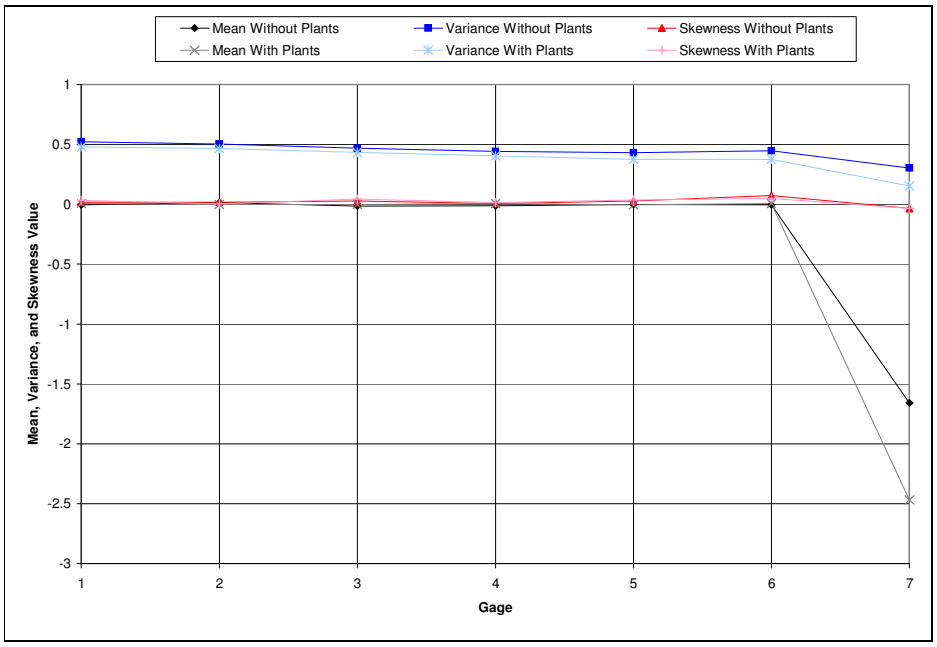

Figure 5.11 Case 3 Without and With Plants Runs Water Surface Elevation Time Series Mean, Variance, and Skewness All Gages

Case 4

Table 5.4 and Figure 5.14 reveal an increase in variance of the water surface elevation time series at gages 6 and 7 and an increasing signal skewness that peaks at gage 6 for the without plants run of case 4 (T_p = 1.5 s and γ = 3.3). The without plants run times series figures (Figures 5.12 and 5.13) show tall wave peaks at gage 6 and a dominant rundown. To a much lesser degree, these patterns are apparent in the with plants run. A steady signal variance results with only a slight peak in signal skewness at gage 6 during the with plants run. Notably, a smooth spilling breaker was observed during much of the with plants run while a more abrupt breaking was observed during the without plants run. The plants became prone in both directions frequently. During the without plants run, the runup/rundown range along the ramp centered about approximately 0.7 cm below still water level. With influence of the plants, this excursion centered about approximately 2 cm below still water level. Typically, during both runs, the rundown was proportional to

the wave height at gage 6 while the magnitude of rundown was generally slightly larger than the wave height during the without plants run. With plants in the flume, the runup/rundown pattern was generally smoother than without plants, i.e. the rundown was not returned up the ramp as abruptly.

Table 5.4 Case 4 Runs Water Surface Elevation Time Series Mean, Variance, and Skewness (a) Without Plants (b) With Plants

(a)	**Gage 1**	**Gage 2**	**Gage 3**	**Gage 4**	**Gage 5**	**Gage 6**	**Gage 7**
Mean	-0.006	-0.003	-0.011	-0.018	-0.034	-0.045	-0.690
Variance	1.380	1.392	1.369	1.362	1.436	2.136	2.499
Skewness	0.252	0.045	0.114	0.204	0.742	2.596	-0.894
(b)	**Gage 1**	**Gage 2**	**Gage 3**	**Gage 4**	**Gage 5**	**Gage 6**	**Gage 7**
Mean	-0.026	-0.032	-0.049	0.009	0.003	-0.031	-1.930
Variance	1.140	1.150	1.104	1.098	1.161	1.292	0.934
Skewness	0.191	0.010	0.064	0.182	0.571	1.199	-0.201

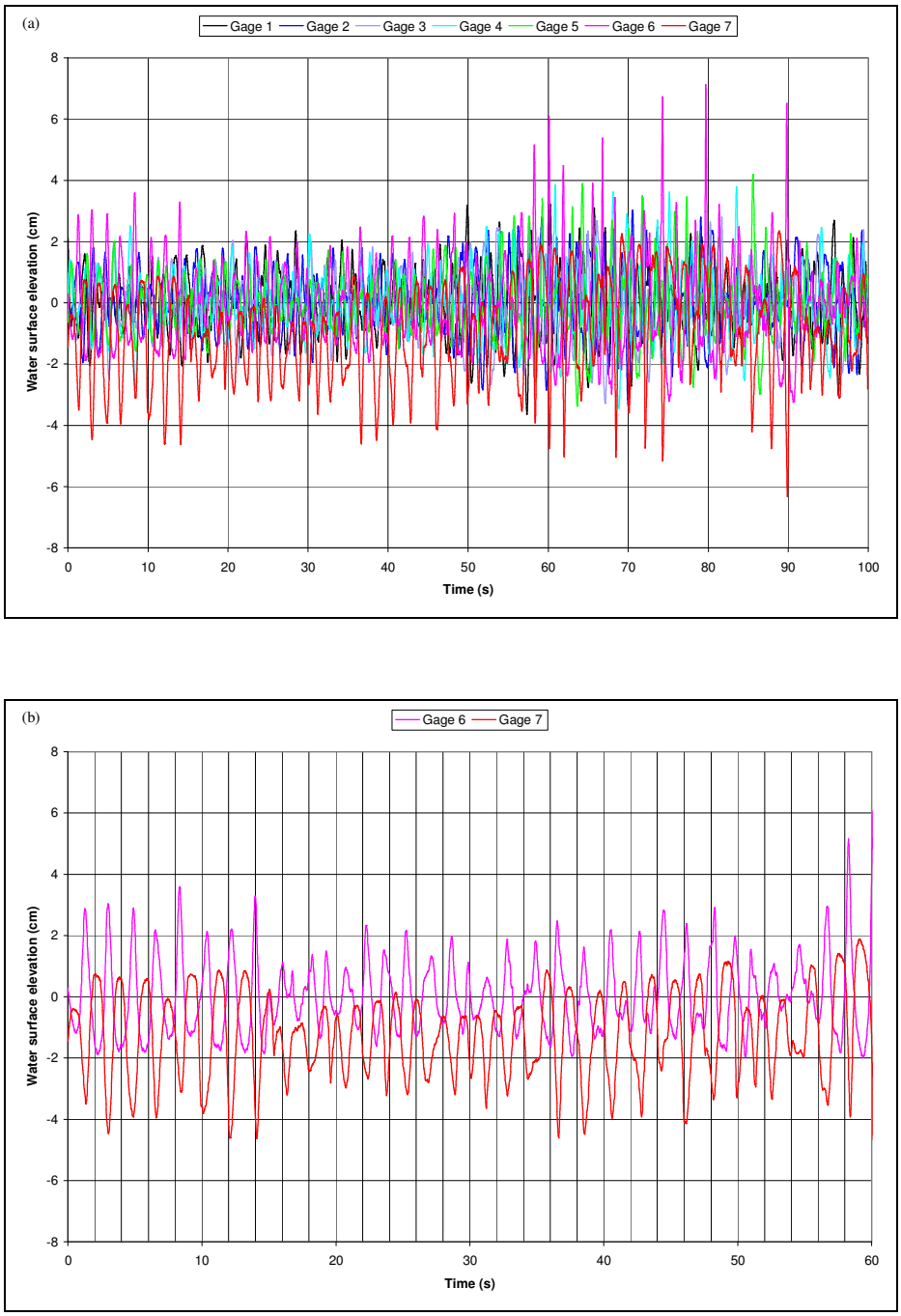

Figure 5.12 Case 4 Without Plants Run Water Surface Elevation Time Series (a) All gages (b) Gages 6 and 7

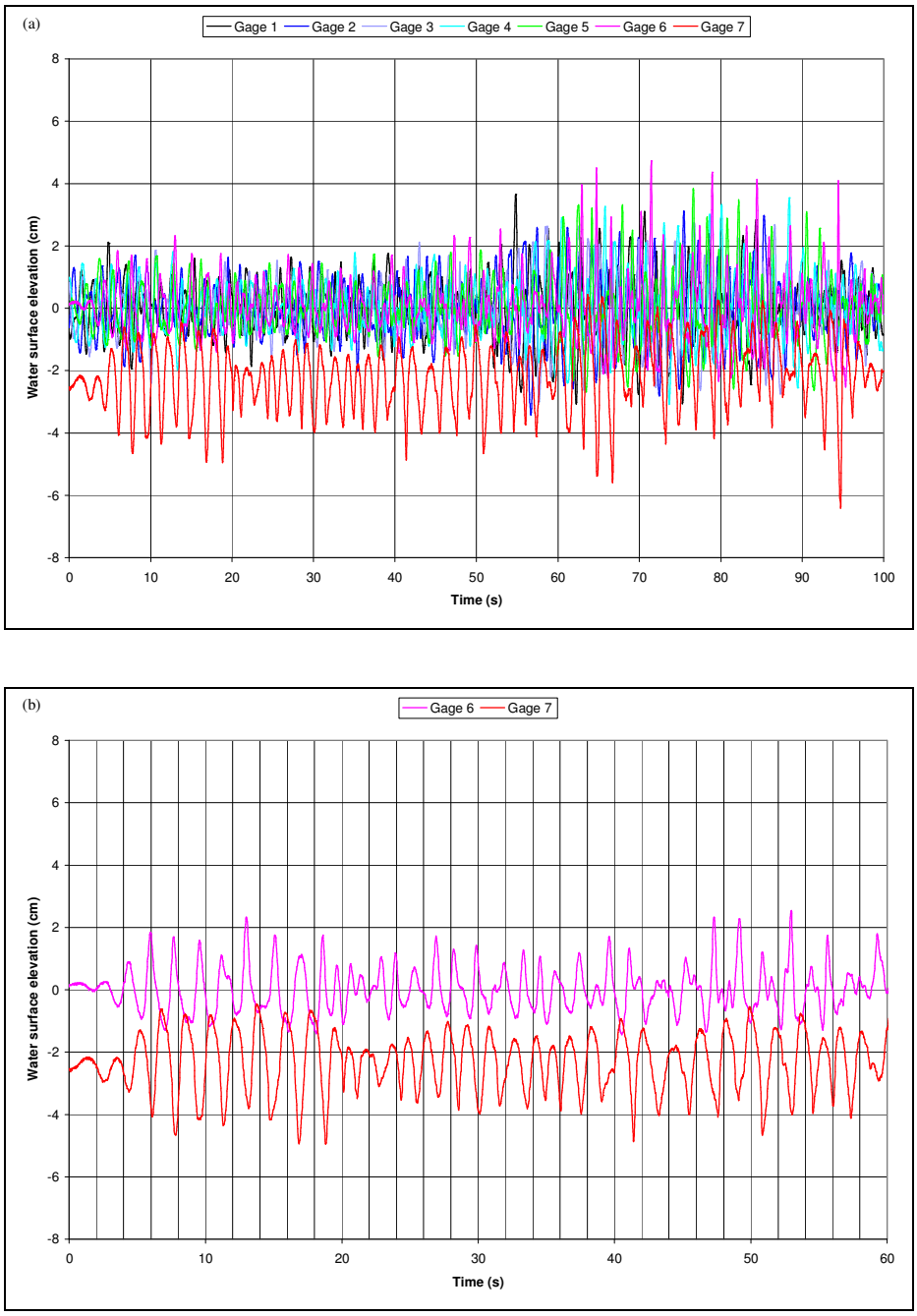

Figure 5.13 Case 4 With Plants Run Water Surface Elevation Time Series (a) All gages (b) Gages 6 and 7

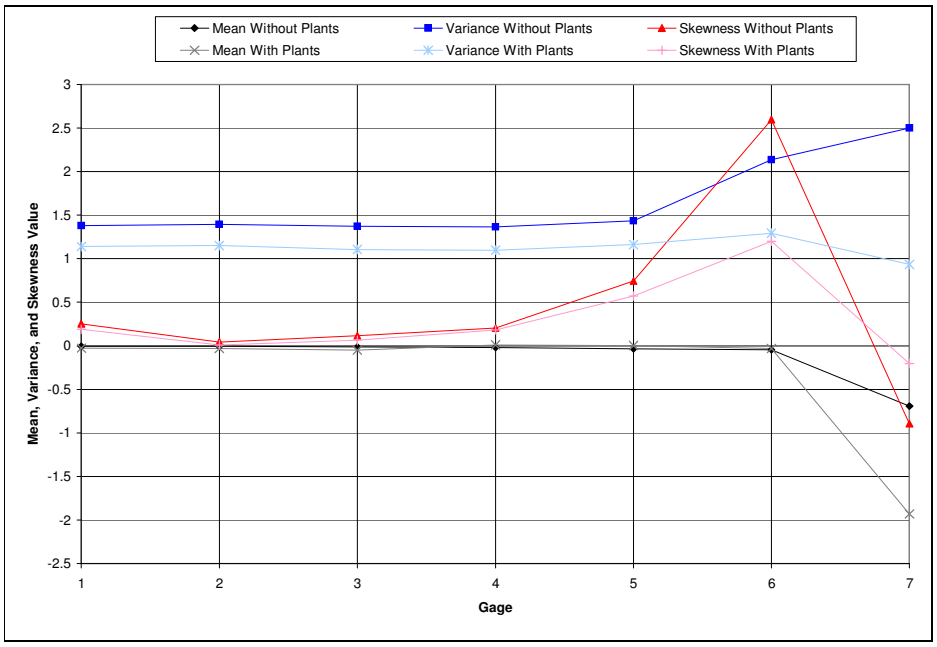

Figure 5.14 Case 4 Without and With Plants Runs Water Surface Elevation Time Series Mean, Variance, and Skewness All Gages

Case 5

The time series figures (Figures 5.15 and 5.16) and water surface elevation time series analysis (Table 5.5 and Figure 5.17) of the case 5 runs (T_p = 1.5 s and γ = 30), reveal very similar results to the corresponding case 4 run. These patterns include an increase in variance of the water surface elevation time series at gages 6 and 7 during the without plants run and a steady variance during the with plants run. An increasing signal skewness peaks at gage 6 during both runs but to a much lesser degree during the with plants run. Observation revealed a sharper breaking wave during the case 5 without plants run as compared to the with plants run. The plants oscillated with the passing waves and frequently became fully prone in both directions. Similar to case 4, the runup/rundown excursion centered about approximately 0.7 cm below still water level during the without plants run and about approximately 2 cm below still water level with plants in the flume. With plants in the flume, the runup and rundown proceeded along the ramp smoothly

while the rundown was more abruptly returned up the ramp without influence of the plants.

Table 5.5 Case 5 Runs Water Surface Elevation Time Series Mean, Variance, and Skewness (a) Without Plants (b) With Plants

(a)	**Gage 1**	**Gage 2**	**Gage 3**	**Gage 4**	**Gage 5**	**Gage 6**	**Gage 7**
Mean	-0.011	-0.004	-0.014	-0.047	-0.023	-0.023	-0.719
Variance	1.472	1.478	1.481	1.406	1.427	2.203	2.178
Skewness	0.202	0.254	0.182	0.438	0.934	2.574	-0.537
(b)	**Gage 1**	**Gage 2**	**Gage 3**	**Gage 4**	**Gage 5**	**Gage 6**	**Gage 7**
Mean	-0.015	-0.046	0.005	0.012	-0.003	-0.041	-1.961
Variance	1.217	1.236	1.200	1.179	1.220	1.368	1.046
Skewness	0.243	0.165	0.135	0.416	0.780	1.558	0.186

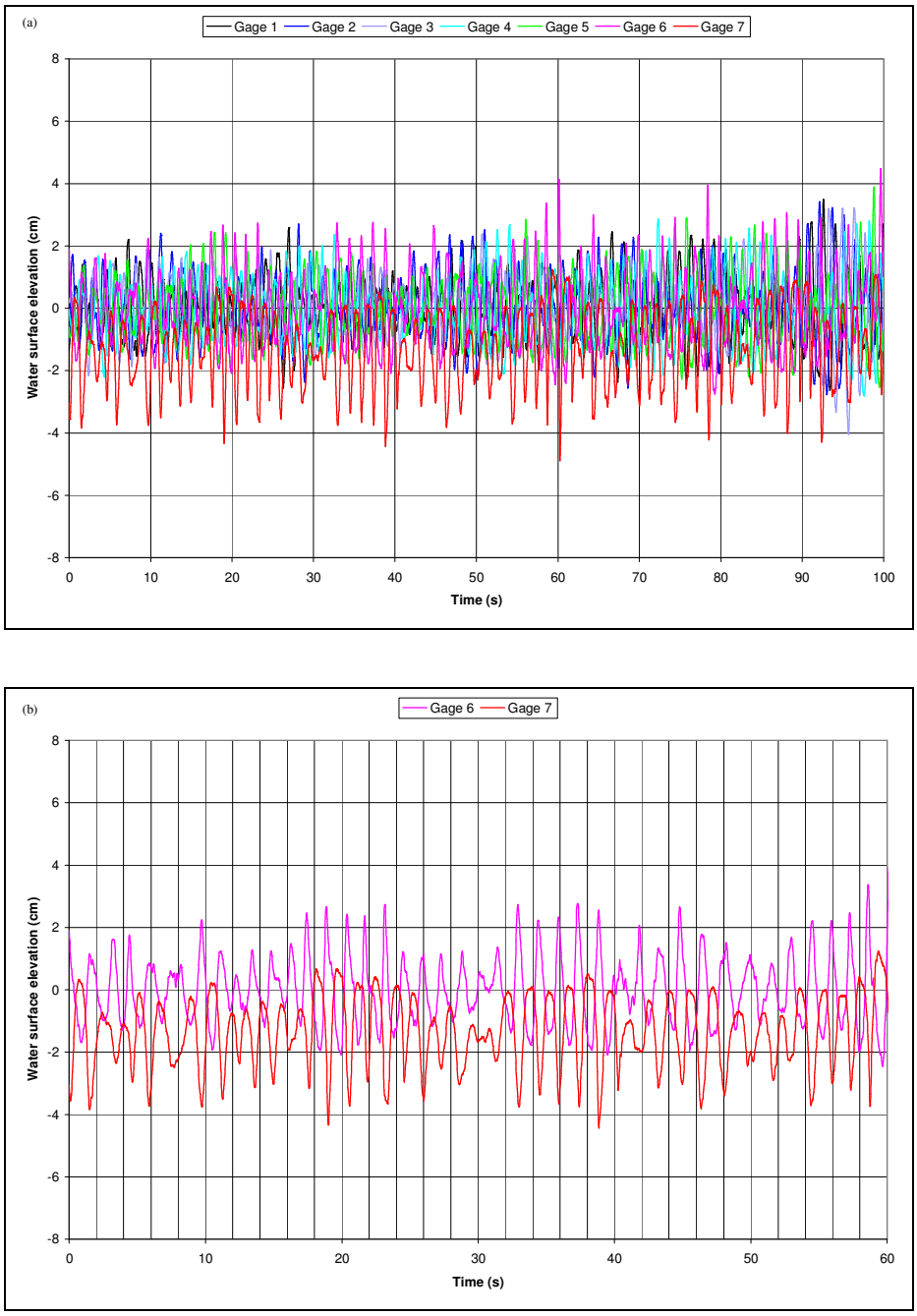

Figure 5.15 Case 5 Without Plants Run Water Surface Elevation Time Series (a) All gages (b) Gages 6 and 7

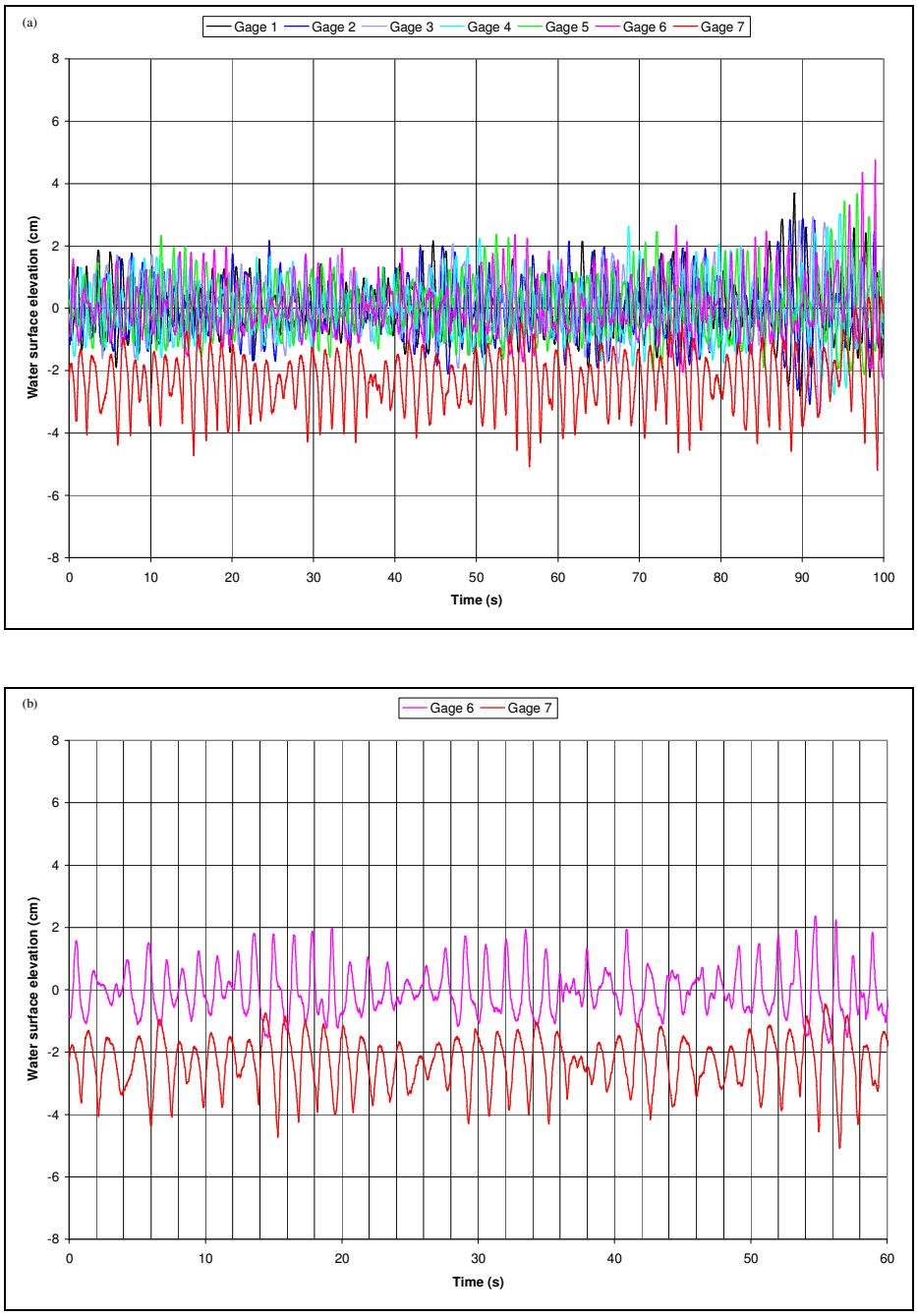

Figure 5.16 Case 5 With Plants Run Water Surface Elevation Time Series (a) All gages (b) Gages 6 and 7

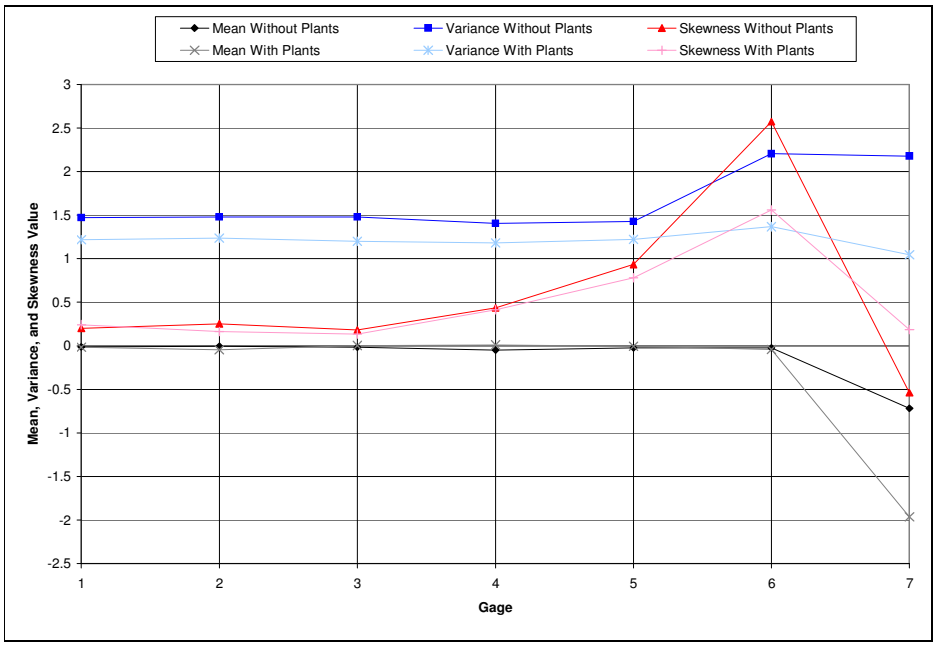

Figure 5.17 Case 5 Without and With Plants Runs Water Surface Elevation Time Series Mean, Variance, and Skewness All Gages

Case 6

For case 6 (T_p = 2 s and γ = 3.3),, the time series figures of the without plants run (Figure 5.18) show a narrow crest height frequently much greater than the broader trough depth at gage 6 and a longer extent of rundown than runup at gage 7. Analysis of the water surface elevation time series of each gage during this run reveals a larger variance at gage 6 and 7 as well as a peak in skewness of the signal at gage 6 (Table 5.6 and Figure 5.20). These same patterns are evident in the with plants run but to a much lesser degree. Notably, a plunging breaker was observed near gage 6 during much of the without plants run while smoother breaking occurred slightly further offshore during much of the with plants run. The plants oscillated with the passing waves and became fully prone in both directions frequently.

The runup/rundown excursion centered about approximately 1 cm below still water level during the without plants run and about approximately 2.5 cm below still

water level with plants in the flume. The excursion along the ramp was generally proportional to but slightly larger than the wave height at gage 6 during both runs, i.e. the taller the crest, the larger the rundown. The runup/rundown pattern was usually smooth during the with plants run but the rundown was abruptly returned up the ramp during the without plants run.

Table 5.6 Case 6 Runs Water Surface Elevation Time Series Mean, Variance, and Skewness (a) Without Plants (b) With Plants

(a)	**Gage 1**	**Gage 2**	**Gage 3**	**Gage 4**	**Gage 5**	**Gage 6**	**Gage 7**
Mean	-0.008	-0.004	-0.017	-0.033	-0.090	-0.047	-1.088
Variance	0.757	0.798	0.831	0.832	0.898	1.397	3.615
Skewness	0.007	0.000	0.019	0.165	0.312	1.889	0.224
(b)	**Gage 1**	**Gage 2**	**Gage 3**	**Gage 4**	**Gage 5**	**Gage 6**	**Gage 7**
Mean	-0.017	-0.022	-0.033	-0.040	-0.033	-0.017	-2.554
Variance	0.336	0.349	0.347	0.361	0.377	0.447	0.963
Skewness	-0.008	-0.013	0.022	0.038	0.073	0.209	-0.216

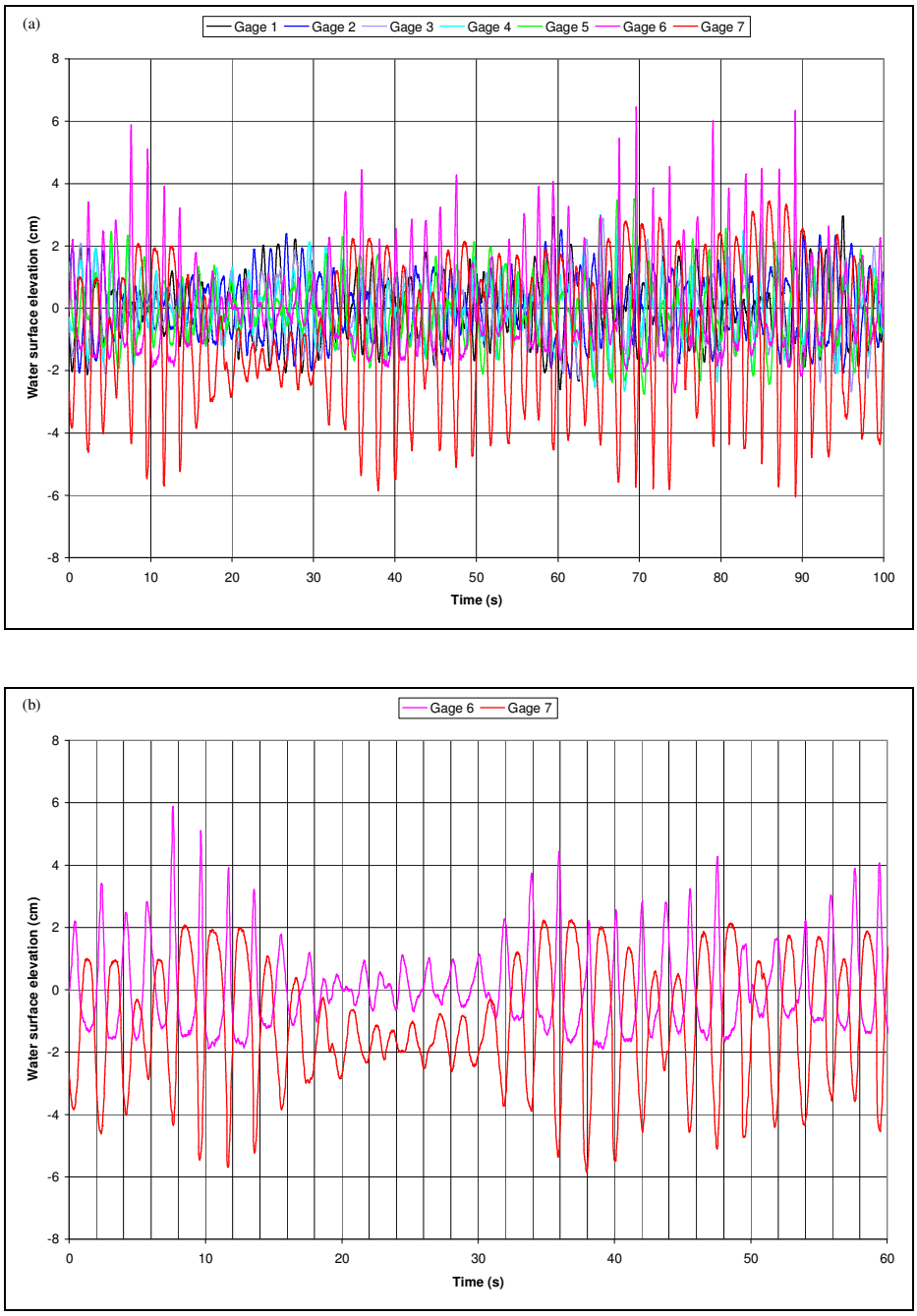

Figure 5.18 Case 6 Without Plants Run Water Surface Elevation Time Series (a) All gages (b) Gages 6 and 7

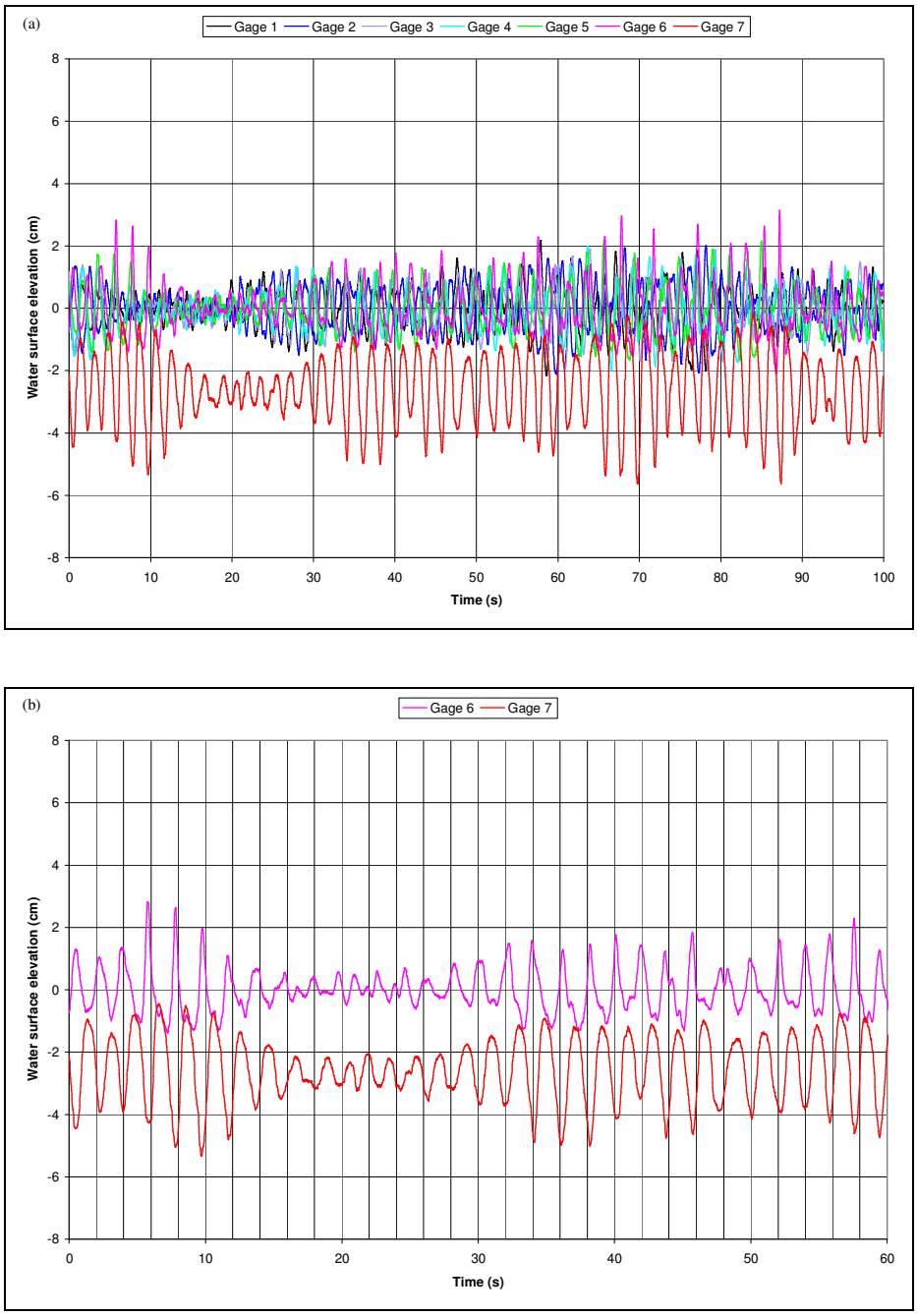

Figure 5.19 Case 6 With Plants Run Water Surface Elevation Time Series (a) All gages (b) Gages 6 and 7

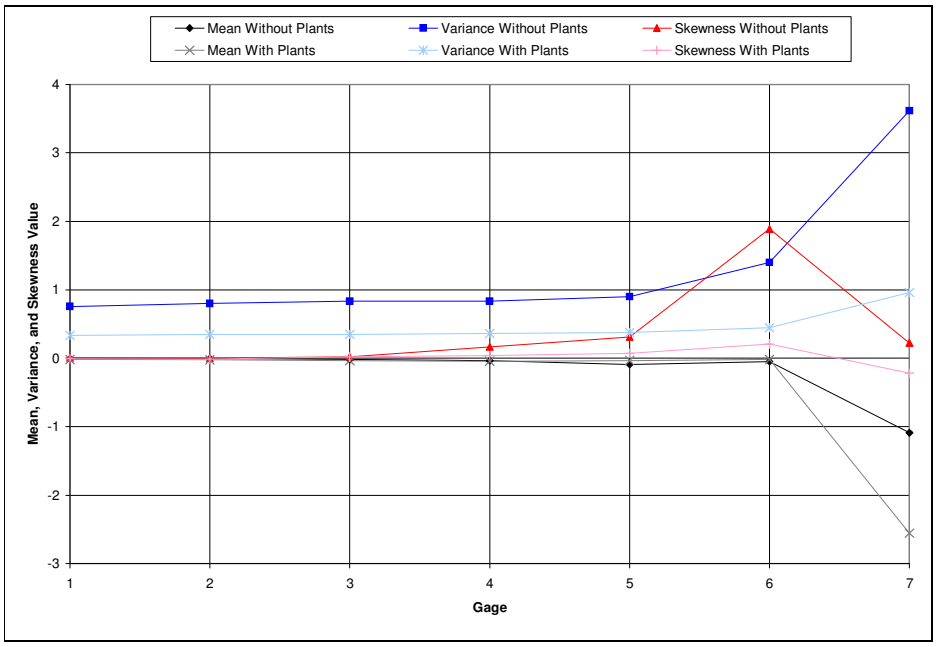

Figure 5.20 Case 6 Without and With Plants Runs Water Surface Elevation Time Series Mean, Variance, and Skewness All Gages

5.2 Spectral Analysis

After analysis of each gage's water surface elevation output time series, the data was transferred into the frequency domain for additional analysis. The power spectral density, or Fourier transform of the autocorrelation function, results from a fast Fourier transform (FFT) utilizing Welch's method with 1,024 data points per segment. The Matlab program, pwelch, estimates the power spectrum of the input time series and allows specification of a windowing function prior to transformation. A rectangular, or "boxcar," window was applied to the time series of the regular wave runs (cases 1 and 2) and a Hanning window to those of the irregular cases (cases 3 – 6). The following figures show the resulting spectra up to 5 Hz which is sufficient to capture relevant information.

5.2.1 Regular Wave Cases

Case 1

For both runs of case 1 (T_p = 1 s), in addition to the prominent 1 Hz frequency peak, the transform captures peaks of decreasing amplitude at multiples of 1 Hz within each gage's output signal (Figure 5.21). Since regular wave conditions developed for 10 minutes prior to data acquisition, these harmonics may be attributed to reflection in the flume during these runs. As seen in Figure 5.22, for both the without and with plants runs, the magnitude of the 1 Hz peak decreases from approximately 200 cm^2/Hz at gage 1 to 70 cm^2/Hz at gage 5 to 20 cm^2/Hz at gage 6 indicating a decrease in energy approaching the beach. The much narrower peak of the first harmonic (2 Hz) has an amplitude two orders of magnitude less than the dominant 1 Hz peak at gage 1. The difference in magnitude between these 2 peaks decreases steadily approaching the beach indicating a lesser degree of reflection, or greater degree of wave energy absorption, at 2 Hz closer to the wave maker. Figure 5.21 reveals a consistently weaker variance at gage 7 than gages 1 – 6 for both the without and with plants runs. Figure 5.22 shows a consistent reduction in energy at gage 7 during the with plants run as compared to the without plants run over the frequency range. Notably, a wide peak centered about approximately 0.375 Hz arises with a magnitude of approximately 1 cm^2/Hz at gage 7 during the without plants run but is not evident during the with plants run.

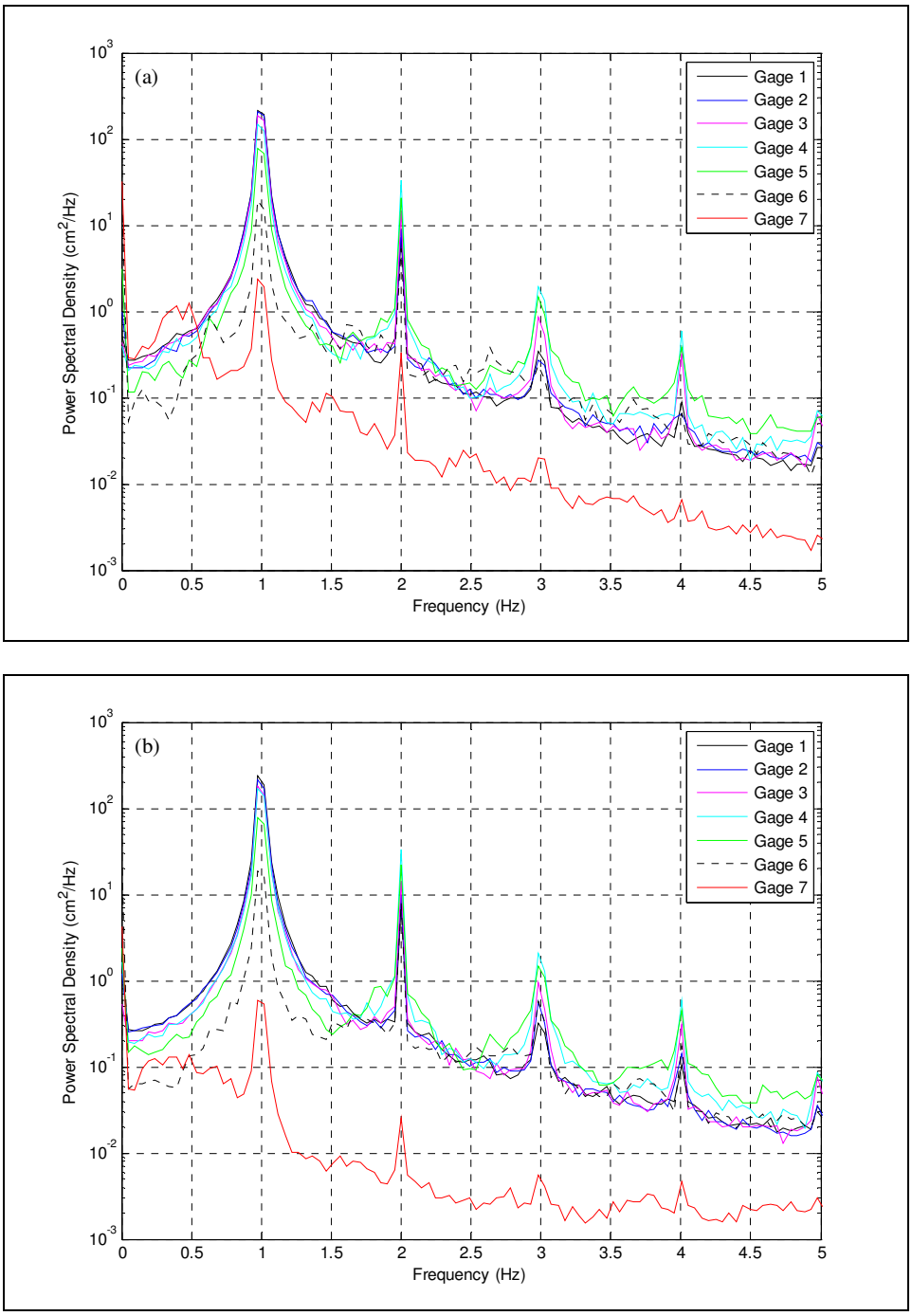

Figure 5.21 Case 1 Runs Power Spectral Density (a) Without Plants (b) With Plants

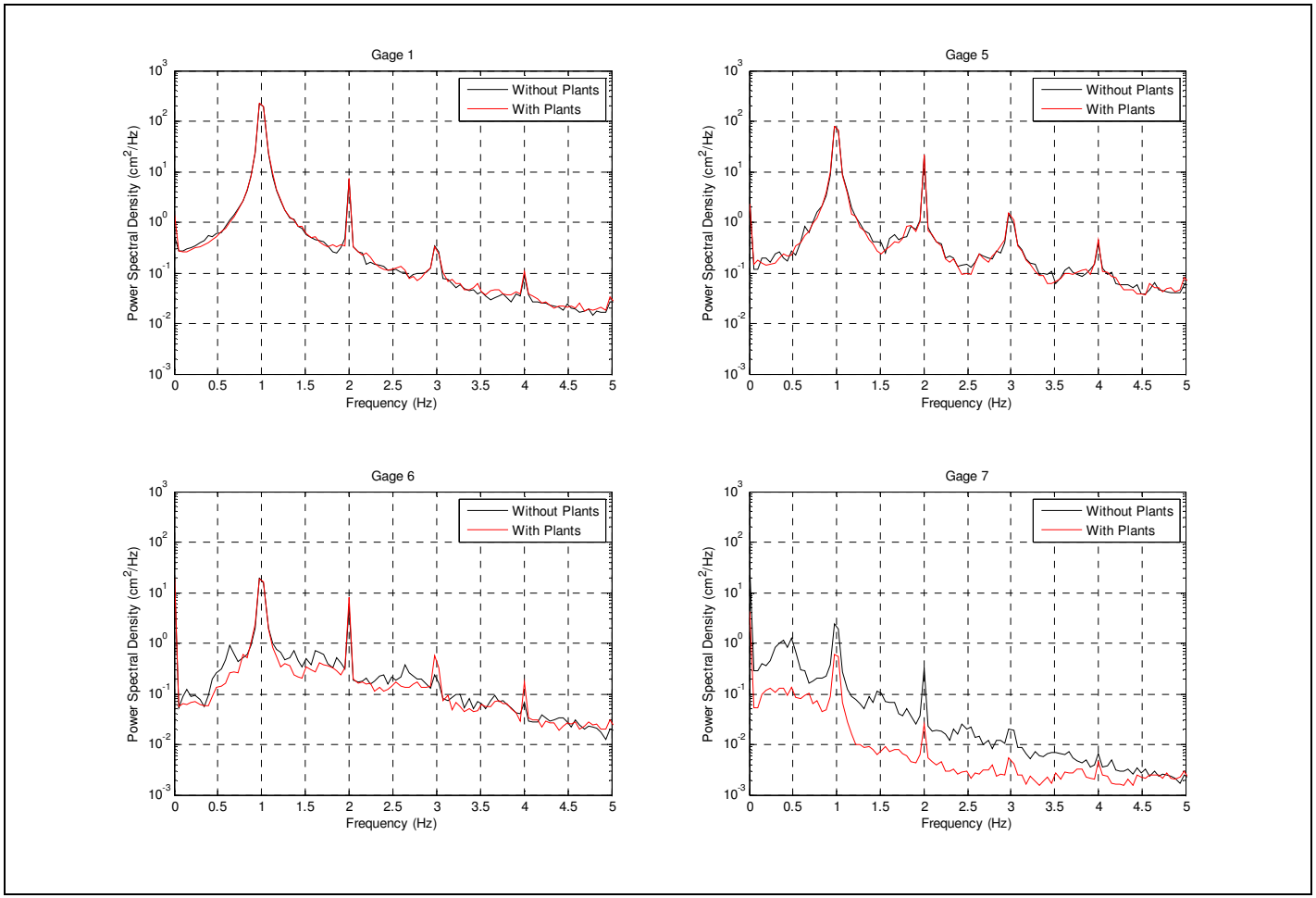

Figure 5.22 Case 1 Runs Power Spectral Density Comparisons

Case 2

As seen in Figure 5.23, similar to case 1, multiple harmonics of decreasing amplitude arise from the frequency transformation of each gage's output signal for both the without and with plants runs for case 2 (T_p = 1.5 s). These additional peaks, at intervals of 0.67 Hz, may be due to reflection resulting from allowing the regular wave condition 10 minutes to develop prior to data acquisition. These peaks are noticeably narrower than those of case 1. Figure 5.24 shows the magnitude of the 0.67 Hz peak decreases from approximately 100 cm^2/Hz at gage 1 to 60 cm^2/Hz at gage 6 for both the without and with plants runs indicating a decrease in energy as the waves approached the beach. The difference in peak magnitude between the 0.67 Hz and first harmonic (1.33 Hz) increases between gages 1 and 5 and then decreases between gages 5 and 7. A larger difference between these peaks indicates a smaller amount of reflection, or greater degree of energy absorption, at that gage. Figure 5.23 indicates a consistently weaker variance at gage 7 than gages 1 – 6 for both the without and with plants runs. Figure 5.24 also reveals a general slight energy reduction at gage 7 during the with plants run versus the without plants run for this case.

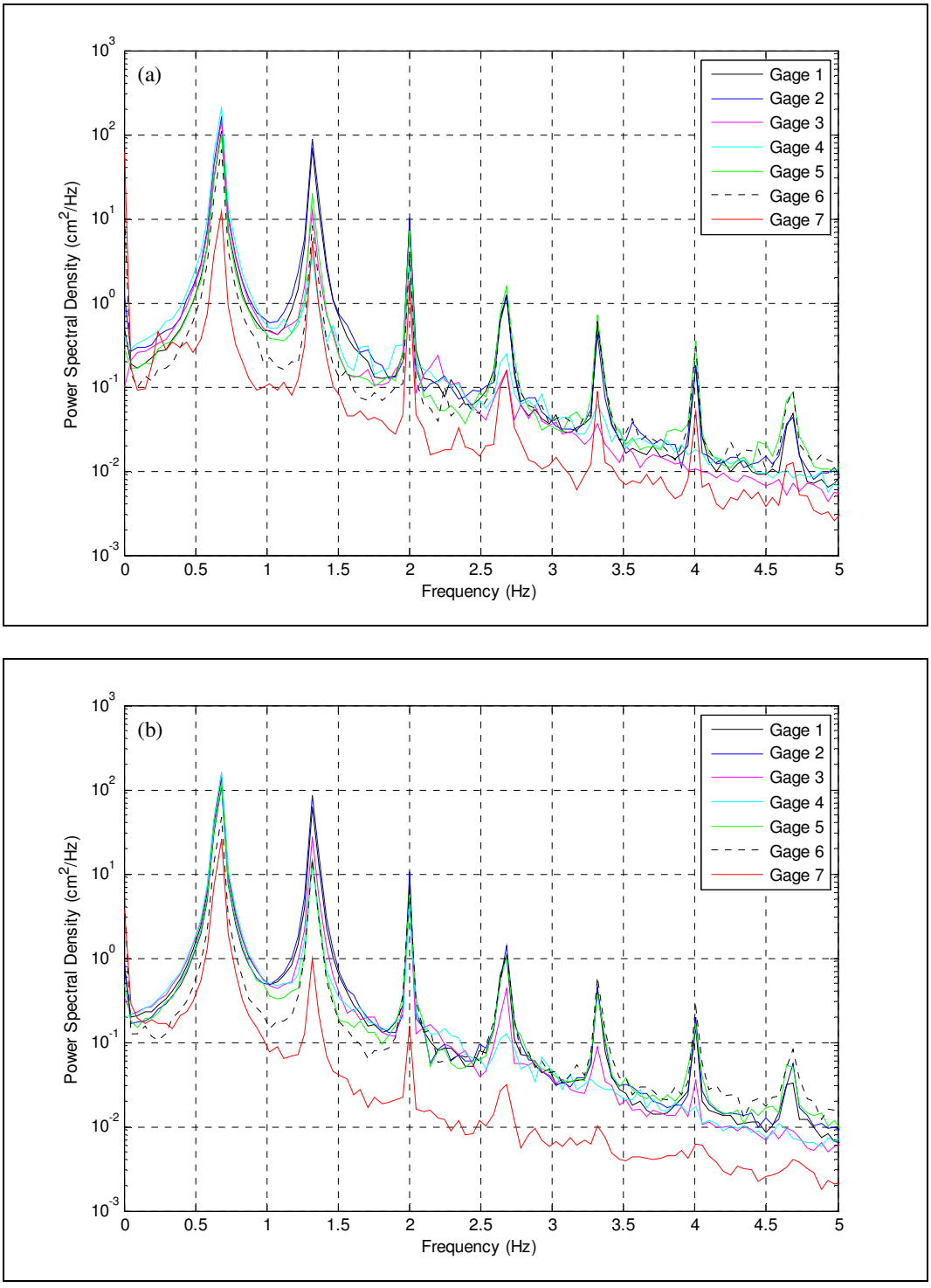

Figure 5.23 Case 2 Runs Power Spectral Density (a) Without Plants (b) With Plants

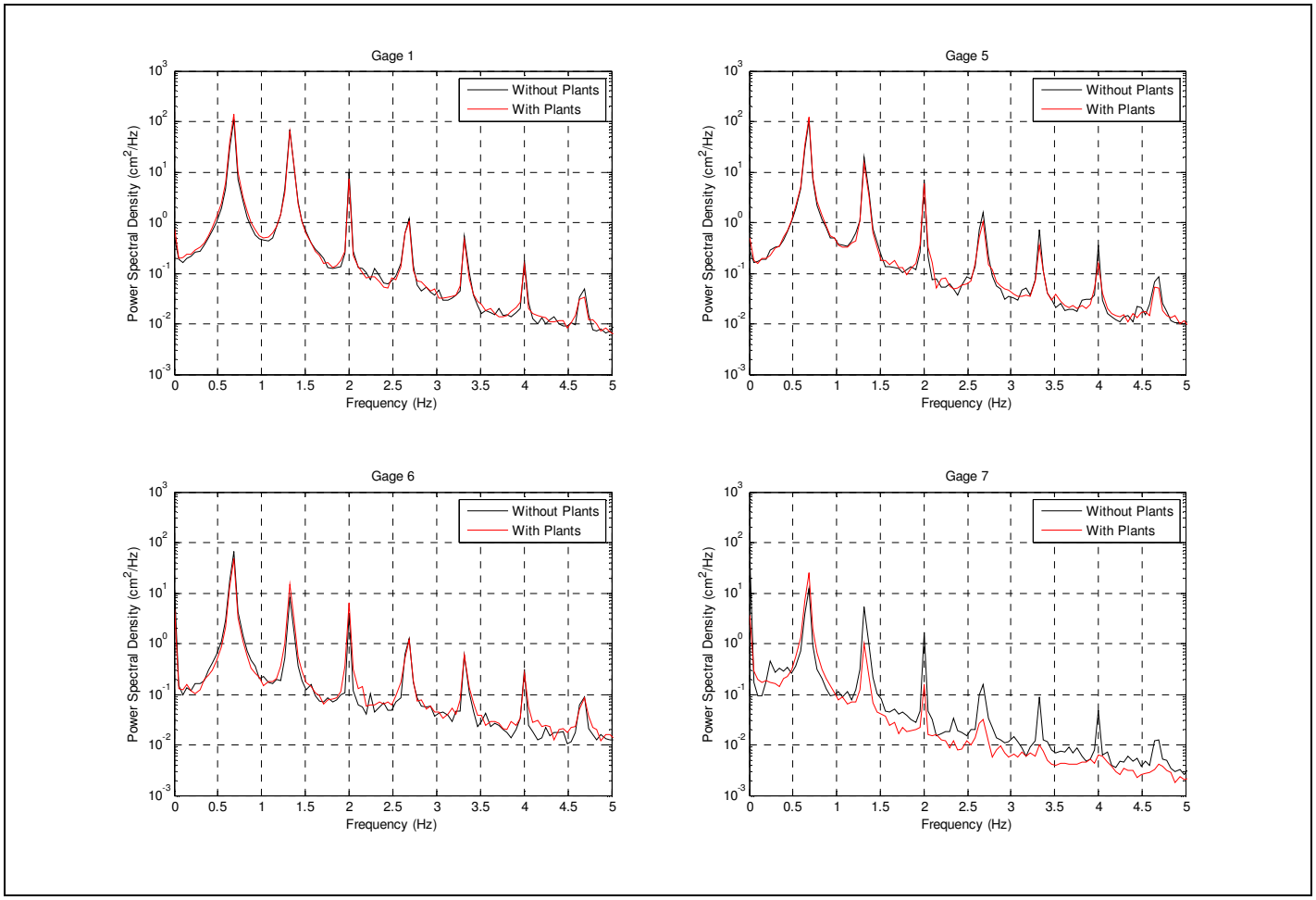

Figure 5.24 Case 2 Runs Power Spectral Density Comparisons

5.2.2 Irregular Wave Cases

Case 3

For case 3 (T_p = 1 s and γ = 3.3), the frequency transformation of each gage's output signal reveals a prominent wide peak centered about approximately 1 Hz for both the without and with plants runs (Figure 5.25). This peak generally retains its amplitude between the 7 gages. For both the without and with plants runs, the magnitude of the 1 Hz peak reaches approximately 2 cm^2/Hz at gage 1, 1 cm^2/Hz at gage 6, and 0.6 cm^2/Hz at gage 7. Notably, as compared to gages 1 – 6, a slight decrease in wave energy appears at gage 7 between 1 Hz and 2.5 Hz for the with plants run. Figure 5.25 reveals this pattern, to a lesser degree, in the spectra of the without plants run. Comparing the without and with plants runs over the frequency range, Figure 5.26 reveals a consistent variance between gages 1, 5, 6, and 7.

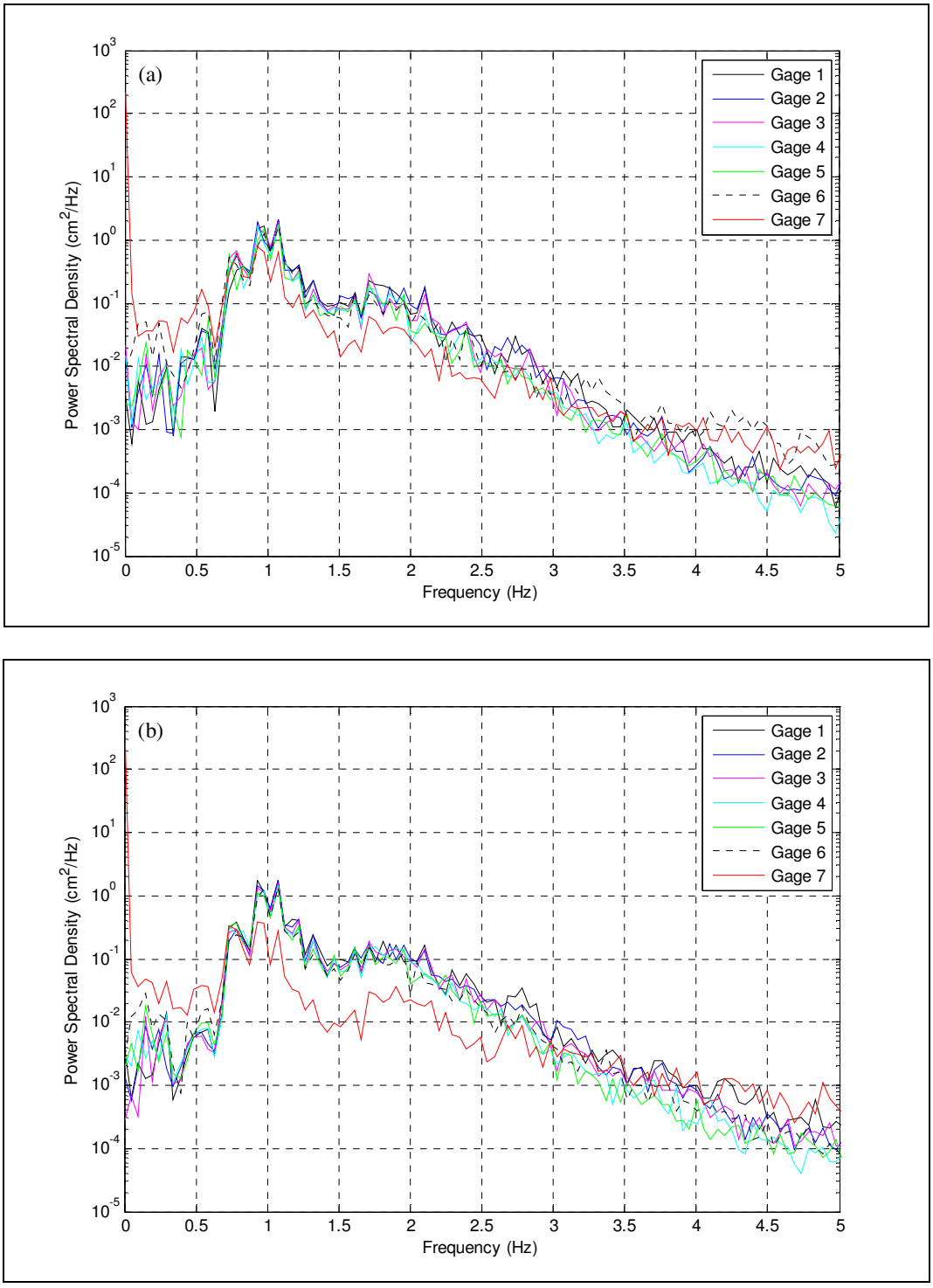

Figure 5.25 Case 3 Runs Power Spectral Density (a) Without Plants (b) With Plants

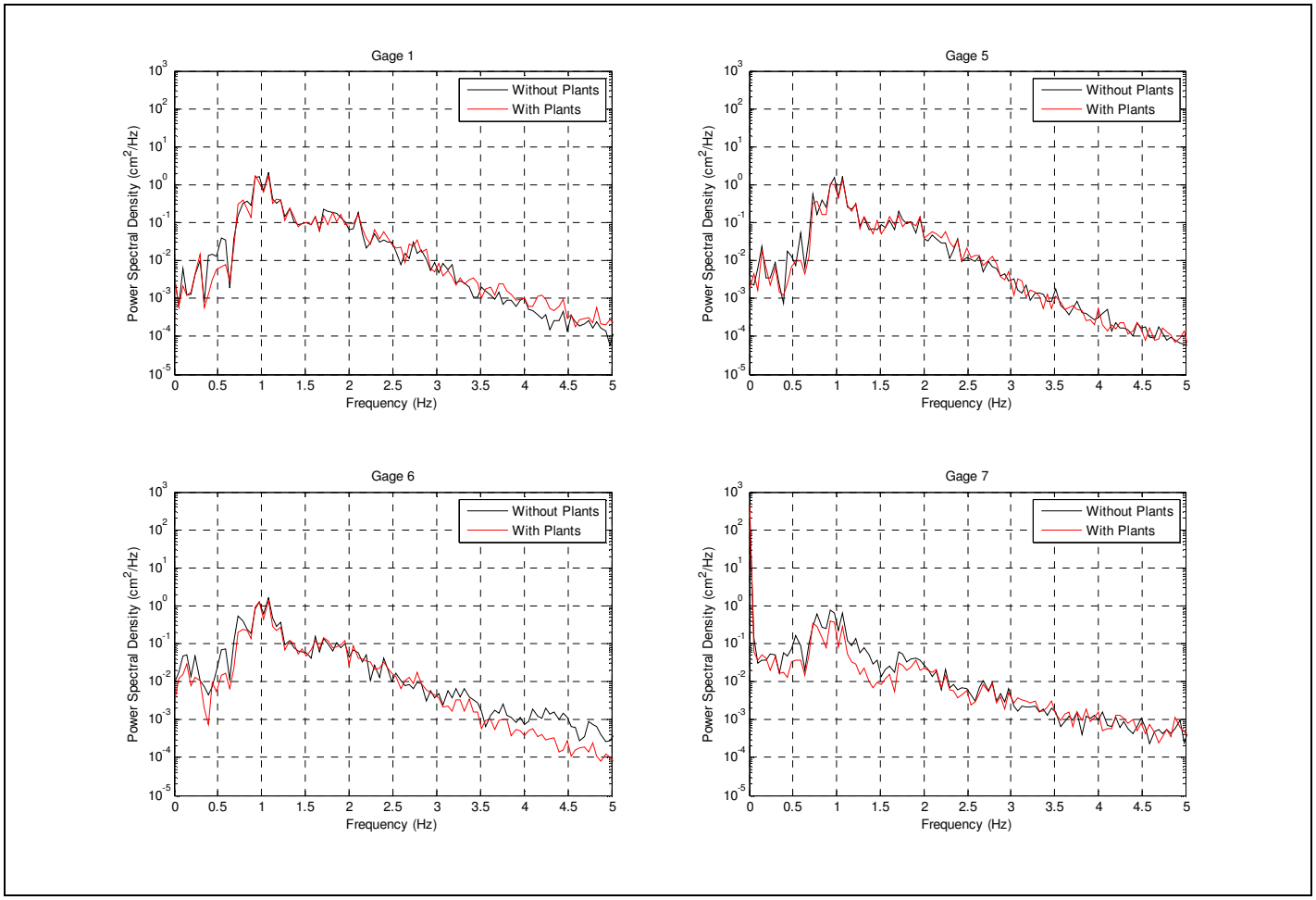

Figure 5.26 Case 3 Runs Power Spectral Density Comparisons

Case 4

The frequency spectrum of each gage's output signal for both the without and with plants runs of case 4 (T_p = 1.5 s and γ = 3.3) shows a wide peak centered about approximately 0.67 Hz (Figure 5.27). During both runs, the magnitude of the prominent frequency peak remains between approximately 2 cm^2/Hz and 10 cm^2/Hz. For both the without and with plants runs, the spectra show greater variance at gages 6 and 7, as compared to gages 1 – 5, at frequencies greater than 3.5 Hz. Figure 5.28 reveals the power spectral density remains generally less at gage 6 and consistently less at gage 7 during the with plants run as compared to the without plants run.

Case 5

For case 5 (T_p = 1.5 s and γ = 30), frequency transformation of each gage's output signal captures a sharper peak at 0.67 Hz with a slightly greater amplitude than the prominent peak seen in case 4 (Figure 5.29). Figure 5.30 shows the magnitude of this prominent peak reaches approximately 20 cm^2/Hz at gage 1 and decreases to approximately 9 cm^2/Hz at gage 7 for both the without and with plants runs. An additional peak centered about approximately 1.33 Hz arises in each gage's spectrum during both the without and with plants runs for this case. The magnitude of this first harmonic peak (1.33 Hz) remains approximately 1 cm^2/Hz at each of the gages during both runs. Similar to case 4, the spectra indicate greater variance at gages 6 and 7, as compared to gages 1 –5, at frequencies greater than 3.5 Hz during both runs. Figure 5.30 indicates the variance remains generally less at gage 6 and consistently less at gage 7 during the with plants run versus the without plants run.

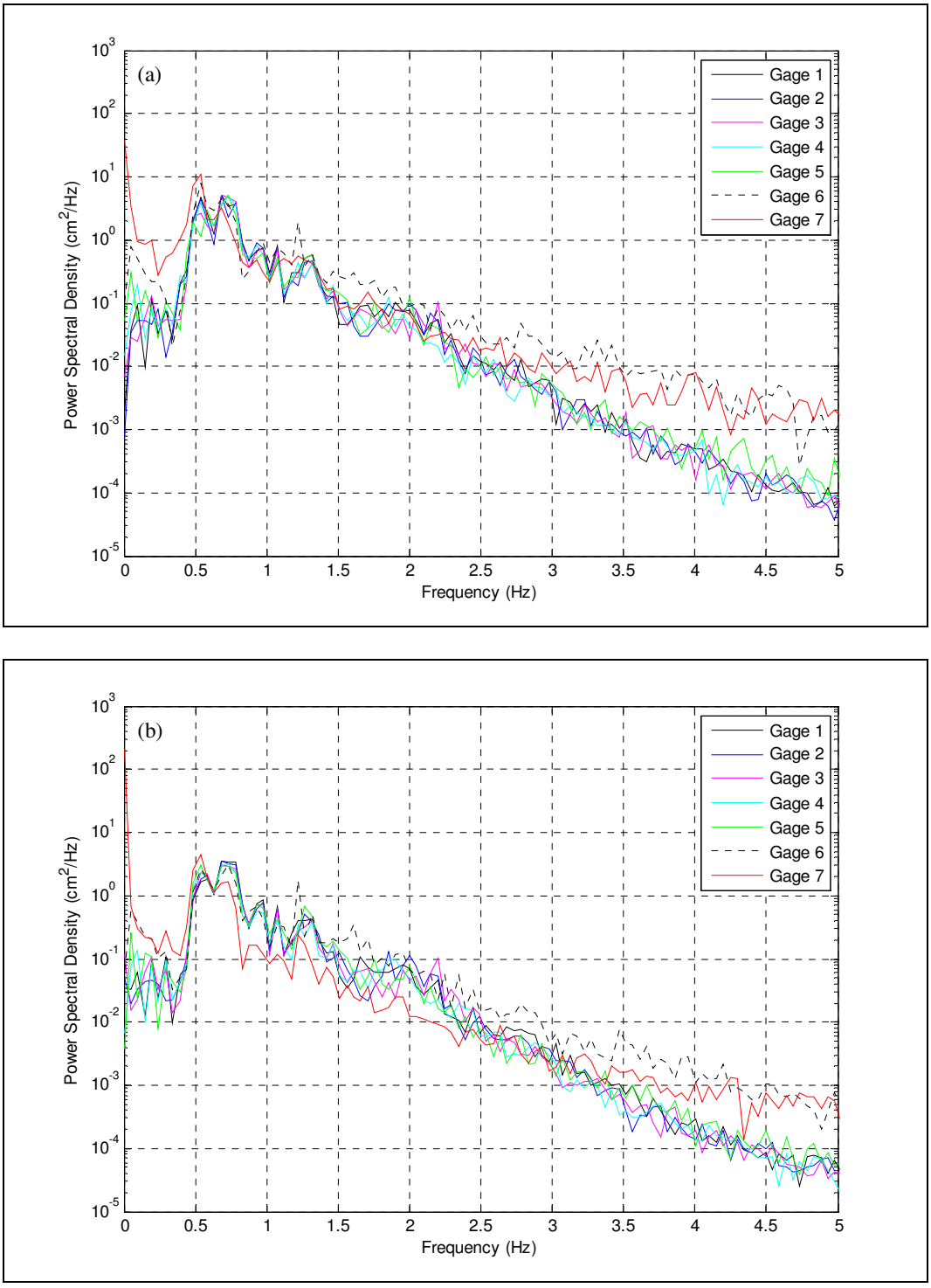

Figure 5.27 Case 4 Runs Power Spectral Density (a) Without Plants (b) With Plants

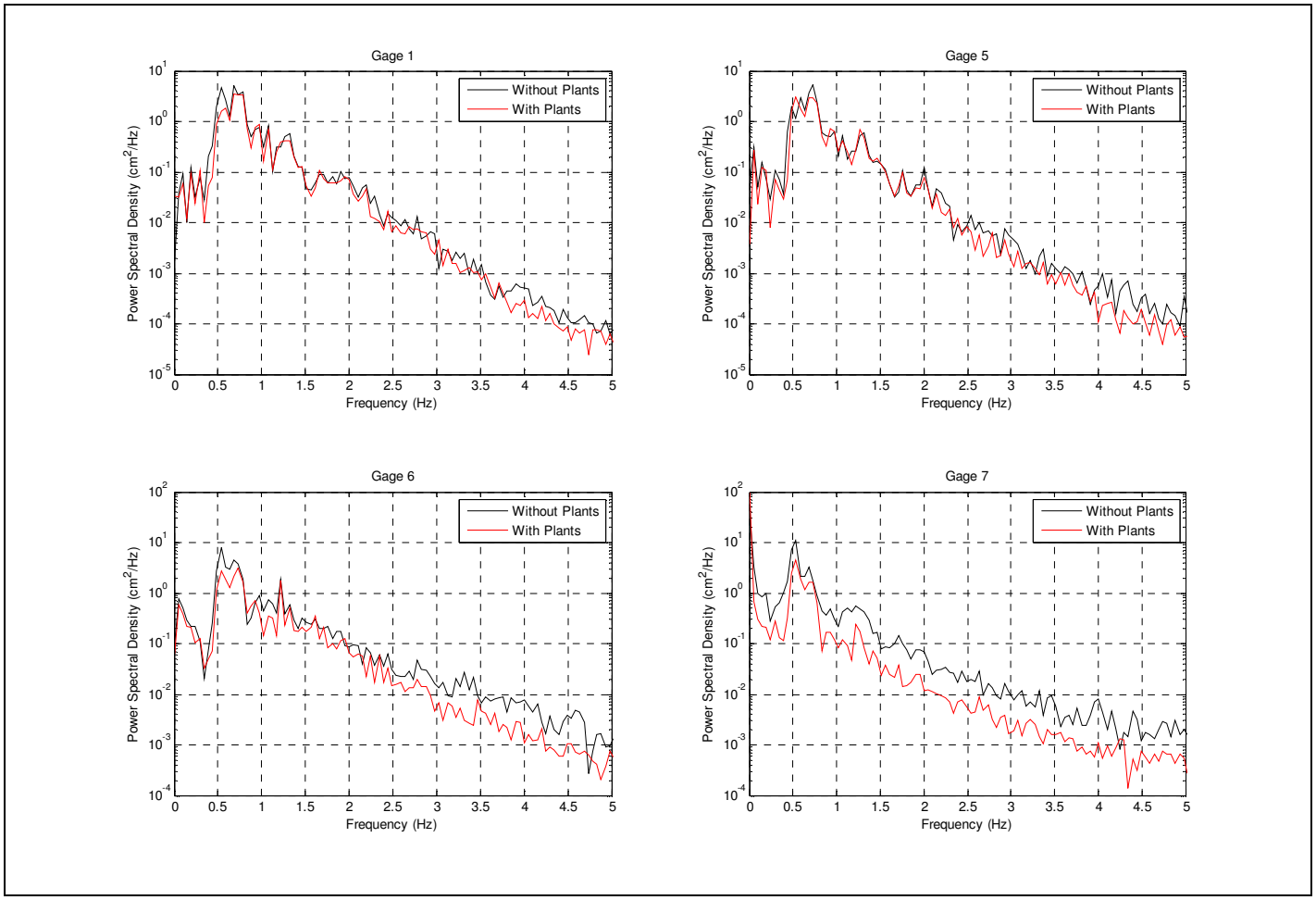

Figure 5.28 Case 4 Runs Power Spectral Density Comparisons

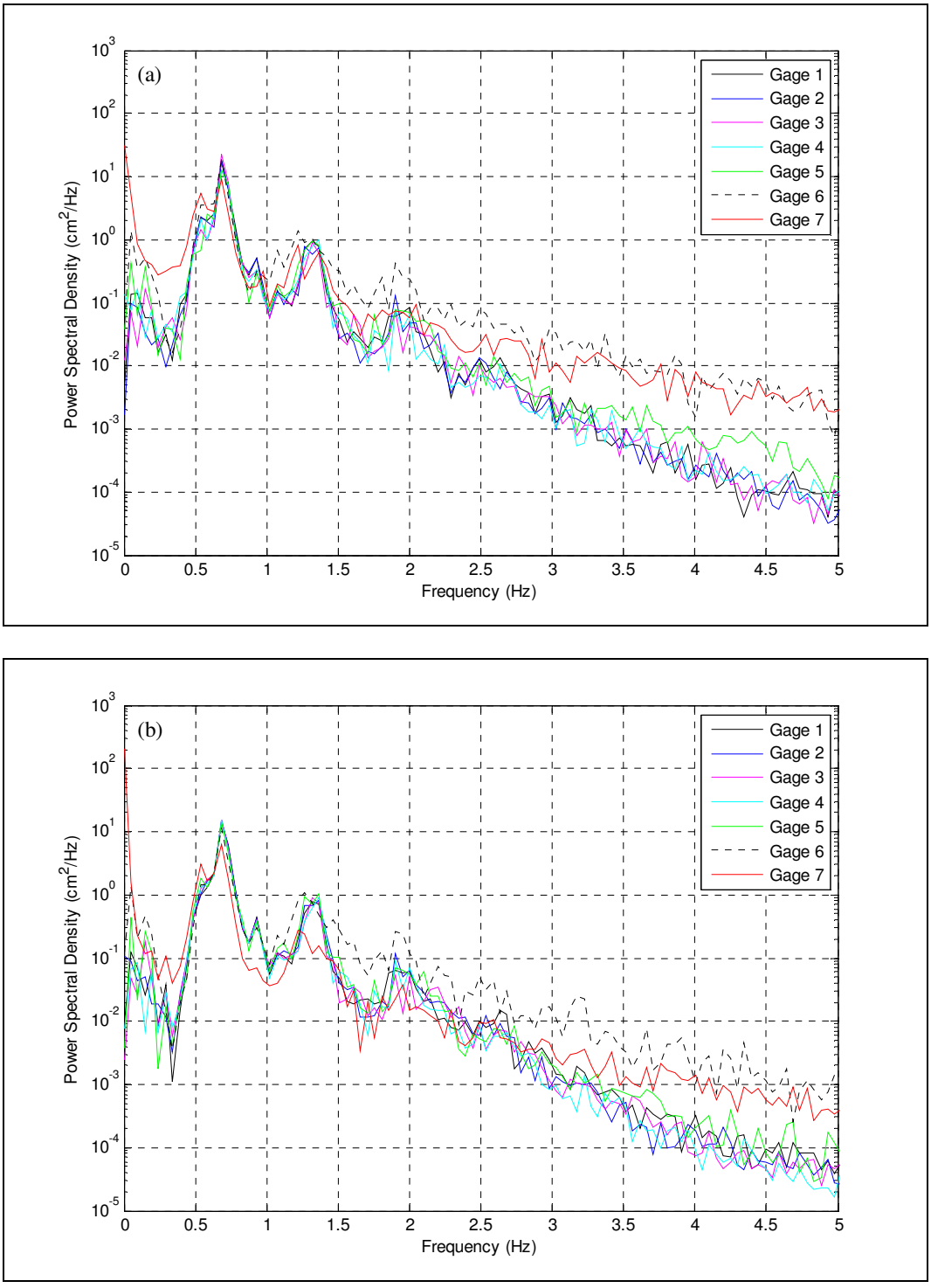

Figure 5.29 Case 5 Runs Power Spectral Density (a) Without Plants (b) With Plants

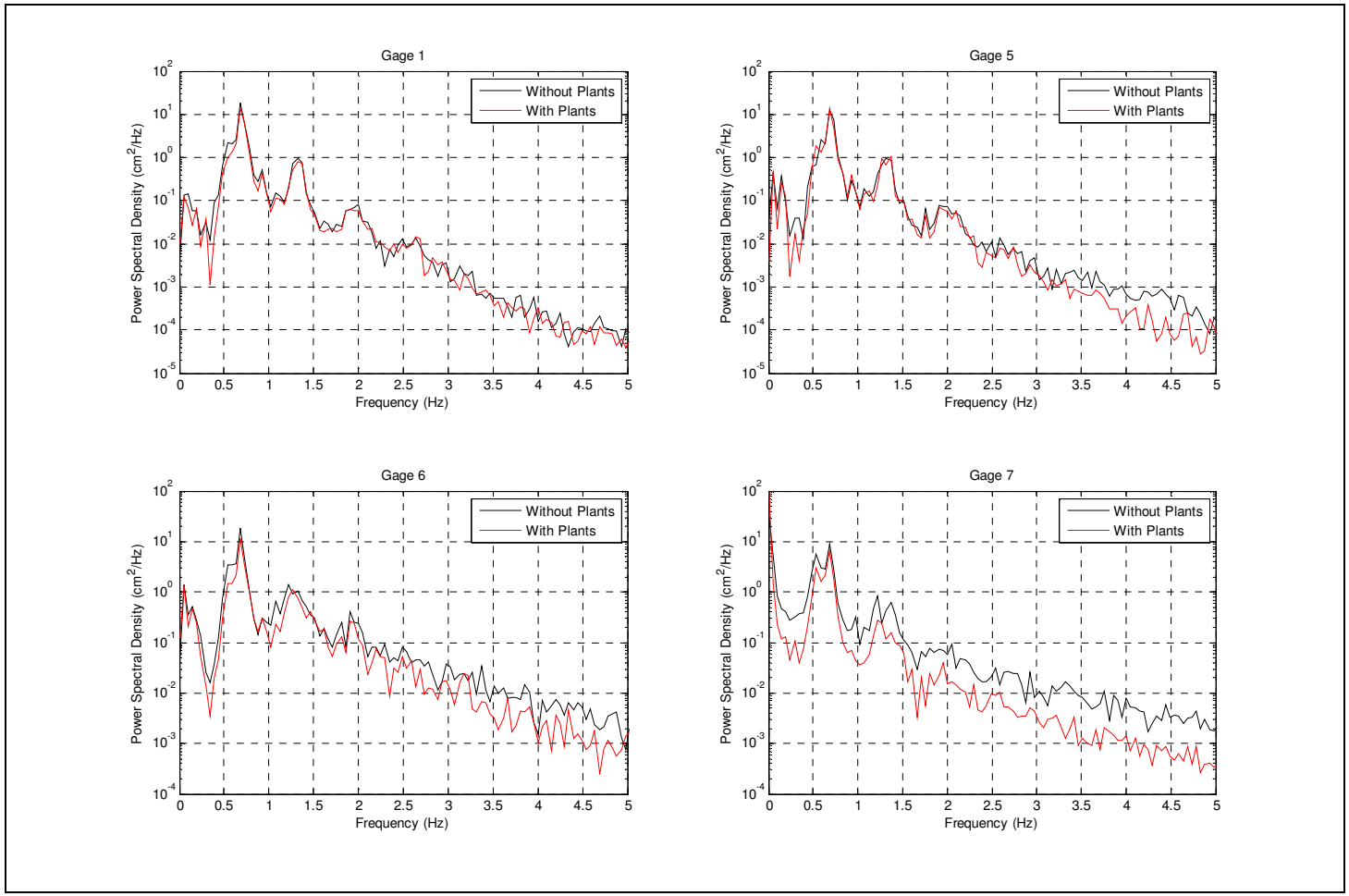

Figure 5.30 Case 5 Runs Power Spectral Density Comparisons

Case 6

The frequency transformation of each gage's output signal for both the without and with plants runs for case 6 (T_p = 2 s and γ = 3.3) produces a prominent peak at 0.5 Hz (Figure 5.31). The magnitude of this peak increases from approximately 10 cm^2/Hz between gages 1 and 6 to approximately 30 cm^2/Hz at gage 7 during the without plants run. To a lesser degree the with plants run shows a similar pattern (from approximately 2 cm^2/Hz between gages 1 and 6 to approximately 9 cm^2/Hz at gage 7). During the without plants run, gages 6 and 7 generally capture greater variance than gages 1 – 5 at frequencies greater than 3 Hz. Figure 5.32 indicates a consistently weaker variance at gages 6 and 7 occurred during the with plants run as compared to the without plants run.

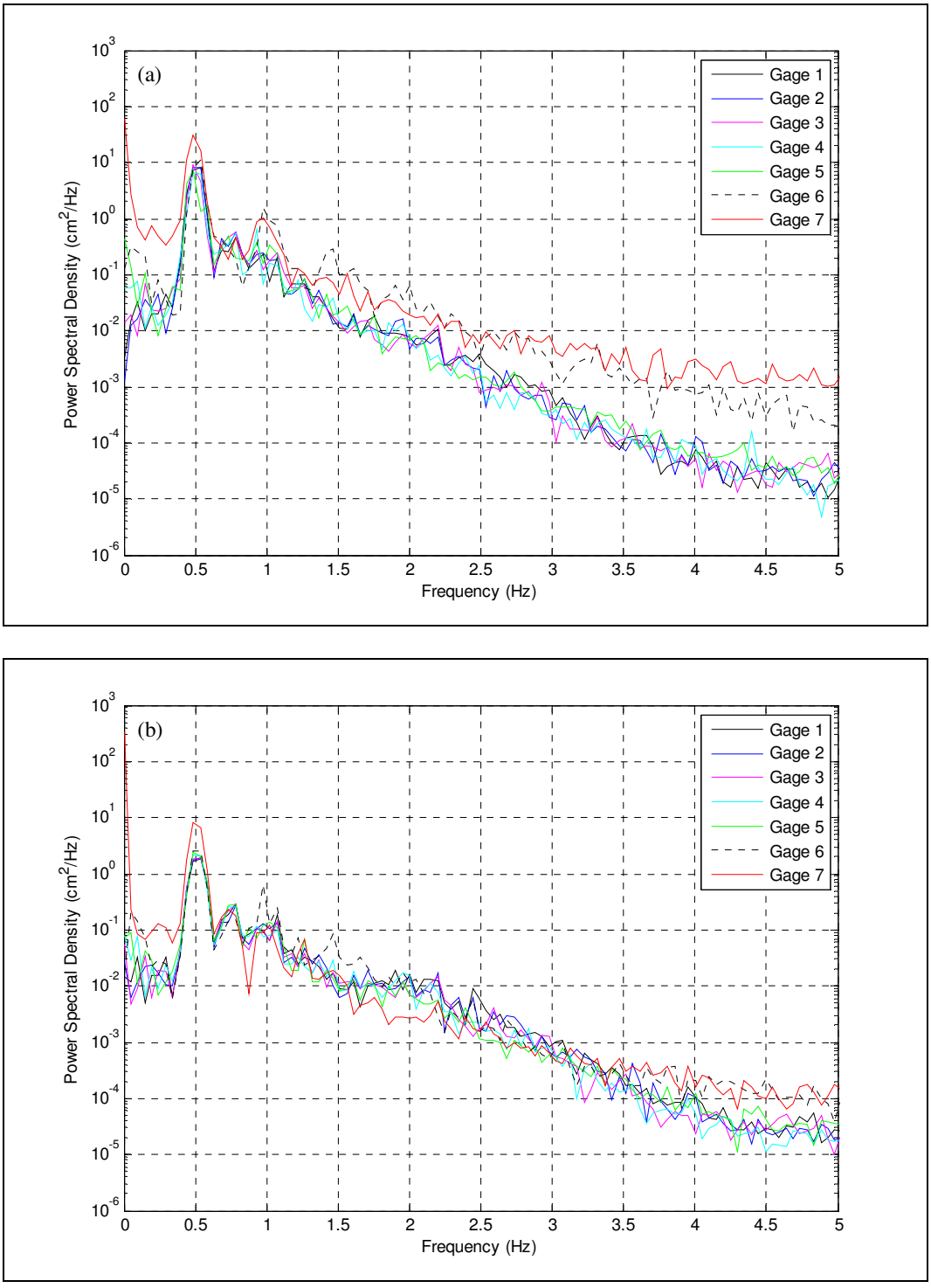

Figure 5.31 Case 6 Runs Power Spectral Density (a) Without Plants (b) With Plants

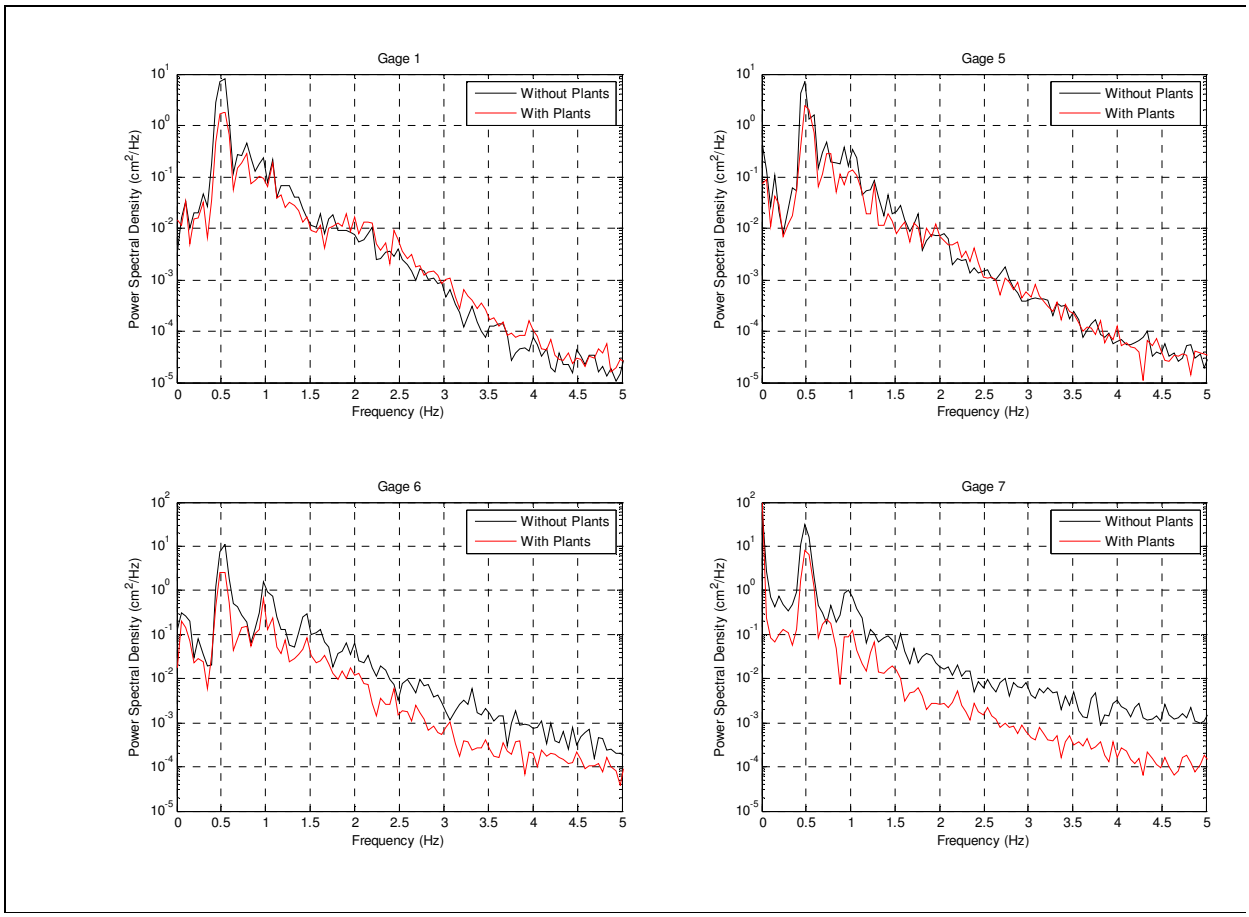

Figure 5.32 Case 6 Runs Power Spectral Density Comparisons

Chapter 6

CONCLUSIONS

6.1 Overview

Studies show wetland vegetation create lower energy environments by dampening wave energy. This study employed laboratory experiments to investigate the effect of a model eelgrass bed on wave runup. Time series analysis reveals insight into the behavior of the waveform as it shoaled up the ramp. Spectral analysis determines the distribution of wave energy over the frequency domain.

6.2 Regular Wave Cases

Case 1

Case 1 employed a regular wave train with a 1 s period. During both runs, at gage 1, the wave measured approximately 14 cm from crest to trough with an approximate 8 cm tall crest. The runup/rundown pattern generally retained the 1 s period but was quite muddled. The excursion remained between approximately 2.5 cm above and 3 cm below still water level during the without plants run and varied between approximately still water level and 2 cm below still water level with plants in the flume. Thus, the plants generally hindered runup above still water level. Notably, the plants oscillated with the passing waves but remained bent toward the wave maker.

The water surface elevation time series variance steadily decreased between gages 1 and 7. Transformation into the frequency domain also revealed a steady decrease in wave energy variance at the 1 Hz peak frequency as the waves approached the beach. Notably, the weakest variance occurred at gage 7 during both runs within the time and

frequency domains. Generally, a slight reduction in energy resulted at gage 7 during the with plants run as compared to the without plants run.

Case 2

Case 2 employed a regular wave train with a 1.5 s period. At gage 1, the wave height measured approximately 12 cm with a slightly taller crest than trough. The runup/rundown pattern generally retained the 1.5 s period. The excursion remained between approximately 3 cm above and 3 cm below still water level during the without plants run and varied between approximately 2 cm above and 2 cm below still water level with plants in the flume. Thus, the plants restricted the runup and rundown to within a more limited range. Notably, the plants oscillated with the oncoming waves becoming prone in both directions and the waves broke further offshore during the with plants run than during the without plants run.

The variance in water surface elevation increased and decreased between gages 1 and 5 without plants in the flume but steadily decreased between gages 1 and 7 during the with plants run. At the 0.67 Hz peak frequency, the power spectra generally match these patterns with the weakest variance occurring at gage 7 during both runs. Also, at this prominent peak, a slightly greater wave energy variance occurred at gage 7 during the with plants run as compared to the without plants run. Overall, a slight reduction in energy occurred at gage 7 with plants in the flume versus without.

Comparison of Regular Wave Cases

Water surface elevation time series and spectral analyses reveal similar patterns during both regular wave cases. During both cases, the plants hindered runup and

rundown to within a smaller range. The runup/rundown patterns also occurred slightly further offshore under the influence of the plants during both cases. The runup/rundown patterns generally retained the initial waveform period but the pattern was more regular during case 2 as compared to case 1.

Comparing each gage's energy spectrum reveals much narrower peaks during case 2 indicating a stronger periodicity as compared to case 1. A reduction in energy occurred at gage 7, as compared to gages 1 – 6, during both runs of each case with a greater reduction during both runs of case 1. Overall, during both runs, a weaker variance occurred at gage 7 with plants in the flume versus without.

6.3 Irregular Wave Cases

Case 3

Using the TMA spectrum Matlab program, case 3 incorporated a 1 s peak period and spectral width parameter of 3.3. Observation revealed minimal wave breaking occurred during both runs. The plants oscillated with the waves but remained positioned toward the wave maker. The mean water level remained slightly lower during the with plants run as compared to the without plants run (2.5 cm below still water level versus 1.6 cm below still water level). Notably, during both runs, the runup was generally proportional to and similar in extent to the wave height at gage 6.

The variance of the water surface elevation remained steady within the time and frequency domains between each of the gages during both runs. A wide peak centered about the 1 Hz peak frequency at each gage during both runs.

Case 4

Case 4 incorporated a 1.5 s peak period and gamma of 3.3. The plants oscillated with the passing waves becoming prone in both directions frequently. The mean water level remained slightly lower during the with plants run as compared to the without plants run (2 cm below still water level versus 0.7 cm below still water level). The runup/rundown pattern was generally smoother and within a smaller range under influence of the plants.

Without plants in the flume, the water surface elevation time series variance remained steady between gages 1 and 5 and increased at gages 6 and 7 while during the with plants run, the variance of each gage's time series remained steady. A prominent wide peak arises at 0.67 Hz within the frequency spectrum of each gage's output signal during both runs. Overall, the wave energy variance generally matches the time series variance with a slight increase at gages 6 and 7 during the without plants run. A general energy reduction at gage 6 and consistent reduction in energy at gage 7 occurred during the with plants run as compared to the without plants run.

Case 5

Case 5 incorporated a 1.5 s peak period and gamma of 30. Notably, a sharper breaking wave occurred without plants in the flume. The plants oscillated with the passing waves becoming prone in both directions frequently. The mean water level remained slightly further down the ramp during the with plants run as compared to the without plants run (2 cm below still water level versus 0.7 cm below still water level). Under the influence of the plants, the runup and rundown generally proceeded smoothly along the ramp while the rundown was returned more abruptly without plants in the flume.

The variance of each gage's output time series remained steady during both runs with exception of an increase at gages 6 and 7 during the without plants run. A prominent sharp peak at 0.67 Hz arises as well as the first harmonic with a smaller amplitude arise within the frequency spectrum of each gage's output signal. Overall, the time series and wave energy variances generally follow similar patterns, i.e. a slight increase at gages 6 and 7 during the with plants run. Wave energy variance remains generally less at gage 6 and consistently less at gage 7 during the with plants run versus the without plants run.

Case 6

Case 6 incorporated a 2 s peak period and gamma of 3.3. Notably, a plunging breaker occurred without plants in the flume while a smoother breaking occurred slightly further offshore under influence of the plants. The plants oscillated with the passing waves and became prone in both directions frequently. The mean water level remained slightly lower during the with plants run as compared to the without plants run (2.5 cm below still water level versus 1 cm below still water level). The runup and rundown generally proceeded smoothly along the ramp under influence of the plants. Without plants in the flume, a larger rundown was seen to return more abruptly up the ramp.

During the without plants run, the variance of each gage's output time series remained steady between gages 1 and 5 and increased at gages 6 and 7. A prominent sharp peak at 0.5 Hz arose within each gage's frequency spectrum with an apparent increase in variance at gages 6 and 7. These same patterns appear in the with plants run analyses but to a lesser degree. Wave energy variance is consistently weaker at gages 6 and 7 during the with plants run as compared to the without plants run.

Comparison of Irregular Wave Cases

Water surface elevation time series and spectral analyses reveal similar patterns between the irregular wave cases. Minimal wave breaking and steady water surface elevation and wave energy variances occurred during both runs of case 3 (T_p = 1 s and γ = 3.3). By increasing the peak period, for case 6 (T_p = 2 s and γ = 3.3), under influence of the plants, smoother breaking occurred slightly further offshore. Similar patterns in time series and wave energy variances occurred during both runs but to a lesser degree with plants in the flume. Unlike the two regular wave conditions, where the water surface elevation and wave energy variances steadily decreased, for case 6, the two variances increased at gages 6 and 7. Analysis of cases 4 and 5 (T_p = 1.5 s) reveal patterns which follow those of case 6 as opposed to those of case 3. In addition to a sharper peak at the prominent 0.67 Hz frequency, a peak at the first harmonic (1.33 Hz) appears with the larger spectral width (3.3 for case 4 and 30 for case 5).

References

Asano, T., Deguchi, H., and Kobayashi, N. (1992). Interaction between water waves and vegetation. *Proceedings of 23rd ICCE*, ASCE, 2710–2723.

Chesapeake Bay Program. (2000). "Chesapeake Bay Submerged Aquatic Vegetation Water Quality and Habitat-Based Requirements and Restoration Targets: A Second Technical Synthesis," Chesapeake Bay Program.

Dalrymple, R. A., Kirby, J. T., and Hwang, P. A. (1984). Wave Diffraction due to areas of energy dissipation. *Journal of Waterway, Port, Coastal, and Ocean Engineering*, **110** (1), 67–79.

Dean, R. G. (1978). "Effects of vegetation on shoreline erosional processes." Wetland Functions and Values: The State of Our Understanding, American Water Resources Association.

Denny, M. W., Gaylord, B. P., and Cowen, E. A. (1997). Flow and flexibility. II. The roles of size and shape in determining wave forces on the bull kelp Ne*reocystis luetkeana*. *Journal of Experimental Biology*, **200**, 3165–3183.

Dubi, A. and Torum, A. (1996). Wave energy dissipation in kelp vegetation. *Proceedings of 25th ICCE*, ASCE, 2626–2639.

Dubi, A. and Torum, A. (1994). Wave damping by kelp vegetation. *Proceedings of 24th ICCE*, ASCE, 142–156.

Elwany, M. H. S., O'Reilly, W. C., Guza, R. T., and Flick, R. E. (1995). Effects of southern California kelp beds on waves. *Journal of Waterway, Port, Coastal, and Ocean Engineering*, **121** (2), 143–150.

Fonseca, M. S., Fisher, J. S., Zieman, J. C., and Thayer, G. W. (1982). Influence of the seagrass, *Zostera marina L*., on current flow. *Estuarine, Coastal, and Shelf Science*, **15**, 351–364.

Fonseca, M, Kenworthy, W., and Thayer, G. (1998). "Guidelines for the Conservation and Restoration of Seagrasses in the United States and Adjacent Waters," NOAA, Silver Spring, MD.

Gambi, M. C., Nowell, A. R. M., and Jumars, P. A. (1990). Flume observations on flow dynamics in *Zostera marina* (eelgrass) beds. *Marine Ecology Progress Series*, **61**, 159–169.

Gaylord, B., Blanchette, C., and Denny, M. (1994). Mechanical consequences of size in wave-swept algae. *Ecological Monographs*, **64** (3), 287–313.

Gaylord, B. and Denny, M. W. (1997). Flow and flexibility. I. Effects of size, shape, and stiffness in determining wave forces on the stipitate kelps *Eisenia arborea* and *Pterygophora californica*. *Journal of Experimental Biology*, **200**, 3141–3164.

Ghisalberti, M. and Nepf, H. M. (2002). Mixing layers and coherent structures in vegetated aquatic flows. *Journal of Geophysical Research*, **107** (C2), 3-2–3-11.

Jackson, G. A. (1984). Internal wave attenuation by coastal kelp stands. *Journal of Physical Oceanography*, **14**, 1300–1306.

Kobayashi, N., Raichle, A., and Asano, T. (1993). Wave attenuation by vegetation. *Journal of Waterway, Port, Coastal, and Ocean Engineering*, **119** (1), 30–48.

Koch, E., Fonseca, M., Whifield, P., and Chiscano-Doyle, C. (2003). "Wave exposure or sediment characteristics: what is limiting the distribution of *Zostera marina* (eelgrass) in Chincoteague Bay, MD, USA?," UMCES, Cambridge, MD.

Kouwen, N. and Li, R. (1980). Biomechanics of vegetative channel linings. *Journal of the Hydraulics Division*, ASCE, **106** (HY6), 1085–1103.

Kouwen, N. and Unny, T. E. (1973). Flexible roughness in open channels. *Journal of the Hydraulics Division*, ASCE, **99** (HY5), 713–728.

Kouwen, N., Unny, T. E., and Hill, H. M. (1969). Flow retardance in vegetated channels. *Journal of the Irrigation and Drainage Division*, ASCE, **95** (IR2), 329–342.

Lovas, S. M. and Torum, A. (2000). Effect of submerged vegetation upon wave damping and run-up on beaches: A case study on *Laminaria Hyperborea*. *Proceedings of 27th ICCE*, ASCE, 851–864.

Nepf, H. M. (1999). Drag, turbulence, and diffusion in flow through emergent vegetation. *Water Resources Research*, **35** (2), 479–489.

Nepf, H. M. and Koch, E. W. (1999). Vertical secondary flows in submersed plant-like arrays. *Limnology and Oceanography*, **44** (4), 1072–1080.

Nepf, H. M. and Vivoni, E. R. (2000). Flow structure in depth-limited, vegetated flow. *Journal of Geophysical Research*, **105** (C12), 28,547–28,557.

Raupach, M. R. and Thom, A. S. (1981). Turbulence In and Above Plant Canopies. *Anuual Review of Fluid Mechanics*, **13**, 97–129.

Stewart, R., McFarland, D., Ward, D., Martin, S., and Barko, J. (1997). "Flume Study Investigation of the Direct Impacts of Navigation-Generated Waves on Submersed Aquatic Macrophytes in the Upper Mississippi River," ENV Report 1, USACE, Vicksburg, MS.

Wallace, S. and Cox, R. (2000). Effects of seagrass on nearshore current and wave dynamics. *Proceedings of 27th ICCE*, ASCE, 878–890.

Wallace, S., Luketina, D., and Cox, R. (1998). Large scale turbulence in seagrass cano-pies. *13th Australasian Fluid Mechanics Conference*, Melbourne, Australia.

Appendix A

FIELD VISIT PHOTOGRAPHS

Figure A1 Plan View of Flume at Gage 6 During Case 6 With Plants Run

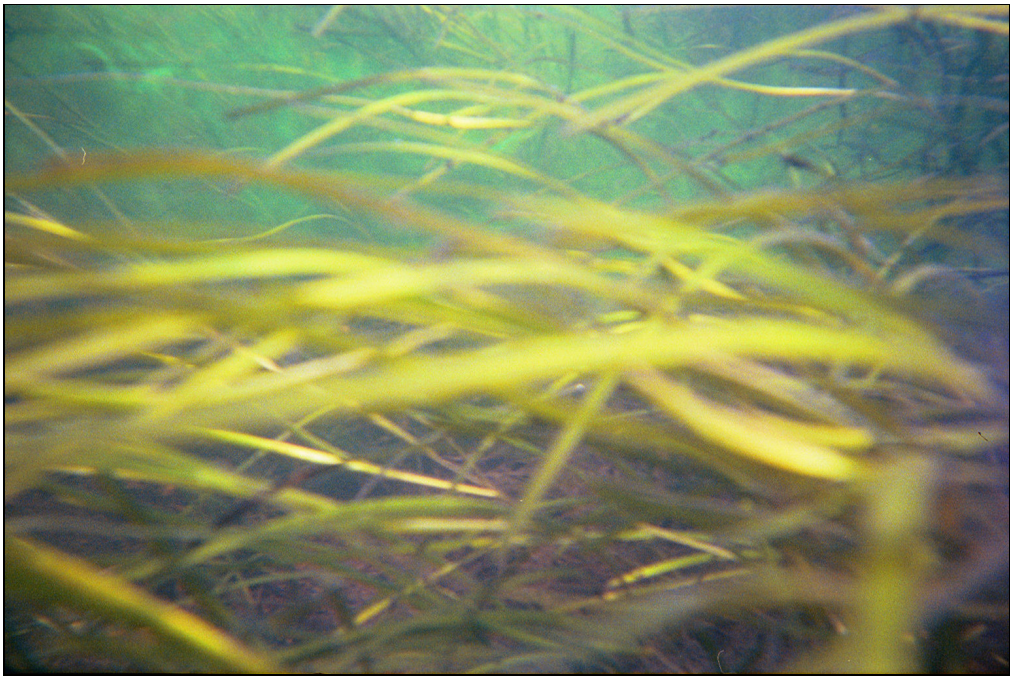

Figure A2 Plan View of Flume at Gage 6 During Case 6 With Plants Run

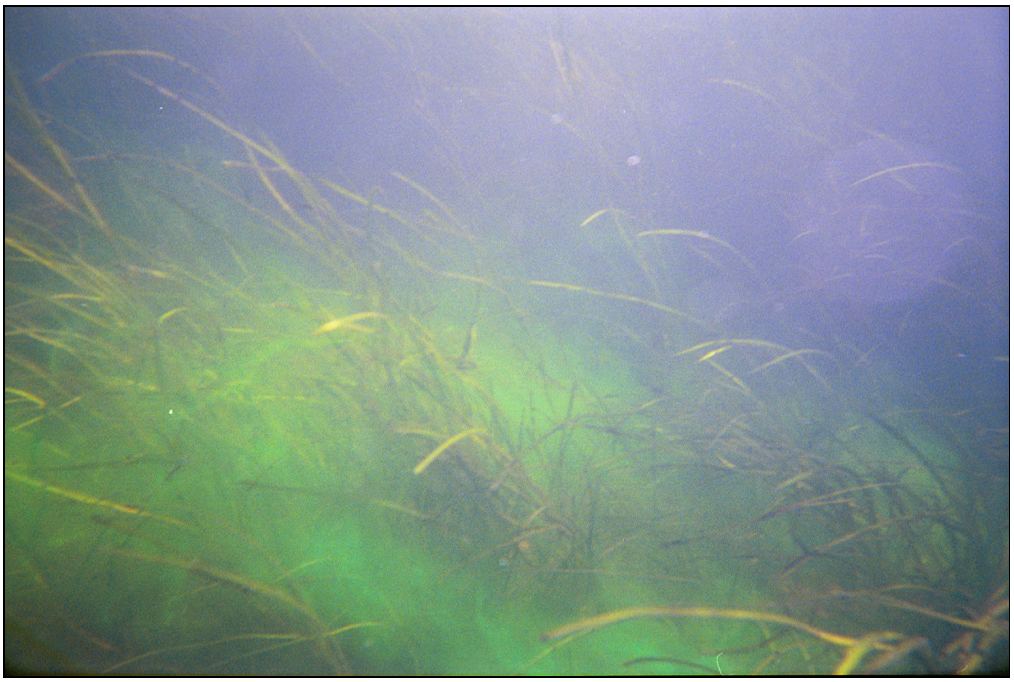

Figure A3 Plan View of Flume at Gage 6 During Case 6 With Plants Run

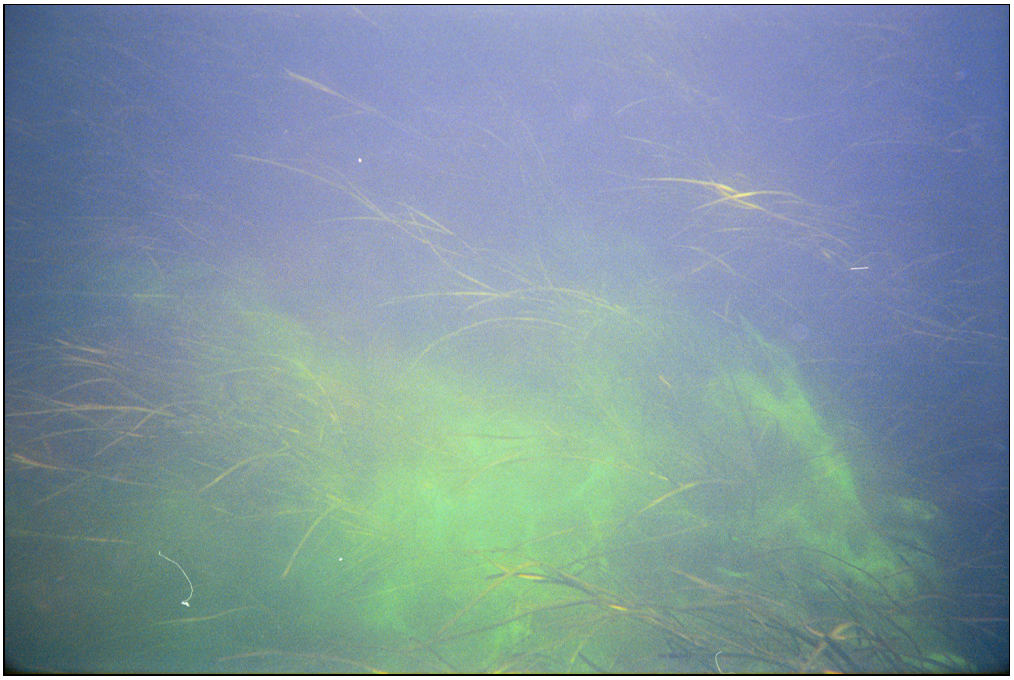

Figure A4 Plan View of Flume at Gage 6 During Case 6 With Plants Run

Appendix B

EXPERIMENT PHOTOGRAPHS

Figure B1 Picture of Gage Setup Facing Wave Maker from Above Ramp

Figure B2 Picture of Beach and Runup Wire Facing Wave Maker from Above Ramp

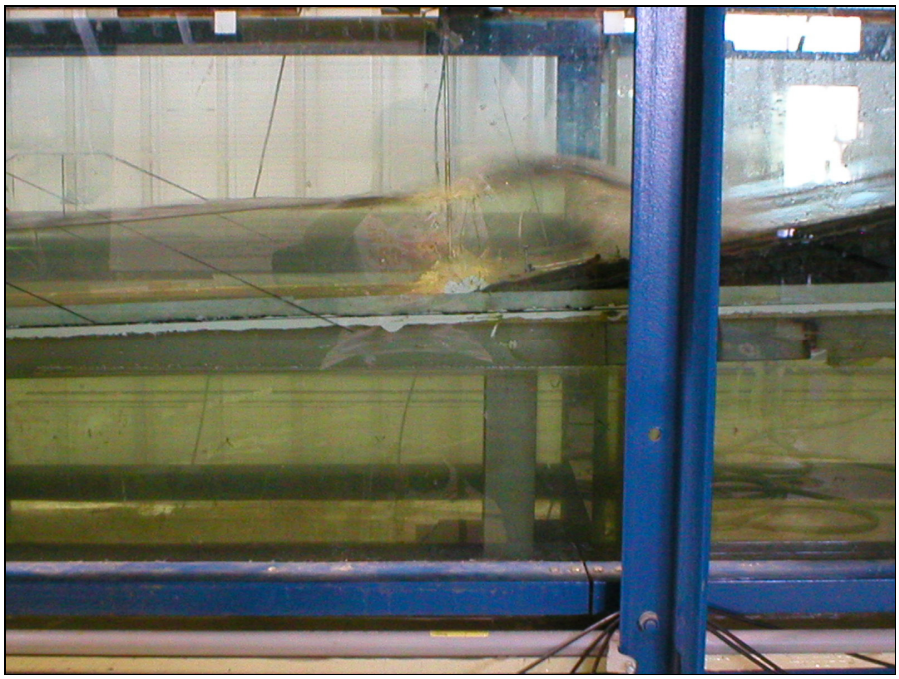

Figure B3 Plan View of Flume at Gage 6 During Case 3 Without Plants Run

Figure B4 Plan View of Flume at Gage 6 During Case 4 With Plants Run

Figure B5 Plan View of Flume at Gage 6 During Case 6 With Plants Run

THE EFFECT OF MODEL SEAGRASS ON WAVE RUNUP: A LABORATORY INVESTIGATION

BY

ALLISON BRIDGES AND JAMES T. KIRBY

RESEARCH REPORT NO. CACR-08-03
MAY 2008

CENTER FOR APPLIED COASTAL RESEARCH

Ocean Engineering Laboratory
University of Delaware
Newark, Delaware 19716

ACKNOWLEDGEMENT

This project was funded by the Delaware Sea Grant Program, Project Number SG2001-04 R/OE-30 and by the Delaware Department of Natural Resources and Environmental Control (DNREC) who purchased the cameras. Also, the Sea Colony Hotel, Bethany Beach, DE who allowing us to install cameras on their roof.

ACKNOWLEDGMENTS

I would like to thank the many individuals at the University of Delaware who helped me during this research, especially, my advisor, Dr. James Kirby, and Michael Davidson. I wish to acknowledge those with whom I consulted outside of the University, especially Ben Anderson, with the Delaware Department of Natural Resources and Environmental Control, and Mike Naylor, with the Maryland Department of Natural Resources. I also wish to extend my appreciation to Dr. Evamaria Koch, with the Horn Point Laboratory at the University of Maryland Center for Environmental Science, for including me in site visits to Chincoteague Bay.

TABLE OF CONTENTS

LIST OF FIGURES

LIST OF TABLES

ABSTRACT

The detrimental impacts of wave forces upon submerged aquatic vegetation (SAV) have been well researched while the effect of these plants on hydrodynamic forces more recently become more aggressively studied. A model eelgrass bed was employed to study the effect of SAV on wave runup along a ramp in a laboratory flume.

Two regular wave conditions revealed similar variance patterns in the time and frequency domains. Time series analysis revealed a steady decrease in water surface elevation variance with the smallest variance along the runup wire. Spectral analysis also showed a steadily decreasing wave energy variance as the waves approached the beach with the smallest variance at the runup wire. Both analyses revealed the ability of the model plants to hinder runup and rundown to within a smaller range than without plants in the flume. Additionally, a weaker variance occurred along the runup wire with plants in the flume versus without.

Four irregular wave cases revealed the influence of peak wave period and spectral width on water surface elevation in the time and frequency domains. With a peak period of 1 s, minimal wave breaking occurred and steady water surface elevation and wave energy variances developed. With a 2 s peak period, smoother breaking occurred slightly further offshore and rundown was restricted to within a smaller range under influence of the plants. Also, an increase in water surface elevation and wave energy variances resulted at and along the ramp. Similarly, cases with a 1.5 s peak period exhibited similar patterns to the 2 s peak period case. An increase in the spectral width parameter (3.3 to

30) revealed a sharper peak at the prominent peak frequency as well as an additional peak at the first harmonic.

Chapter 1

INTRODUCTION

1.1 Opening

A delicate balance exists between fluid dynamics and submerged aquatic vegetation (SAV). While the detrimental impacts of wave and current forces upon SAV have been well researched and documented, the significance of these plants to reduce current flow and dampen wave energy has more recently become an important field of study. By creating lower energy conditions, these plants help maintain a healthy productive environment. This is well regarded as a major benefit of these wetlands vegetation. The sustainability of SAV is largely due to their ability to adapt to hydrodynamic forces. In nature, large groups of plants wave in an organized manner with the direction of water particle velocity. While field studies provide insight, in order to develop a better understanding of the relationship between SAV and hydrodynamics, laboratory research provides a more controlled environment. The laboratory allows creation of specific conditions and isolation of individual parameters. The use of model plants, as opposed to live, creates a more regulated environment as long as the model plants accurately mimic their natural counterpart.

This study utilizes laboratory experiments to investigate the effects of model flexible SAV on wave runup under both regular and irregular wave conditions. Time series analysis provides insight into the behavior of the waveform while spectral analysis determines the distribution of wave energy over the frequency domain.

1.2 Outline

Chapter 2 discusses the motivation for this research and reviews results from previous studies. Chapter 3 discusses development of the model eelgrass bed while Chapter 4 outlines the preparation for the laboratory experiments. Chapter 5 presents time series and spectral analyses and Chapter 6 summarizes the findings. A list of references follows Chapter 5. Appendix A contains pictures taken during field investigations and Appendix B contains pictures taken during laboratory experiments.

Chapter 2

BACKGROUND

2.1 Wetlands and Seagrass

Wetlands have experienced tremendous losses due to human-induced changes in the coastal environment. In the United States, in the late 1960s, public awareness of the environmental benefits of wetlands began to increase. Areas once labeled “wasted” land soon became an important aspect of federal policy.

The National Environmental Protection Act of 1969 required an annual Environmental Quality Report denoting the status and condition of major natural environmental classes such as wetlands. A package of wetland reforms, Protecting America’s Wetlands: A Fair, Flexible, and Effective Approach, created on August 24, 1993, set the goal of “no net loss” of wetlands. Since initiation of the “no net loss” goal, wetland area has begun to stabilize.

With the onset of increasing public awareness and federal policy implementation, the general function and resource value of wetlands became more extensively researched and documented. Research shows wetlands preserve biodiversity by providing habitat to an assortment of species, provide erosion and flood control, stabilize flow, recharge underground aquifers, and filter water, i.e. denitrification.

Within the unique wetland environment are specialized aquatic vegetation adapted for growing within the hydric soil of this inundated or saturated environment. Studies have concluded submerged aquatic vegetation sustainability is extremely sensitive

to light availability, water clarity, hydrodynamic forcings, boat traffic, and mechanical harvesting impacts (Stewart et al., 1997; Fonseca et al., 1998; Chesapeake Bay Program, 2000; Koch et al., 2003).

Studies also provide evidence of a feedback mechanism between SAV sustainability and hydrodynamics. An example cycle begins with a dense SAV bed. The dense bed decreases current velocity, dampens wave energy, and allows sediment deposition. This creates an environment more conducive to plant reproduction. Due to the increased density of the bed, and resulting decrease in current velocity and wave energy, the inundation of organic matter reaches a point that the high phytotoxin levels cause the plants to die back. As the bed density becomes reduced, current velocity and wave energy increase. This increased flow reduces the organic matter and phytotoxins. Eventually, the plants are able to begin to reproduce again, due to increased light availability, and establish a dense bed.

Due to human interference, factors that inhibit the ability of SAV to thrive have become more abundant which decreases the ability of SAV to recover. Notably, SAV beds are depleted quickly but recovery is a very slow process (Fonseca et al., 1998). The loss of seagrass has extreme detrimental biological and environmental implications. Seagrasses supply food, shelter, and protection to an assortment of aquatic organisms to create an excellent breeding ground, incubation area, and nursery or permanent residence. At the same time, SAV acts as a sediment trap with its extensive root and rhizome system and baffles current and wave energy with its canopy of stems and shoots (Fonseca et al., 1998). An SAV bed can reduce current velocity, attenuate waves, and change the height of the water column. Researchers have noted currents in SAV beds to be 2 – 10 times slower than in adjacent unvegetated areas (Chesapeake Bay Program, 2000).

2.2 Past Studies

Different techniques have been implemented to better understand the dynamic relationship between fluid dynamics and flexible vegetation. A value of Manning's n, a function of U X R, where U is the average flow velocity and R is the hydraulic radius, has been roughly determined for a variety of vegetative channel linings through both field and laboratory tests. Kouwen et al. (1969) improved upon the friction factor n by introduction of a relative roughness parameter y/k, where y is the water depth and k is the deflected height of the vegetation. This deflected height refers to the location of the roughness tips from the bed during the majority of time. The resulting formula describing flow retardance in vegetated channels

$$\frac{U}{u_*} = C_1 + C_2 \ln\left(\frac{y}{k}\right) \tag{2.1}$$

incorporates vegetation characteristics, where C_1 is a function of vegetation bed density and C_2 is a function of individual vegetation stiffness. Kouwen and Unny (1973) expanded upon these results by showing flexible plastic roughness elements behave hydraulically similar to the natural vegetation they model. Kouwen and Li (1980) examined the deflected roughness height between erect, waving, and prone motions.

As flow velocity increases, the vertical plants bend and become more streamlined. The area perpendicular to the flow (projected area) decreases which results in a decrease in drag. Similarly, as a wave passes over the vertical plants, the plants bend in the direction of the horizontal particle velocity. Gaylord et al. (1984) determined the optimal size of flexible plants, such as seagrass, is limited by mechanical factors, such as drag, not biological factors alone, such as sunlight availability. Denny et al. (1997) suggest the ability

of flexible vegetation, such as seagrass, to reorient itself with the flow may benefit larger plants but be detrimental to smaller plants. Reorientation, most effective for plants longer than the diameter of the wave-driven water orbit, allows the plant to bend slightly but not to a degree severe enough to cause breakage before the water motion reverses (Gaylord and Denny, 1997).

A major complication encountered in modeling flexible roughness elements is incorporation of a damping coefficient due to this ability to reorient with the flow. Dalrymple et al. (1984) modeled a cluster of rigid vertical cylinders as a region of localized energy dissipation with drag constant over depth. They found a shadow region of wave damping developed onshore of the cylinders in the direction of the oblique wave. Gaylord and Denny (1997) and Denny et al. (1997) investigated a simple numerical model based on vertically oriented cantilever beams. The model incorporated forces, including drag, virtual buoyancy, and a restoring force, on a point mass at the end of a kelp stipe, however, it lacked a vertically directed force balance.

Kobayashi et al. (1993) developed an analytical solution to the vertically two-dimensional problem of waves propagating over submerged vegetation by introducing a damping coefficient. This calibrated drag coefficient varied greatly for the different wave cases of the artificial seaweed experiment (Asano et al., 1988). Asano et al. (1992) incorporated the swaying motion of the flexible element, including the vegetation size and proximity of surrounding elements, into the constant drag model. By including the plant motion, the drag coefficient value was found to be approximately 0.5. This value proves much better agreement to the experimental data than the 0.1 value determined by Kobayashi et al. (1993).

Wang and Torum (1994) developed a theoretical model based on limited experimental data. They found the damping coefficient increased with increasing wave period until reaching an asymptotic value based on plant density. Dubi and Torum (1996) expanded this study by using both theoretical and experimental means to determine the damping rate. They found the drag coefficient increased as the wave period increased for short period waves, reached a maximum, and then decreased gradually with longer period waves. They also determined the damping coefficient was governed by water depth and plant population density. Field and laboratory studies reveal a positive correlation between wave attenuation by flexible vegetation and the percentage of water column the plants occupy (Chesapeake Bay Program, 2000).

Dean (1978) found the dense root system of aquatic vegetation creates strong durable plants. Since these plants decrease bottom shear stress, deposition of sediment rather than erosion may result. Also, these plants have the ability to decrease wave energy, or wave height, and, ultimately, wave steepness. By changing breaking wave conditions, accretional rather than erosional conditions may develop along the shoreline. Lovas and Torum (2000) show, similar to live vegetation, model kelp reduces wave breaking as an effect of wave damping. Notably, wave attenuation begins in deeper water and less runup occurs on the beach when the kelp is present.

Chapter 3

MODEL DEVELOPMENT

3.1 Field Visits

To develop a better understanding of the plants and environment I intended to model, I joined Dr. Evamaria Koch and associates to Chincoteague Bay. We visited Wildcat Marsh in southeastern Chincoteague Bay and Mills and Tizzard Islands along southwestern Chincoteague Bay. Figure 3.1, taken from Google Maps, shows these areas.

The Chincoteague Bay is a coastal barrier island or lagoon system located at the southeastern edge of the Delmarva Peninsula near the mouth of the Chesapeake Bay. Wave exposure in the Chincoteague Bay is relatively low as compared to the rest of the Chesapeake Bay. However, Koch et al. (2003) points out, within Chincoteague Bay, extensive dense eelgrass beds thrive on the eastern shore while sparse, isolated beds are present on the western side.

According to the Maryland Department of Natural Resources (DNR), of the bay grass species found in the high-salinity areas of Chesapeake Bay, eelgrass, *Zostera marina*, is one of the most abundant and persistent. Figure 3.2 shows a picture of an eelgrass plant from the DNR website. An eelgrass plant consists of a single shoot arising from a rhizome node. The underground creeping rhizome, and roots which grow from its nodes, bind the sediment and stabilize the shoot. A tubular sheath surrounds 3 – 5 ribbon-like leaves which sprout from this single shoot. New leaves sprout in an alternating pattern as the shoot grows for protection.

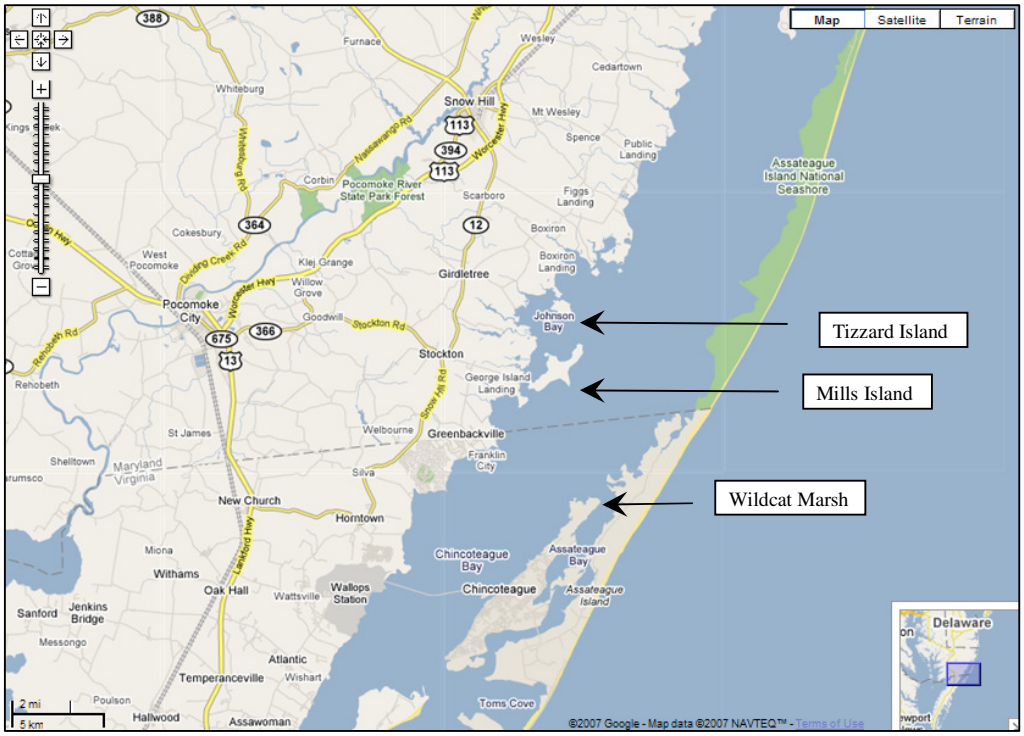

Figure 3.1 Map of Chincoteague Bay Area

Figure 3.2 Picture of Natural Eelgrass Plant

Initial observation of an eelgrass bed revealed organized oscillatory swaying of the plants with wave interaction. Closer inspection revealed the flexibility of each individual plant to become prone in both directions. Basic fluorocene dye tests performed within these beds showed the effect of the plant waving on the flow. When released near the bottom, the dye moved back and forth with the plant swaying but remained concentrated near the bottom. The dye dispersed very slowly toward the surface and horizontally. Dye released within a sparsely populated area within the bed also remained near the bottom but quicker vertical dispersion occurred here than within a more densely populated portion of the bed. Appendix A contains pictures taken during these field investigations.

3.2 Model Eelgrass Bed

During these visits I collected samples of *Zostera marina* from multiple sites. Attempts to measure flexural properties of live eelgrass by machine failed due to the sensitivity of the plant membrane and the inability to retain water within the plant during measurement. Based on field observation and basic flexural rigidity tests, I decided to model an eelgrass plant with Mylar strips.

A model eelgrass plant consisted of a 7.5 cm tall basal stem with 4 – 7 mm wide 0.1016 mm thick blades (Figure 3.3). The length of the blades were, in order facing the oncoming waves – 21.5 cm, 16.5 cm, 18.5 cm, and 29.5 cm. Individual model plants were glued into 0.5 cm deep holes drilled in 2 cm thick 2.5 m X 58 cm Plexiglas sheets. The silicone glue attachment allowed the plants movement as in natural substrate. The canopy consisted of a regular matrix configuration to reduce shelter effects by surrounding plants. The matrix was comprised of alternating rows of 18 and 19 plants with 1.4 cm spacing (twice the blade width) between the plants and rows. The Plexiglas sheet was attached to the sidewalls and bottom of the ramp with silicone and water-resistant tape (Figure 3.4).

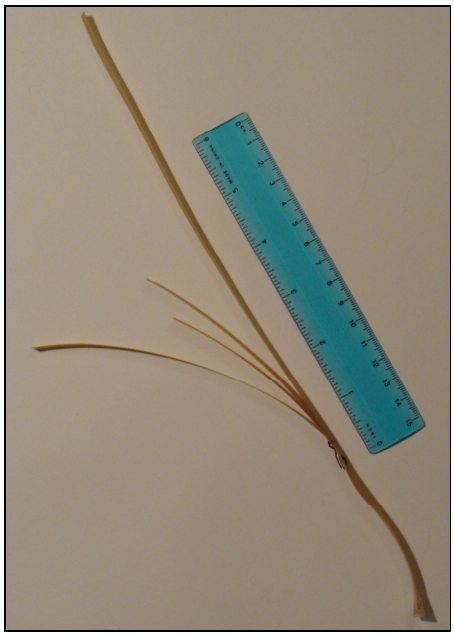

Figure 3.3 Picture of Model Eelgrass Plant

Figure 3.4 Picture of Model Eelgrass Bed in Flume Facing Wave Maker

Chapter 4

LABORATORY EXPERIMENTS

4.1 Experimental Setup

4.1.1 Flume Preparation

Laboratory experiments were conducted at the Center for Applied Coastal Research at the University of Delaware. The facility houses a 30 m long, 0.6 m wide, and 1.0 m deep two-dimensional wave flume. The hydraulically-driven piston-type wave maker generated waves for the experimental cases. Within the limitations of paddle motion, the wave maker has the capability to create both regular and irregular waves. A user-defined input voltage signal time series determines the rate and magnitude of paddle displacement. Since the correlation between paddle displacement and resulting wave height was not determined prior to the experiments, direct observation served as verification of resulting wave parameters. Notably, the wave maker does not have the ability to absorb reflected waves.

Beginning 9.1 m from the wave maker paddle neutral position, a series of bottom slopes was installed to produce depth-limited breaking waves (Figure 4.1). The first ramp, with an initial slope of 1:15, extended between 9.1 m and 10.4 m from the wave maker paddle neutral position. The second ramp, with a 1:35 slope, extended 10.7 m from the first ramp. The third ramp, serving as the beach, extended 1.2 m from the second ramp with a slope of 1:5.

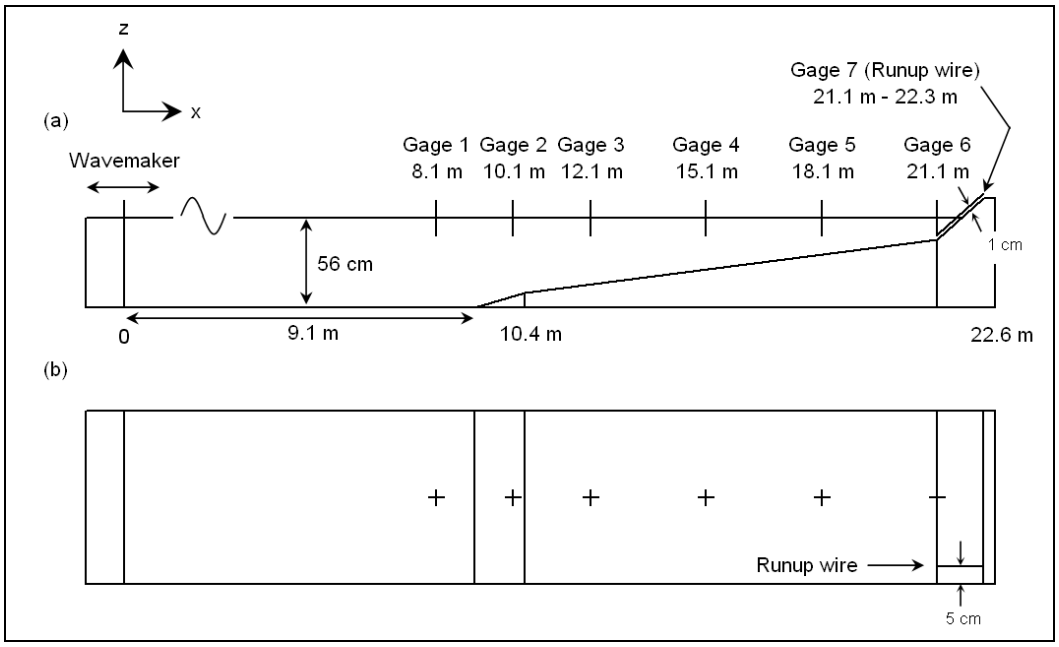

Figure 4.1 Flume Setup (a) Plan View (b) View From Above

4.1.2 Waves

Regular wave trial runs were conducted to determine an approximate relationship between input voltage magnitude and resulting wave height. Input of these sinusoidal voltage time series helped determine the time necessary to obtain a steady regular wave condition. Comparisons of regular wave patterns up to 60 minutes indicated steady regular wave motion developed after 10 minutes.

An irregular wave voltage time series was created based on a Texel, Marsen, Arsloe (TMA) spectrum. The spectrum was produced via a Matlab program dependent on user inputs of significant wave height, peak frequency, and the spectral width parameter (γ). While these parameters determine the shape of the energy spectrum, wave height and period magnitudes are not established a priori. An infinite number of voltage time series can be produced based on the same criteria.

4.1.3 Data Acquisition Equipment

The following laboratory experiments incorporated a total of 7 capacitance gages with a sampling frequency of 50 Hz. Figure 4.1 outlines the experimental layout of the flume. Six capacitance gages were placed along the center of the flume to measure the water surface fluctuation over time. Gages 1 through 6 were placed 8.1 m, 10.1 m, 12.1 m, 15.1 m, 18.1 m, and 21.1 m from the wave maker paddle neutral position. These gages were aligned manually to face directly into the oncoming waves. The calibration procedure accounted for any alignment inaccuracy. A seventh capacitance gage stretched from the top of the 2nd ramp to the top of the beach (3rd ramp) to record runup along the beach. This gage was installed 5 cm from the flume sidewall, parallel to the bottom. The gage was strategically placed 1 cm from the bottom to record the maximum runup without encountering viscous effects. An intricate calibration procedure ensured accurate results.

The capacitance gage calibration procedure consisted of obtaining a voltage reading while varying the water depth in the flume in 1 cm increments. The calibration procedure began with the still water level positioned in the middle of the runup wire (56 cm from the horizontal bottom of the flume). The six gages were adjusted vertically so the water level was positioned in the center of the gage wires and the voltage of each of the seven gages was zeroed. A voltage reading was recorded at each 1 cm interval as the water depth was increased from 56 cm to 68 cm (upper limit of the runup wire), decreased to 46 cm (lower limit of the runup wire), and returned to 56 cm.

For the 6 capacitance gages along the center of the flume, the calibration procedure ultimately produces a calibration coefficient relating the linear relationship between the water surface elevation and gage voltage. A 3rd order regression curve fit to

the runup wire (gage 7) calibration data related water surface elevation and voltage for this gage.

4.2 Experimental Procedure

After determining accurate operation of the wave maker and gages, trial runs determined acceptable regular and irregular wave parameters. The resulting waves needed to capture the majority of the runup wire but not overtop the beach. Table 4.1 outlines the parameters of each experimental case. Note, the spectral width parameter is represented by γ. In order to densely populate the frequency spectra, the length of record corresponding to each case captured 800 waves.

For each case, the wave maker received the same input voltage time series for the without and with plants runs. Prior to each run, the gages recorded the still water level (56 cm depth) for 30 s. The average value was removed from the gage output prior to processing. Data acquisition for the regular wave conditions began 10 minutes after initiation of the waves. Figure 4.2 shows the TMA spectrum corresponding to each irregular wave case and Figure 4.3 shows the input voltage signal time series for each of these cases. Appendix B contains pictures taken during these laboratory experiments.

Table 4.1 Experimental Cases

Experimental Runs		T_p (s)	H_s (cm)	γ
Regular Wave Cases	**Case 1**	1	-	-
	Case 2	1.5	-	-
Irregular Wave Cases	**Case 3**	1	6	3.3
	Case 4	1.5	6	3.3
	Case 5	1.5	6	30
	Case 6	2	3	3.3

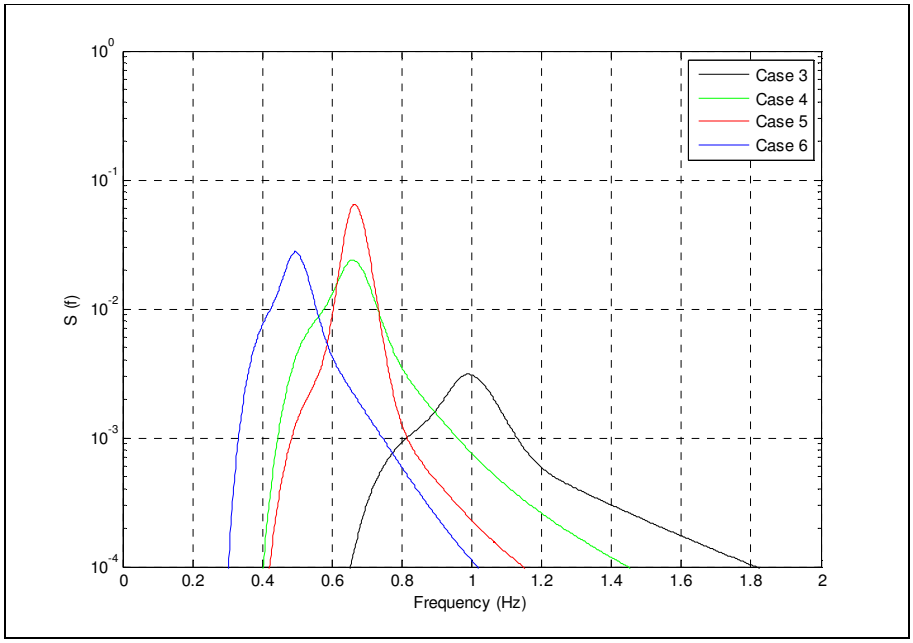

Figure 4.2 TMA Spectra for Irregular Wave Cases

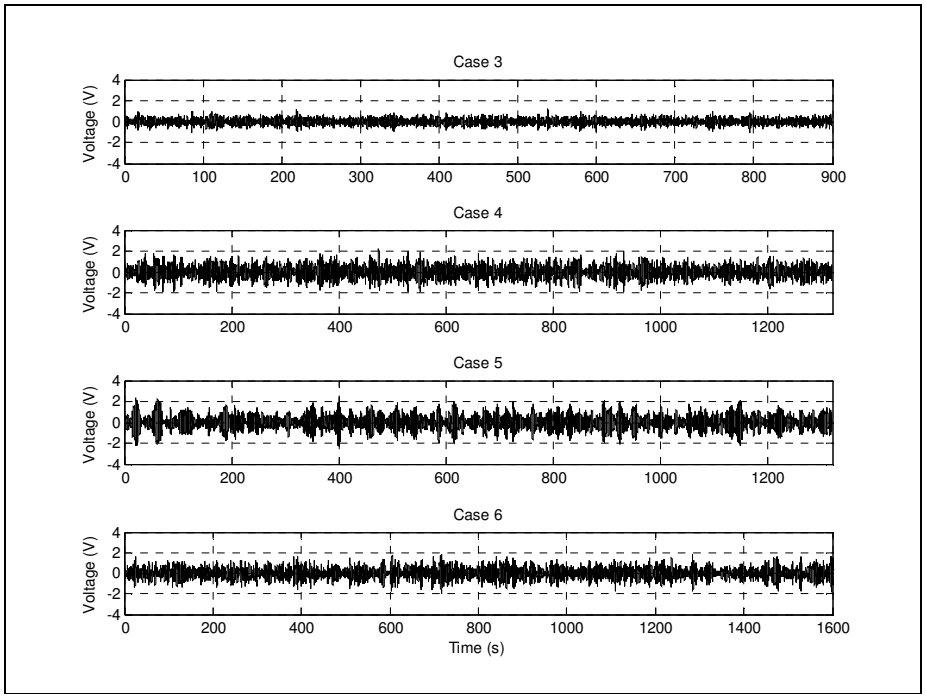

Figure 4.3 Time Series of Irregular Wave Cases

Chapter 5

DATA ANALYSIS

5.1 Time Series Analysis

Analysis of multiple segments of gage output (water surface elevation) revealed general trends in wave height and period during each run. Included are sections of water surface elevation time series indicative of the findings. The mean water level at each gage reveals the accumulation of water at that location while the variance and skewness of each gage's output signal provides insight into the behavior of the waveform during its shoaling process. For a simple regular linearly shoaling wave, it is expected that the variance of the water surface elevation decreases slightly as the wave approaches breaking while the skewness of the signal increases toward and then decreases following breaking.

5.1.1 Regular Wave Cases

Case 1

As seen from the time series figures (Figures 5.1 – 5.3), the waveform proceeded with similar dimensions in the without and with plants runs of case 1 (T_p = 1 s), until gage 7. The 1 s period was retained throughout both runs. At gage 1, the wave measured approximately 14 cm from peak to trough with a slightly taller crest than trough. The waveform became steeper as it shoaled up ramps 1 and 2 and began spilling near gage 5. Notably, the plants oscillated with the passing waves but remained bent toward the oncoming waves. Analysis of the water surface elevation time series at each gage reveals a steadily decreasing signal variance and a signal skewness that peaked at gage 4 (Table 5.1 and Figure 5.4).

The runup/rundown patterns during both runs retain the 1 s period but are quite muddled. The runup typically proceeded up the ramp slowly but was abruptly returned up the ramp during rundown. For the without plants run, the increasing mean water level at gages 6 and 7 indicates an accumulation of water landward of the breaking wave. Without influence of the plants, after breaking, the wave excursion varied between approximately 2.5 cm above and 3 cm below still water level along the runup wire (Table 5.1 and Figure 5.3). For the with plants run, the slightly negative mean water level at gage 7 indicates the runup generally remained below still water level (between approximately still water and 2 cm below still water level). As evidenced by Figure 5.3, the plants generally hindered runup above still water level.

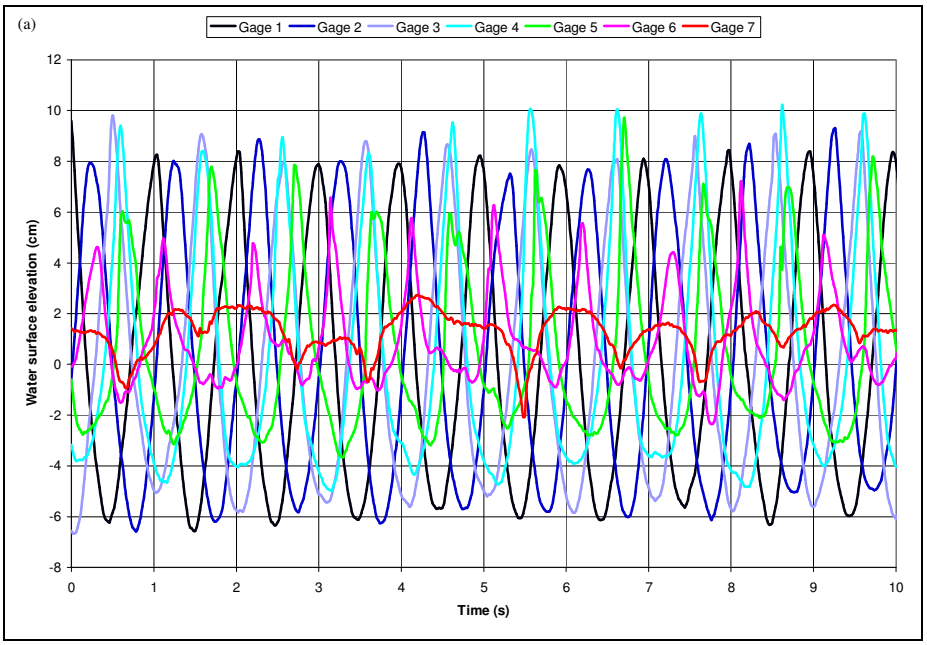

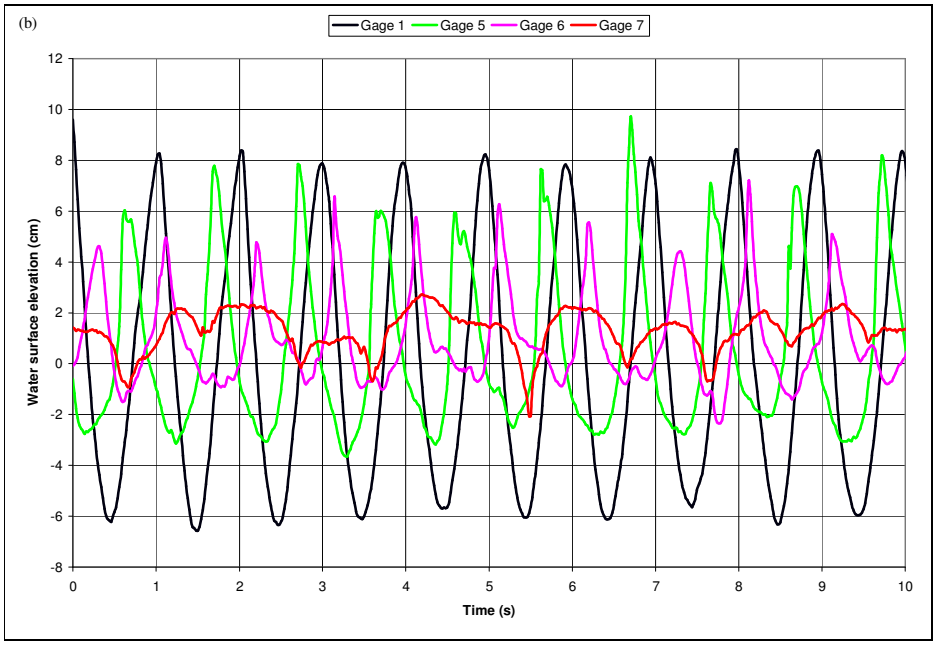

Figure 5.1 Case 1 Without Plants Run Water Surface Elevation Time Series (a) All gages (b) Gages 1, 5, 6, and 7

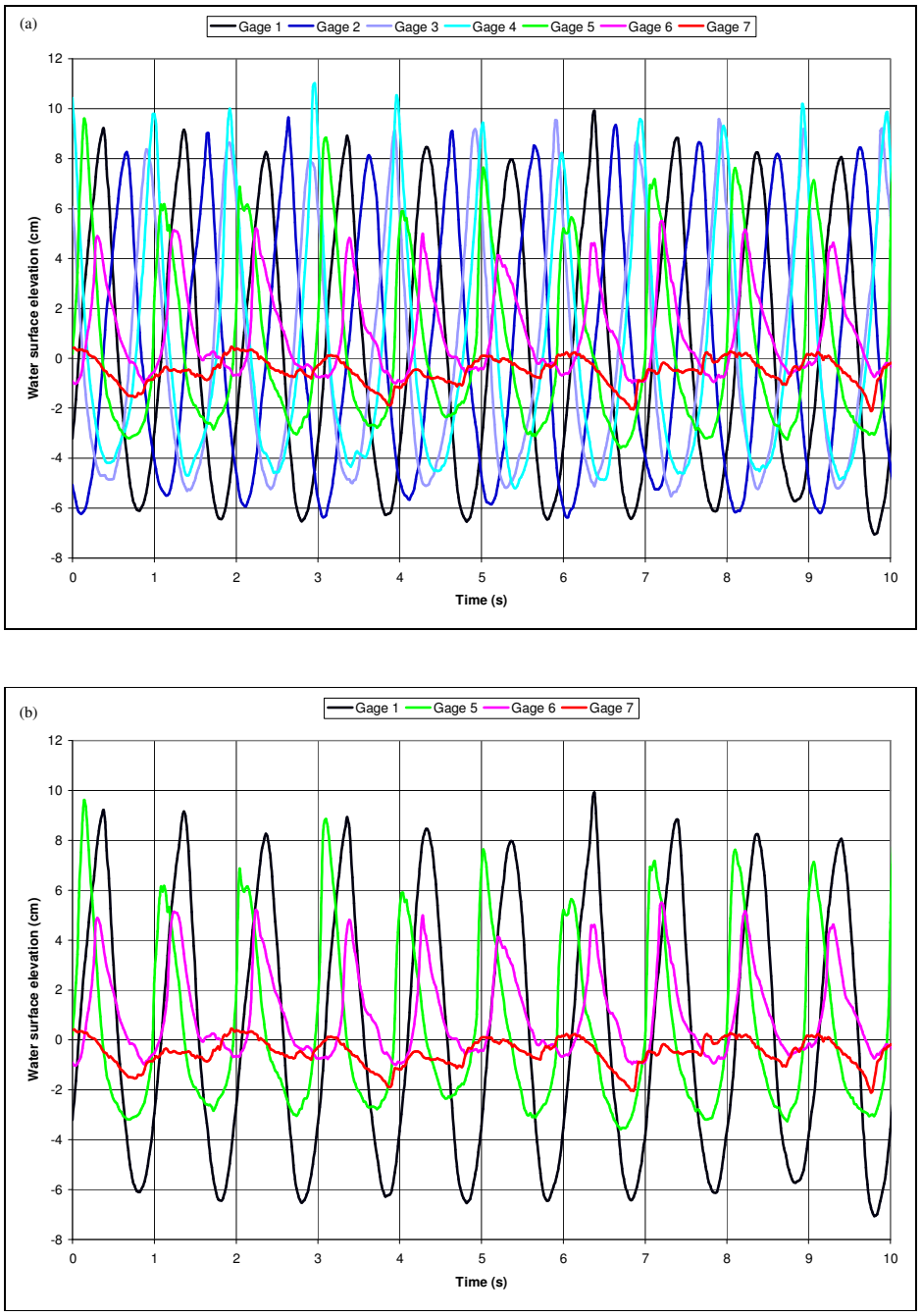

Figure 5.2 Case 1 With Plants Run Water Surface Elevation Time Series (a) All gages (b) Gages 1, 5, 6, and 7

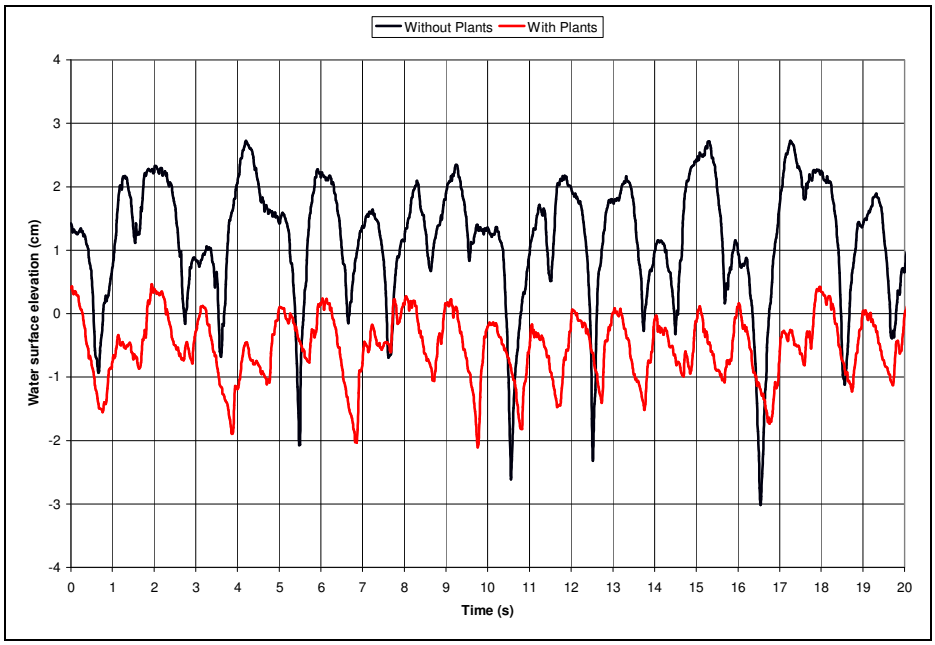

Figure 5.3 Case 1 Without and With Plants Runs Water Surface Elevation Time Series Gage 7

Table 5.1 Case 1 Runs Water Surface Elevation Time Series Mean, Variance, and Skewness (a) Without Plants (b) With Plants

(a)	**Gage 1**	**Gage 2**	**Gage 3**	**Gage 4**	**Gage 5**	**Gage 6**	**Gage 7**
Mean	0.133	0.205	0.122	0.116	0.383	0.964	1.243
Variance	25.284	24.542	22.130	18.846	10.997	3.245	0.819
Skewness	32.245	35.771	43.805	62.218	30.661	6.132	-0.492
(b)	**Gage 1**	**Gage 2**	**Gage 3**	**Gage 4**	**Gage 5**	**Gage 6**	**Gage 7**
Mean	0.247	0.229	0.144	0.272	0.330	0.981	-0.446
Variance	26.255	23.972	20.589	20.850	11.023	3.130	0.169
Skewness	33.862	37.729	39.961	68.321	30.356	5.714	-0.022

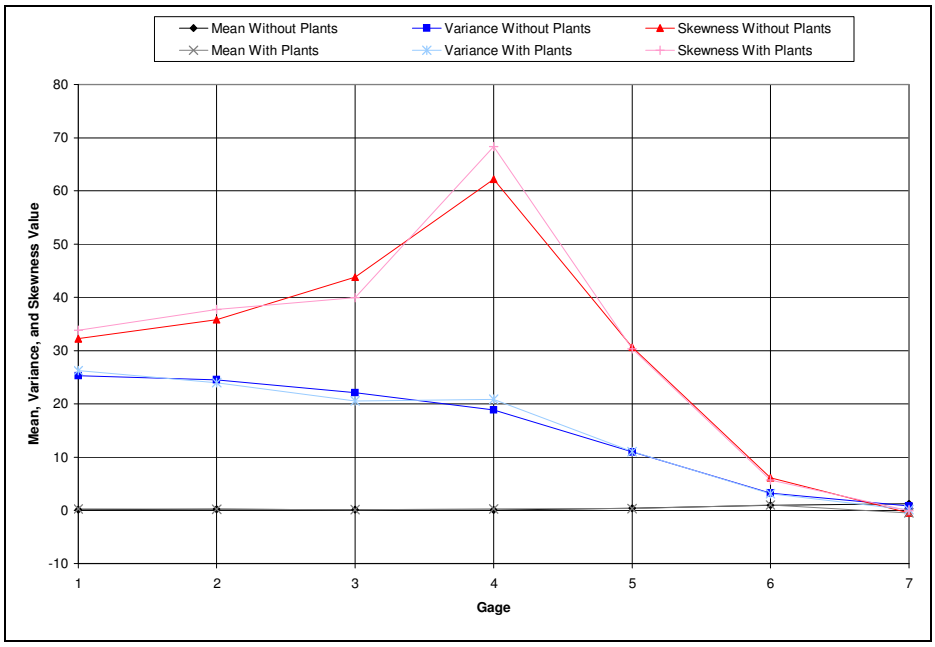

Figure 5.4 Case 1 Without and With Plants Runs Water Surface Elevation Time Series Mean, Variance, and Skewness All Gages

Case 2

For case 2 (T_p = 1.5 s), the time series figures (Figures 5.5 – 5.7) indicate a waveform with similar dimensions and a consistent 1.5 s period propagated during the without and with plants runs. The wave measured approximately 12 cm from peak to trough at gage 1 with an approximate 8 cm tall crest. At gage 2, the crest height increased slightly, as indicated by the peak in water surface elevation skewness in Table 5.2 and Figure 5.8. The wave continued to shoal as it propagated up ramp 2 with an approximate 10 cm wave height at gage 5. The waves were seen to begin spilling between gages 5 and 6 and finally break along the runup wire. Notably, wave breaking was seen to begin slightly further offshore with plants in the flume than without. The plants oscillated with the oncoming waves by bending toward the oncoming wave during rundown and then backwards as the wave proceeded up the ramp.

Figure 5.7 shows a very similar runup/rundown pattern between the without and with plants runs. Both patterns generally retained the 1.5 s period of the initial waveform. Without influence of the plants, wave runup reached approximately 3 cm above still water level along the ramp while the rundown varied between still water level and 3 cm below still water level. With plants in the flume, the runup only reached approximately 2 cm above still water level and the rundown only reached approximately 2 cm below still water level. The figures indicate the plants restricted wave runup and rundown to within a more limited, regular pattern than without plants in the flume.

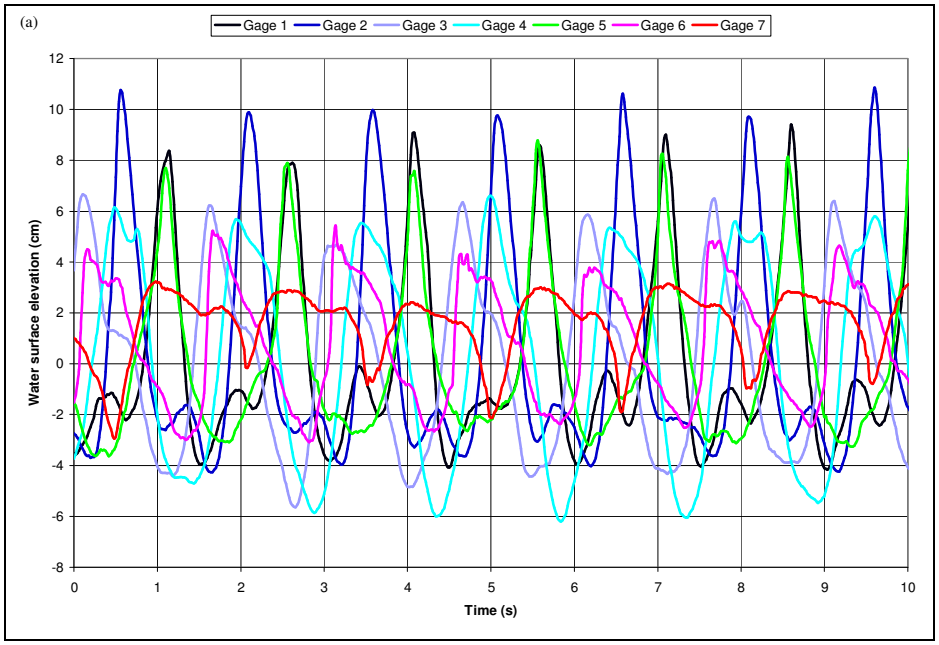

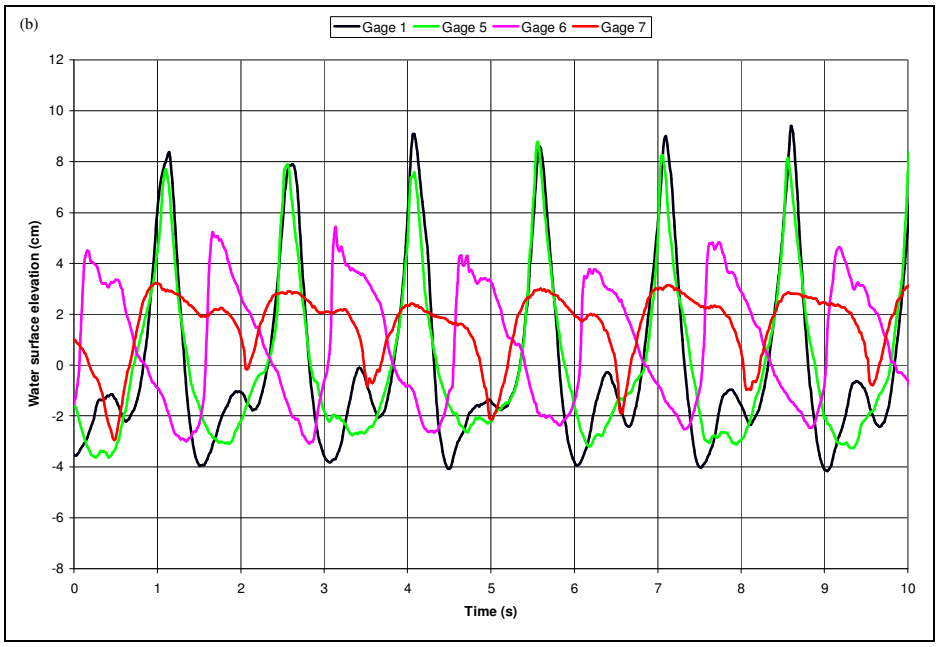

Figure 5.5 Case 2 Without Plants Run Water Surface Elevation Time Series (a) All gages (b) Gages 1, 5, 6, and 7

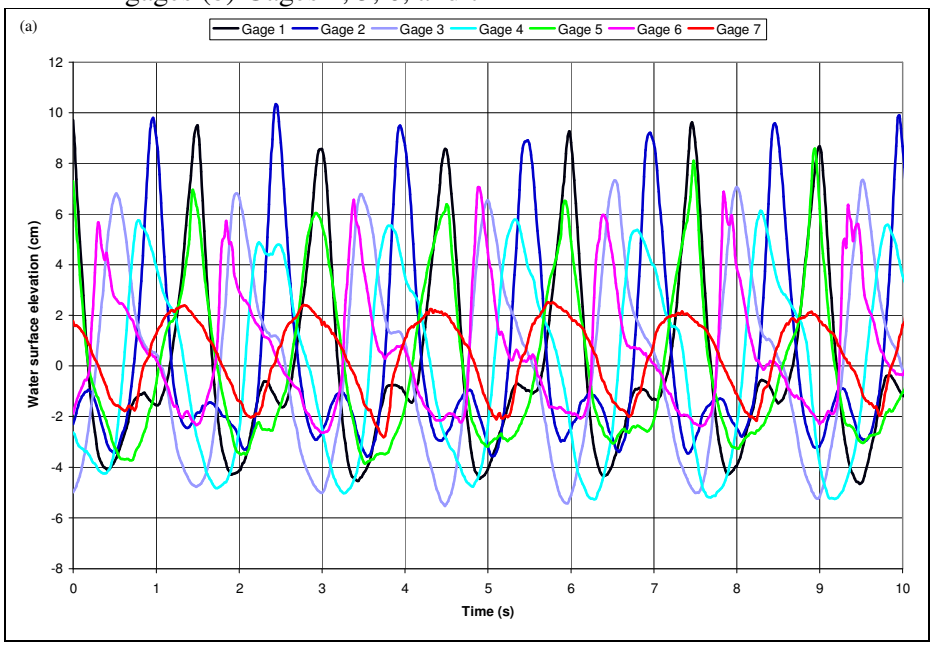

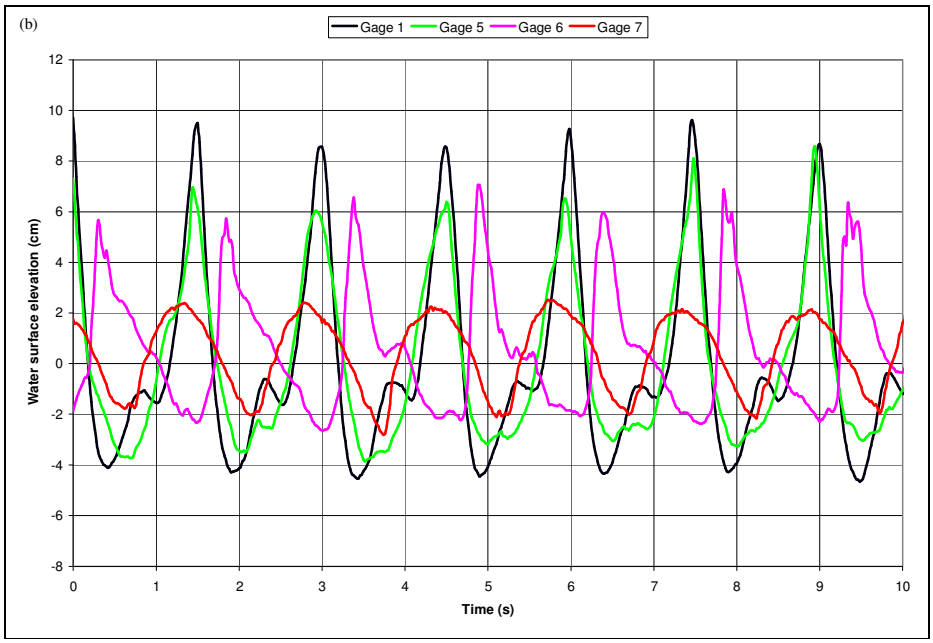

Figure 5.6 Case 2 With Plants Run Water Surface Elevation Time Series (a) All gages (b) Gages 1, 5, 6, and 7

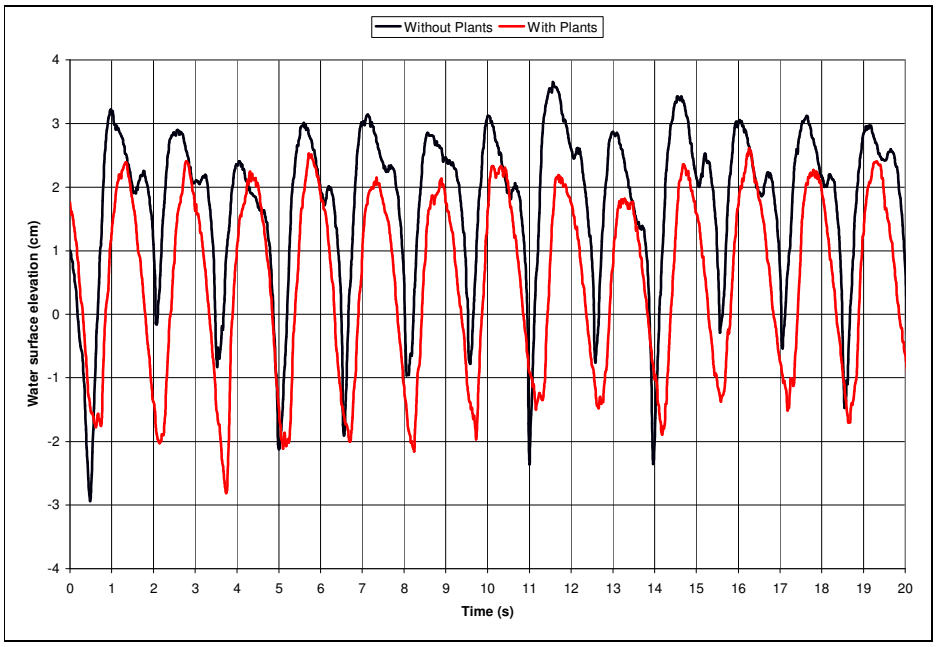

Figure 5.7 Case 2 Without and With Plants Runs Water Surface Elevation Time Series Gage 7

Table 5.2 Case 2 Runs Water Surface Elevation Time Series Mean, Variance, and Skewness (a) Without Plants (b) With Plants

(a)	**Gage 1**	**Gage 2**	**Gage 3**	**Gage 4**	**Gage 5**	**Gage 6**	**Gage 7**
Mean	0.140	0.227	0.009	0.111	0.100	0.724	1.726
Variance	13.374	18.529	12.137	16.568	9.687	5.924	1.568
Skewness	51.628	93.179	6.831	3.296	32.371	1.273	-2.563
(b)	**Gage 1**	**Gage 2**	**Gage 3**	**Gage 4**	**Gage 5**	**Gage 6**	**Gage 7**
Mean	0.180	0.190	0.107	0.060	0.141	0.484	0.403
Variance	15.100	14.646	13.712	13.487	10.351	5.207	2.082
Skewness	38.788	70.265	15.986	4.151	27.553	8.051	-1.392

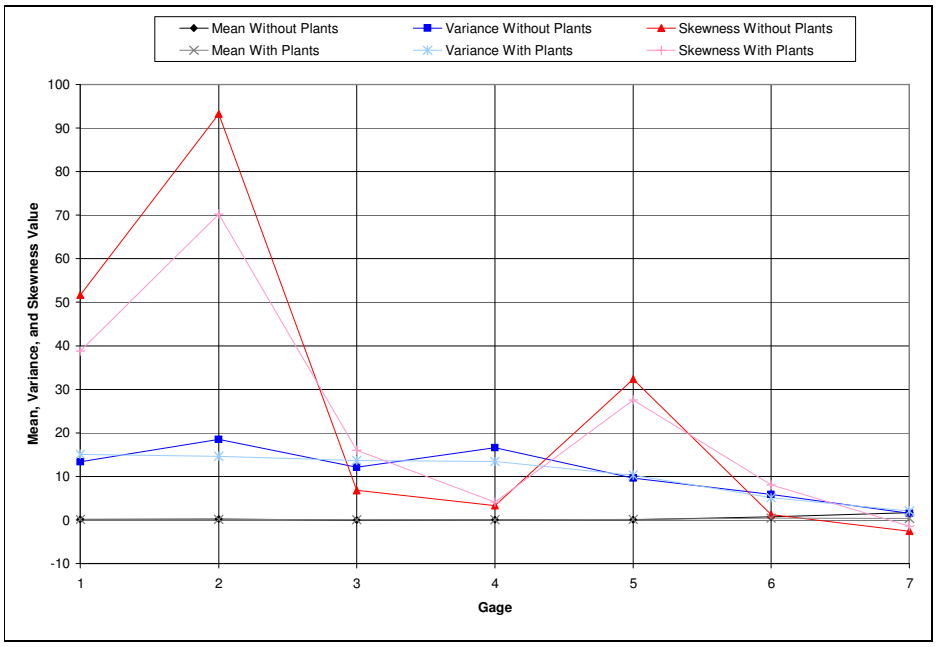

Figure 5.8 Case 2 Without and With Plants Runs Water Surface Elevation Time Series Mean, Variance, and Skewness All Gages

5.1.2 Irregular Wave Cases

Case 3

Minimal wave breaking occurred during both the without and with plants runs of case 3 (T_p = 1 s and γ = 3.3), as indicated by the constant variance and skewness of each gage's output signal (Table 5.3 and Figure 5.11). The plants oscillated with the passing waves but did not bend backwards. During both runs, the waves typically proceeded up the ramp slowly but were abruptly returned up the ramp during rundown. The negative mean water level at gage 7 during both the without and with plants runs indicates the runup/rundown pattern typically remained below still water level. Without plants in the flume, the wave excursion along the ramp centered about approximately 1.6 cm below still water level. With influence of the plants, this excursion centered about approximately 2.5 cm below still water level. Notably, the runup was generally proportional to and similar in extent to the wave height at gage 6 during both runs (Figures 5.9 and 5.10).

Table 5.3 Case 3 Runs Water Surface Elevation Time Series Mean, Variance, and Skewness (a) Without Plants (b) With Plants

(a)	**Gage 1**	**Gage 2**	**Gage 3**	**Gage 4**	**Gage 5**	**Gage 6**	**Gage 7**
Mean	-0.006	0.014	-0.016	-0.014	-0.004	-0.005	-1.659
Variance	0.522	0.502	0.468	0.441	0.430	0.445	0.302
Skewness	0.016	0.016	0.028	0.006	0.026	0.074	-0.035
(b)	**Gage 1**	**Gage 2**	**Gage 3**	**Gage 4**	**Gage 5**	**Gage 6**	**Gage 7**
Mean	0.007	-0.004	-0.002	0.006	-0.005	0.005	-2.467
Variance	0.478	0.465	0.431	0.404	0.374	0.374	0.152
Skewness	0.032	0.004	0.045	0.013	0.036	0.048	-0.034

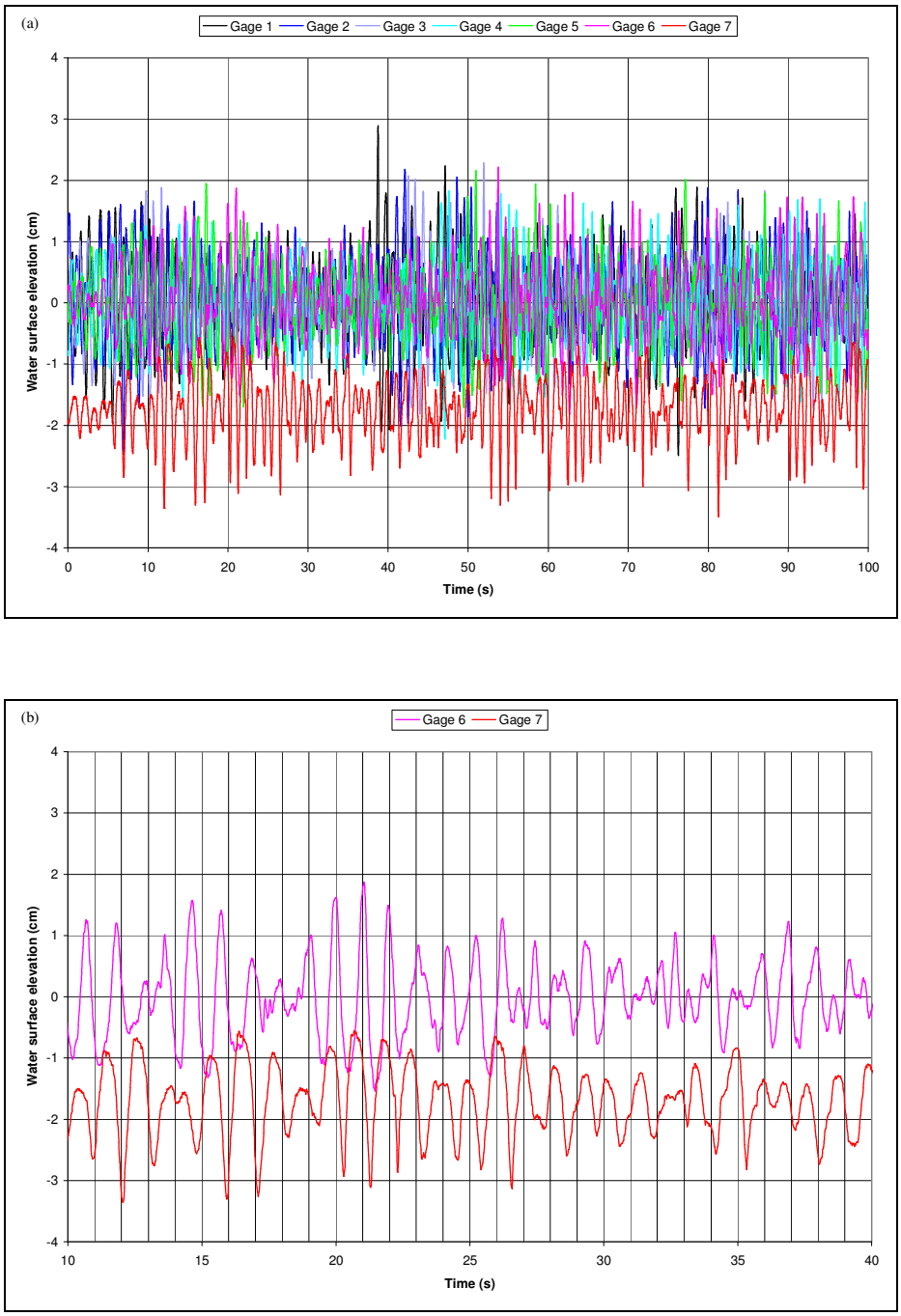

Figure 5.9 Case 3 Without Plants Run Water Surface Elevation Time Series (a) All gages (b) Gages 6 and 7

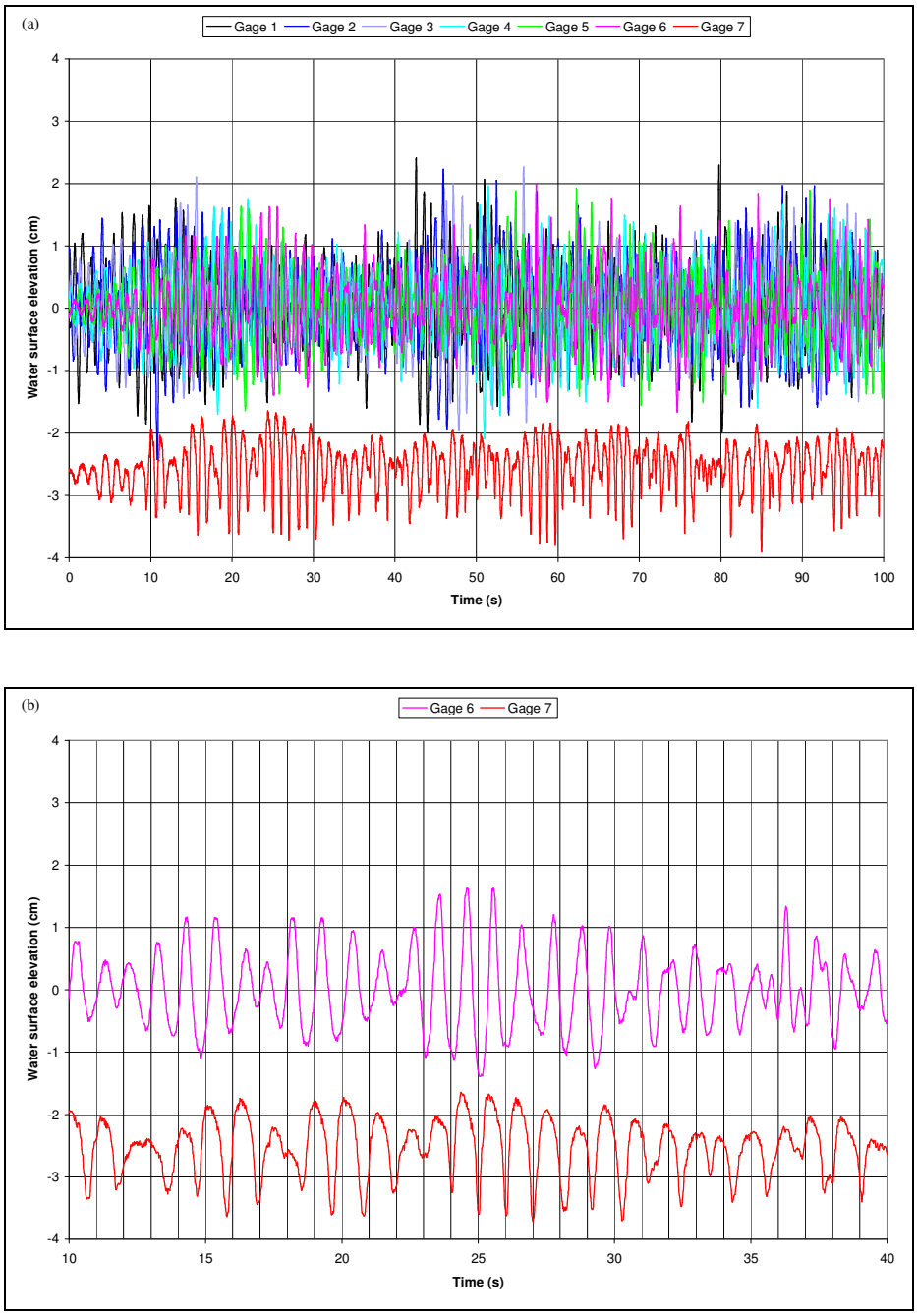

Figure 5.10 Case 3 With Plants Run Water Surface Elevation Time Series (a) All gages (b) Gages 6 and 7

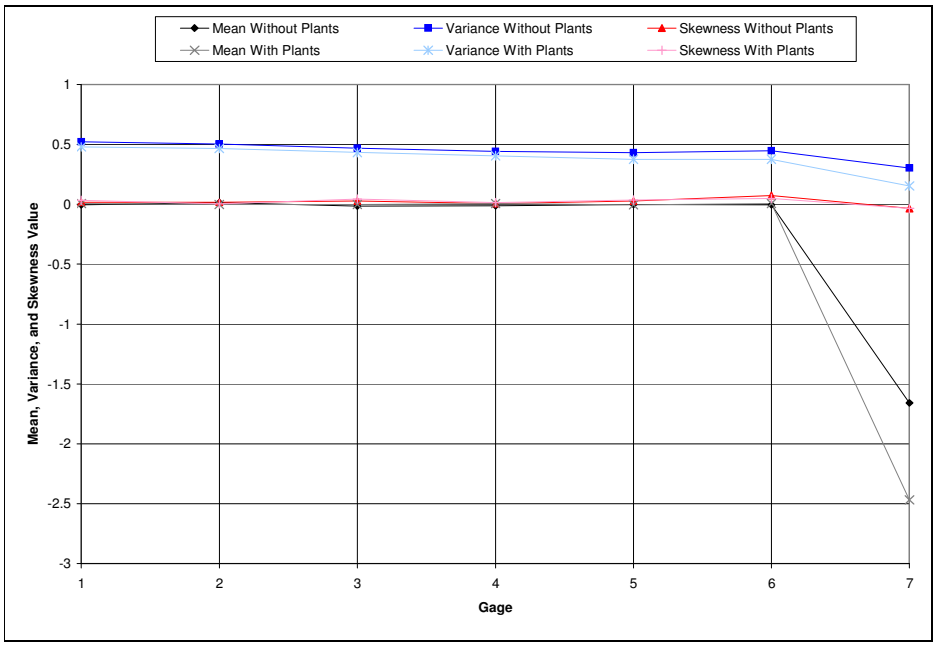

Figure 5.11 Case 3 Without and With Plants Runs Water Surface Elevation Time Series Mean, Variance, and Skewness All Gages

Case 4

Table 5.4 and Figure 5.14 reveal an increase in variance of the water surface elevation time series at gages 6 and 7 and an increasing signal skewness that peaks at gage 6 for the without plants run of case 4 (T_p = 1.5 s and γ = 3.3). The without plants run times series figures (Figures 5.12 and 5.13) show tall wave peaks at gage 6 and a dominant rundown. To a much lesser degree, these patterns are apparent in the with plants run. A steady signal variance results with only a slight peak in signal skewness at gage 6 during the with plants run. Notably, a smooth spilling breaker was observed during much of the with plants run while a more abrupt breaking was observed during the without plants run. The plants became prone in both directions frequently. During the without plants run, the runup/rundown range along the ramp centered about approximately 0.7 cm below still water level. With influence of the plants, this excursion centered about approximately 2 cm below still water level. Typically, during both runs, the rundown was proportional to

the wave height at gage 6 while the magnitude of rundown was generally slightly larger than the wave height during the without plants run. With plants in the flume, the runup/rundown pattern was generally smoother than without plants, i.e. the rundown was not returned up the ramp as abruptly.

Table 5.4 Case 4 Runs Water Surface Elevation Time Series Mean, Variance, and Skewness (a) Without Plants (b) With Plants

(a)	**Gage 1**	**Gage 2**	**Gage 3**	**Gage 4**	**Gage 5**	**Gage 6**	**Gage 7**
Mean	-0.006	-0.003	-0.011	-0.018	-0.034	-0.045	-0.690
Variance	1.380	1.392	1.369	1.362	1.436	2.136	2.499
Skewness	0.252	0.045	0.114	0.204	0.742	2.596	-0.894
(b)	**Gage 1**	**Gage 2**	**Gage 3**	**Gage 4**	**Gage 5**	**Gage 6**	**Gage 7**
Mean	-0.026	-0.032	-0.049	0.009	0.003	-0.031	-1.930
Variance	1.140	1.150	1.104	1.098	1.161	1.292	0.934
Skewness	0.191	0.010	0.064	0.182	0.571	1.199	-0.201

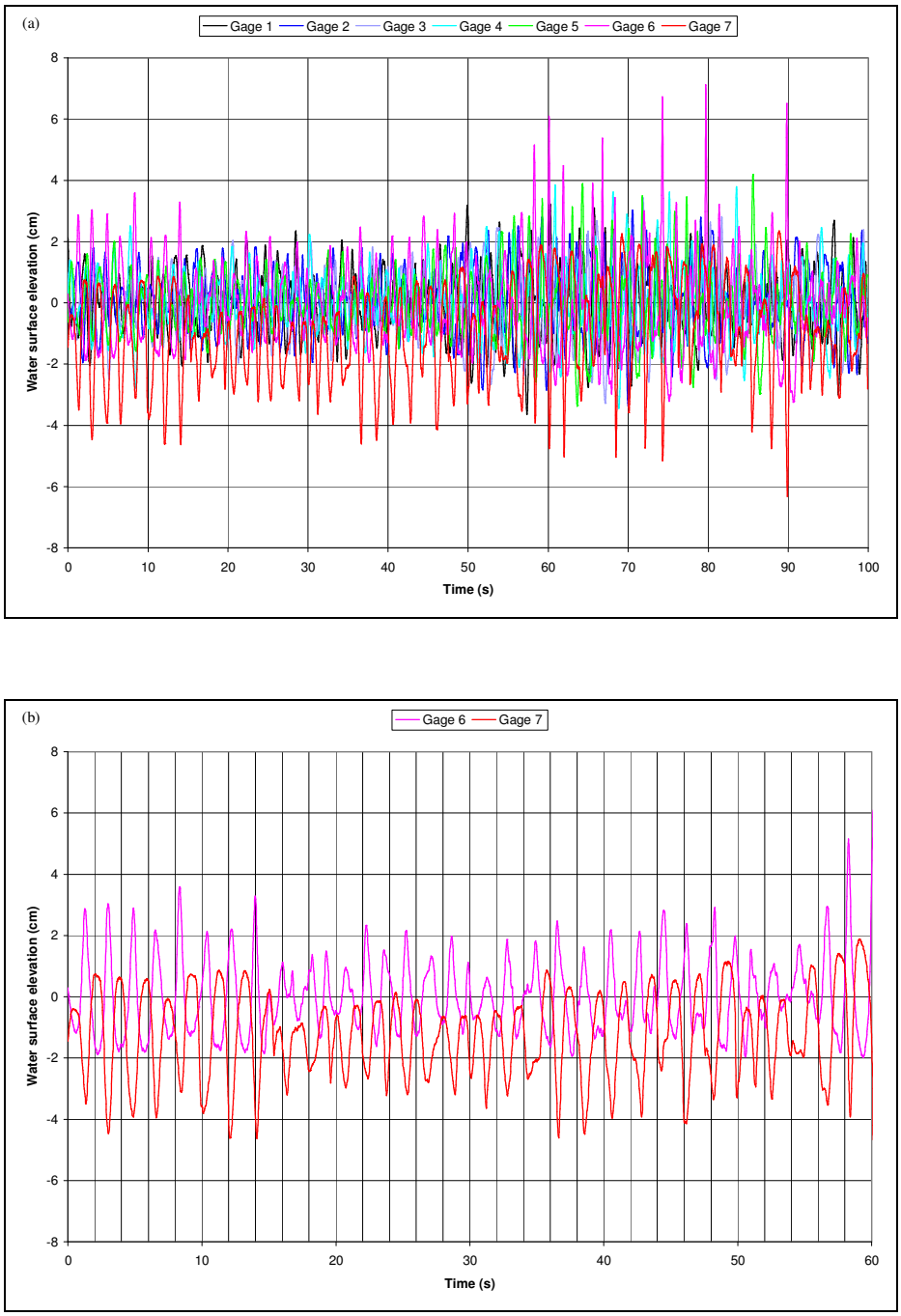

Figure 5.12 Case 4 Without Plants Run Water Surface Elevation Time Series (a) All gages (b) Gages 6 and 7

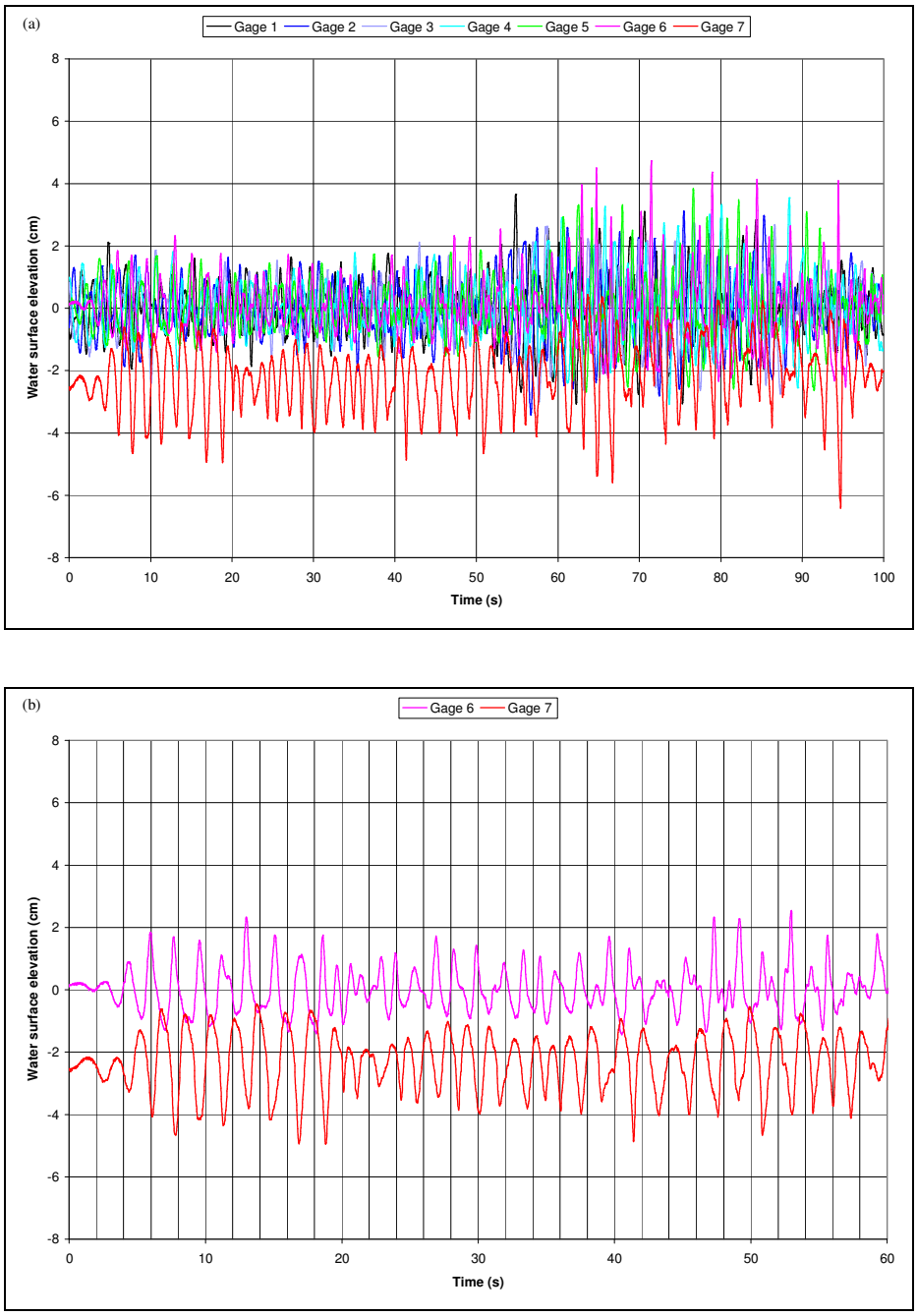

Figure 5.13 Case 4 With Plants Run Water Surface Elevation Time Series (a) All gages (b) Gages 6 and 7

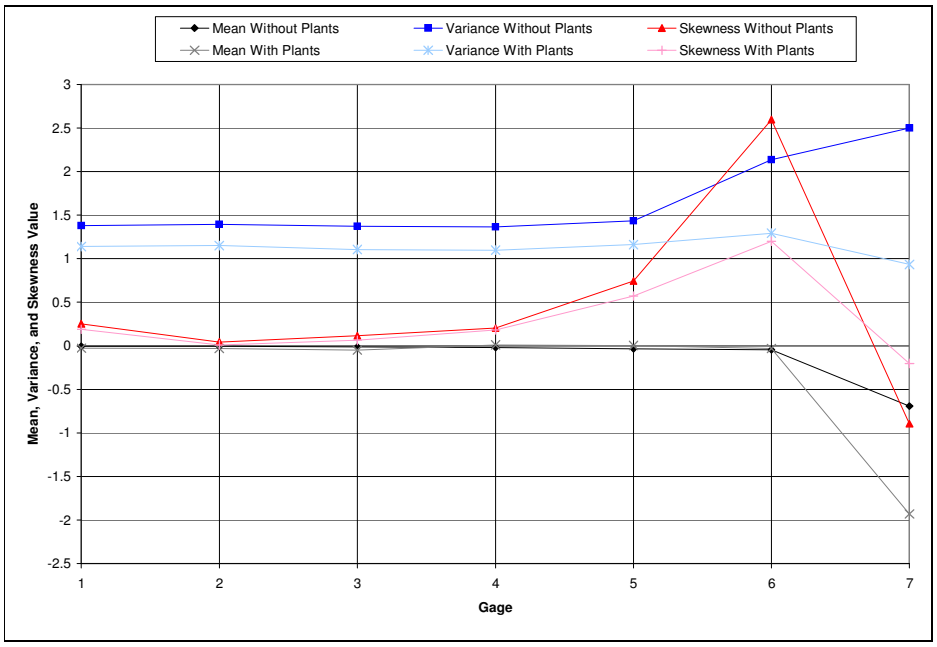

Figure 5.14 Case 4 Without and With Plants Runs Water Surface Elevation Time Series Mean, Variance, and Skewness All Gages

Case 5

The time series figures (Figures 5.15 and 5.16) and water surface elevation time series analysis (Table 5.5 and Figure 5.17) of the case 5 runs (T_p = 1.5 s and γ = 30), reveal very similar results to the corresponding case 4 run. These patterns include an increase in variance of the water surface elevation time series at gages 6 and 7 during the without plants run and a steady variance during the with plants run. An increasing signal skewness peaks at gage 6 during both runs but to a much lesser degree during the with plants run. Observation revealed a sharper breaking wave during the case 5 without plants run as compared to the with plants run. The plants oscillated with the passing waves and frequently became fully prone in both directions. Similar to case 4, the runup/rundown excursion centered about approximately 0.7 cm below still water level during the without plants run and about approximately 2 cm below still water level with plants in the flume. With plants in the flume, the runup and rundown proceeded along the ramp smoothly

while the rundown was more abruptly returned up the ramp without influence of the plants.

Table 5.5 Case 5 Runs Water Surface Elevation Time Series Mean, Variance, and Skewness (a) Without Plants (b) With Plants

(a)	**Gage 1**	**Gage 2**	**Gage 3**	**Gage 4**	**Gage 5**	**Gage 6**	**Gage 7**
Mean	-0.011	-0.004	-0.014	-0.047	-0.023	-0.023	-0.719
Variance	1.472	1.478	1.481	1.406	1.427	2.203	2.178
Skewness	0.202	0.254	0.182	0.438	0.934	2.574	-0.537
(b)	**Gage 1**	**Gage 2**	**Gage 3**	**Gage 4**	**Gage 5**	**Gage 6**	**Gage 7**
Mean	-0.015	-0.046	0.005	0.012	-0.003	-0.041	-1.961
Variance	1.217	1.236	1.200	1.179	1.220	1.368	1.046
Skewness	0.243	0.165	0.135	0.416	0.780	1.558	0.186

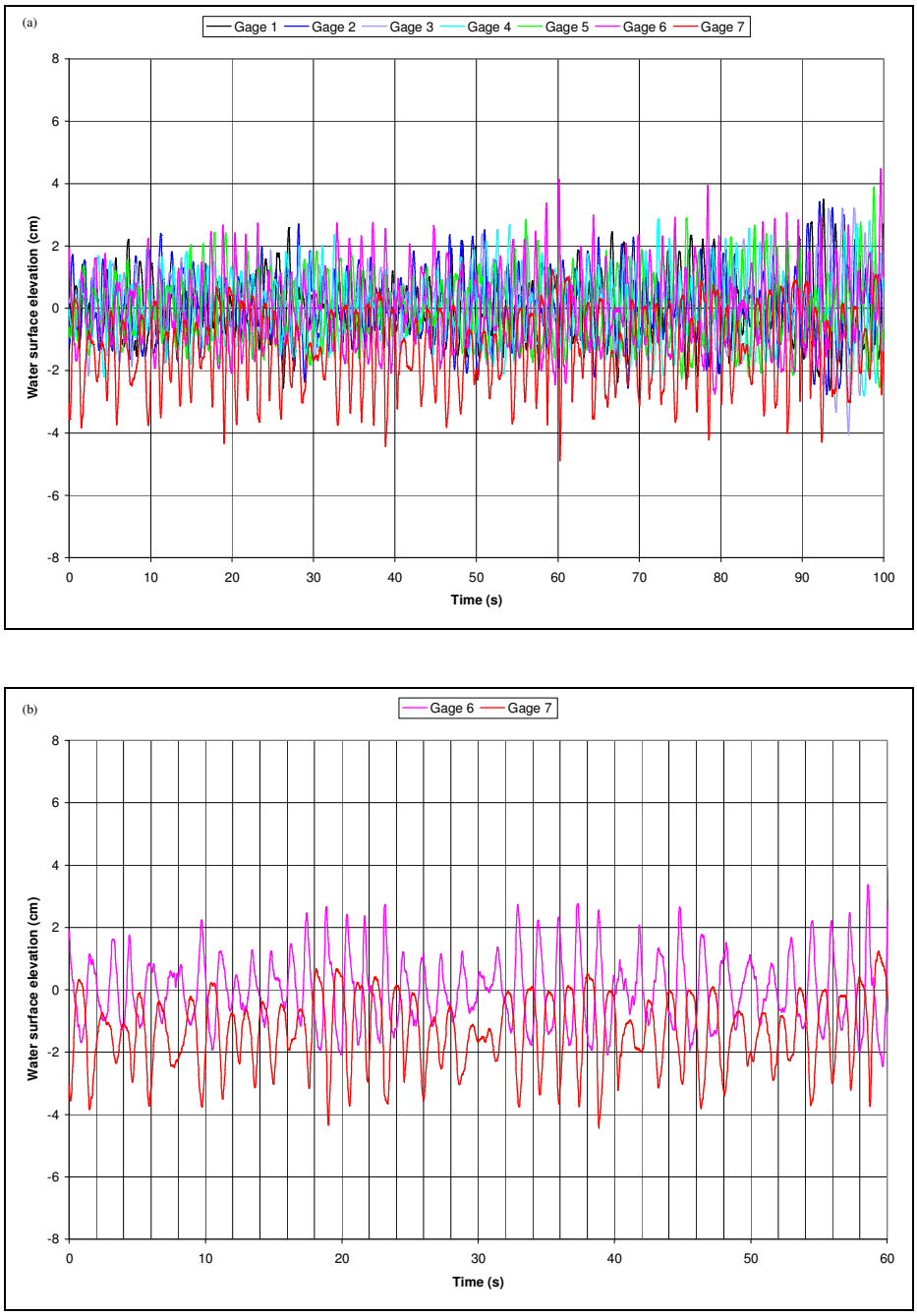

Figure 5.15 Case 5 Without Plants Run Water Surface Elevation Time Series (a) All gages (b) Gages 6 and 7

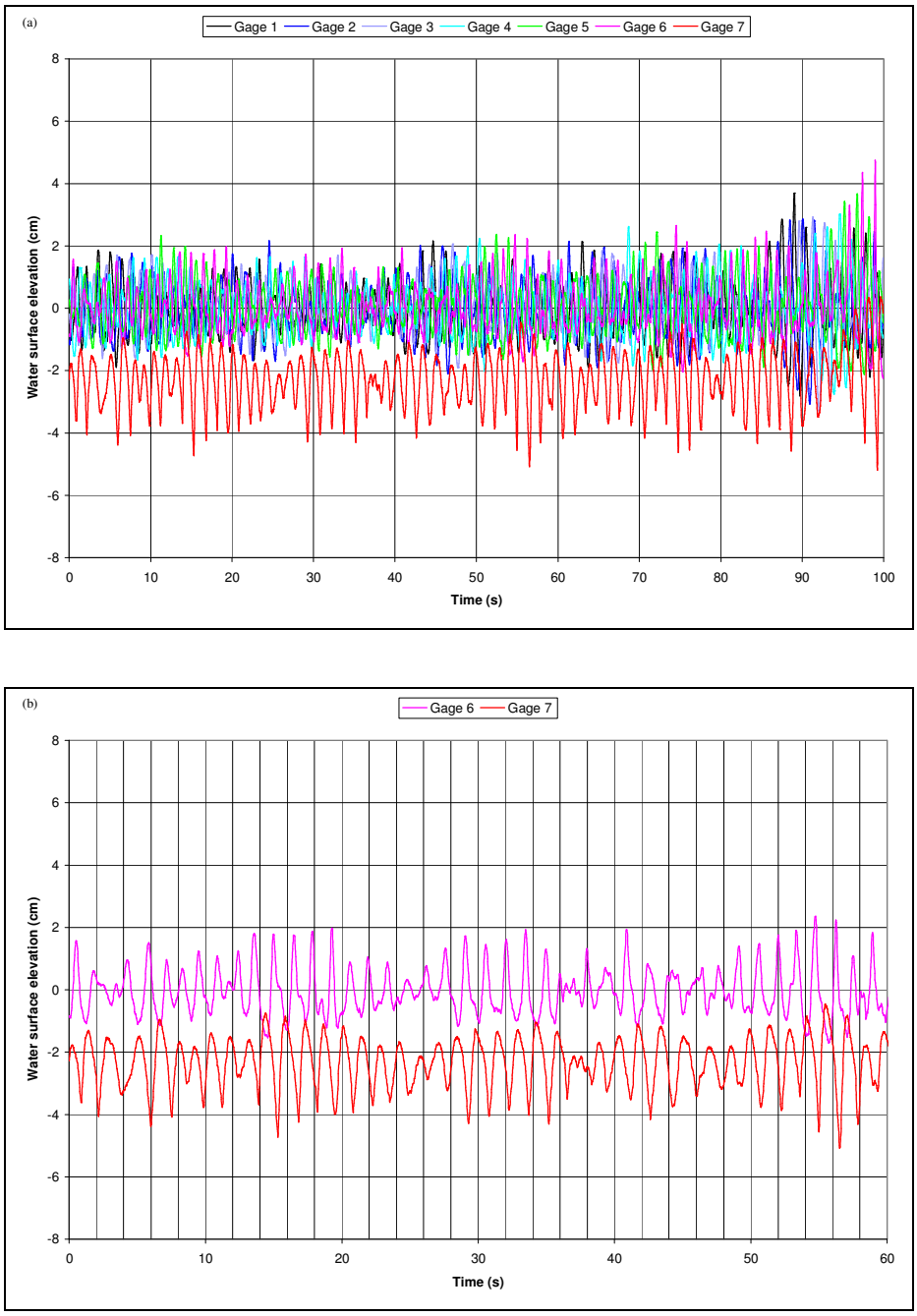

Figure 5.16 Case 5 With Plants Run Water Surface Elevation Time Series (a) All gages (b) Gages 6 and 7

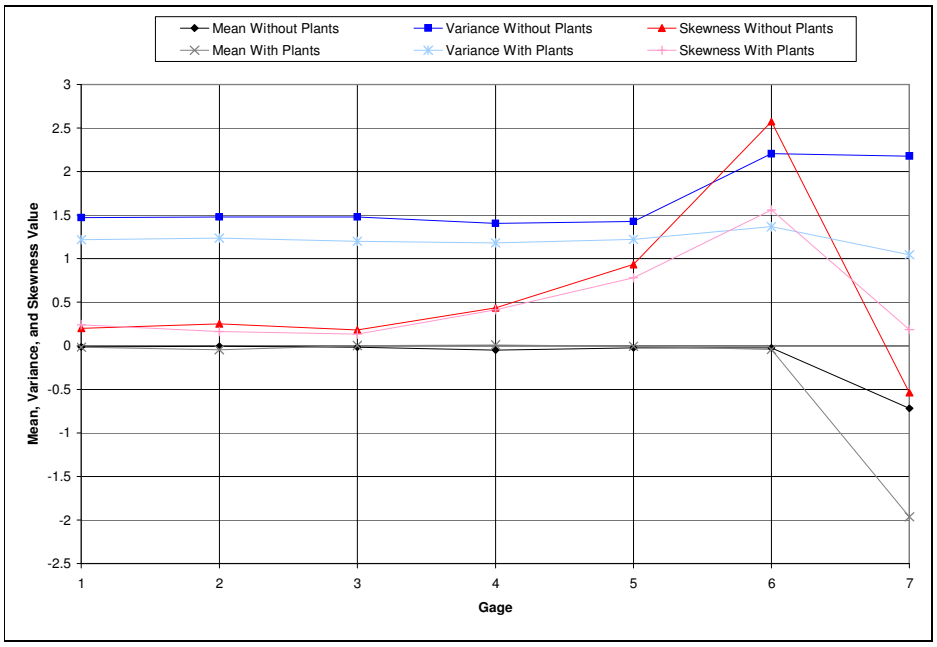

Figure 5.17 Case 5 Without and With Plants Runs Water Surface Elevation Time Series Mean, Variance, and Skewness All Gages

Case 6

For case 6 (T_p = 2 s and γ = 3.3),, the time series figures of the without plants run (Figure 5.18) show a narrow crest height frequently much greater than the broader trough depth at gage 6 and a longer extent of rundown than runup at gage 7. Analysis of the water surface elevation time series of each gage during this run reveals a larger variance at gage 6 and 7 as well as a peak in skewness of the signal at gage 6 (Table 5.6 and Figure 5.20). These same patterns are evident in the with plants run but to a much lesser degree. Notably, a plunging breaker was observed near gage 6 during much of the without plants run while smoother breaking occurred slightly further offshore during much of the with plants run. The plants oscillated with the passing waves and became fully prone in both directions frequently.

The runup/rundown excursion centered about approximately 1 cm below still water level during the without plants run and about approximately 2.5 cm below still

water level with plants in the flume. The excursion along the ramp was generally proportional to but slightly larger than the wave height at gage 6 during both runs, i.e. the taller the crest, the larger the rundown. The runup/rundown pattern was usually smooth during the with plants run but the rundown was abruptly returned up the ramp during the without plants run.

Table 5.6 Case 6 Runs Water Surface Elevation Time Series Mean, Variance, and Skewness (a) Without Plants (b) With Plants

(a)	**Gage 1**	**Gage 2**	**Gage 3**	**Gage 4**	**Gage 5**	**Gage 6**	**Gage 7**
Mean	-0.008	-0.004	-0.017	-0.033	-0.090	-0.047	-1.088
Variance	0.757	0.798	0.831	0.832	0.898	1.397	3.615
Skewness	0.007	0.000	0.019	0.165	0.312	1.889	0.224
(b)	**Gage 1**	**Gage 2**	**Gage 3**	**Gage 4**	**Gage 5**	**Gage 6**	**Gage 7**
Mean	-0.017	-0.022	-0.033	-0.040	-0.033	-0.017	-2.554
Variance	0.336	0.349	0.347	0.361	0.377	0.447	0.963
Skewness	-0.008	-0.013	0.022	0.038	0.073	0.209	-0.216

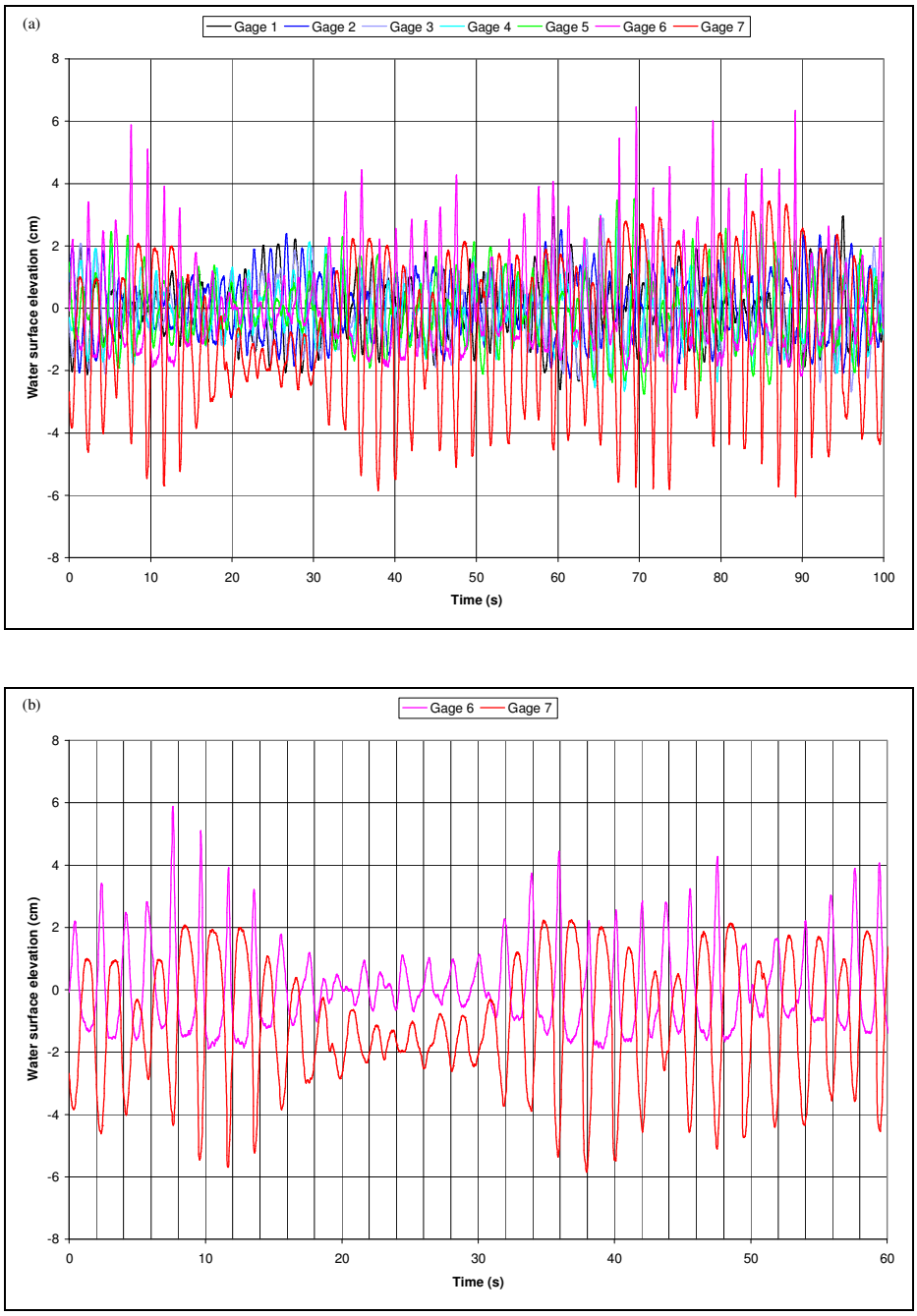

Figure 5.18 Case 6 Without Plants Run Water Surface Elevation Time Series (a) All gages (b) Gages 6 and 7

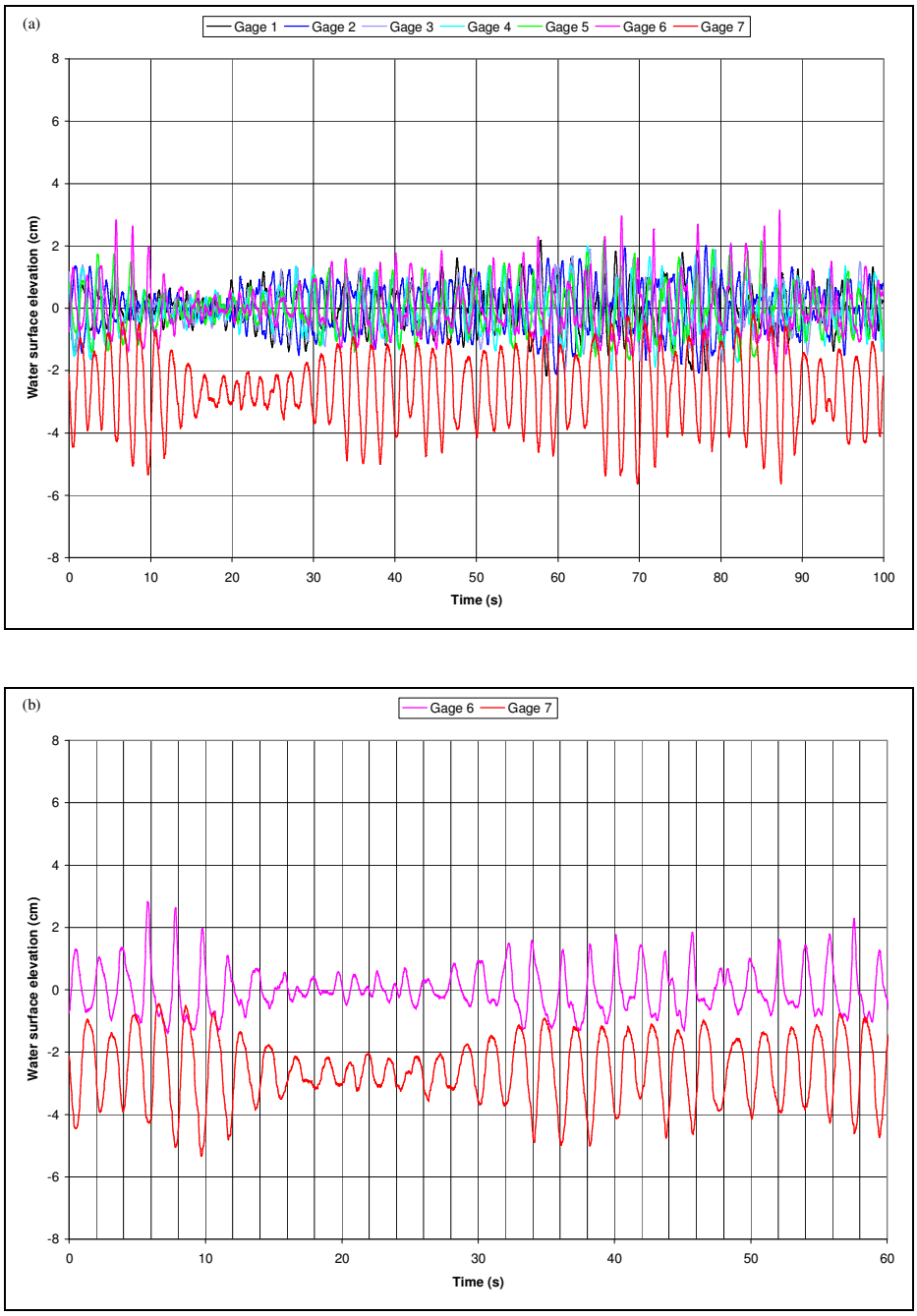

Figure 5.19 Case 6 With Plants Run Water Surface Elevation Time Series (a) All gages (b) Gages 6 and 7

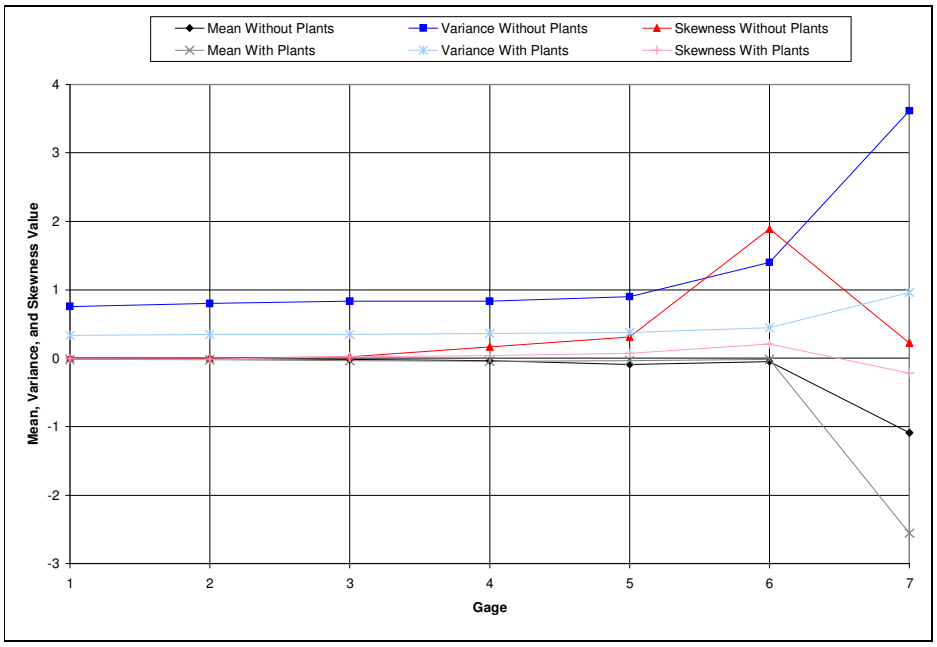

Figure 5.20 Case 6 Without and With Plants Runs Water Surface Elevation Time Series Mean, Variance, and Skewness All Gages

5.2 Spectral Analysis

After analysis of each gage's water surface elevation output time series, the data was transferred into the frequency domain for additional analysis. The power spectral density, or Fourier transform of the autocorrelation function, results from a fast Fourier transform (FFT) utilizing Welch's method with 1,024 data points per segment. The Matlab program, pwelch, estimates the power spectrum of the input time series and allows specification of a windowing function prior to transformation. A rectangular, or "boxcar," window was applied to the time series of the regular wave runs (cases 1 and 2) and a Hanning window to those of the irregular cases (cases 3 – 6). The following figures show the resulting spectra up to 5 Hz which is sufficient to capture relevant information.

5.2.1 Regular Wave Cases

Case 1

For both runs of case 1 (T_p = 1 s), in addition to the prominent 1 Hz frequency peak, the transform captures peaks of decreasing amplitude at multiples of 1 Hz within each gage's output signal (Figure 5.21). Since regular wave conditions developed for 10 minutes prior to data acquisition, these harmonics may be attributed to reflection in the flume during these runs. As seen in Figure 5.22, for both the without and with plants runs, the magnitude of the 1 Hz peak decreases from approximately 200 cm^2/Hz at gage 1 to 70 cm^2/Hz at gage 5 to 20 cm^2/Hz at gage 6 indicating a decrease in energy approaching the beach. The much narrower peak of the first harmonic (2 Hz) has an amplitude two orders of magnitude less than the dominant 1 Hz peak at gage 1. The difference in magnitude between these 2 peaks decreases steadily approaching the beach indicating a lesser degree of reflection, or greater degree of wave energy absorption, at 2 Hz closer to the wave maker. Figure 5.21 reveals a consistently weaker variance at gage 7 than gages 1 – 6 for both the without and with plants runs. Figure 5.22 shows a consistent reduction in energy at gage 7 during the with plants run as compared to the without plants run over the frequency range. Notably, a wide peak centered about approximately 0.375 Hz arises with a magnitude of approximately 1 cm^2/Hz at gage 7 during the without plants run but is not evident during the with plants run.

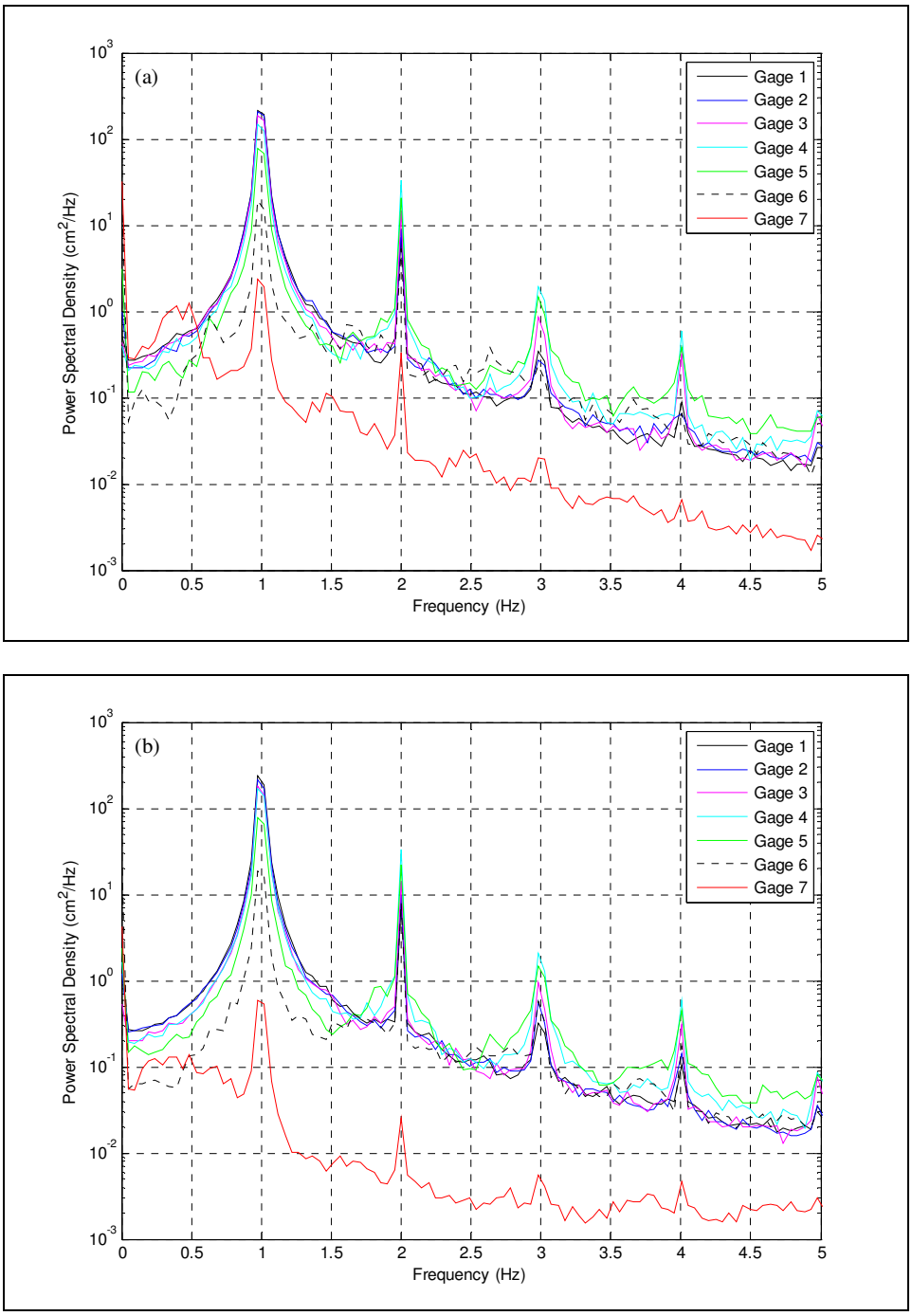

Figure 5.21 Case 1 Runs Power Spectral Density (a) Without Plants (b) With Plants

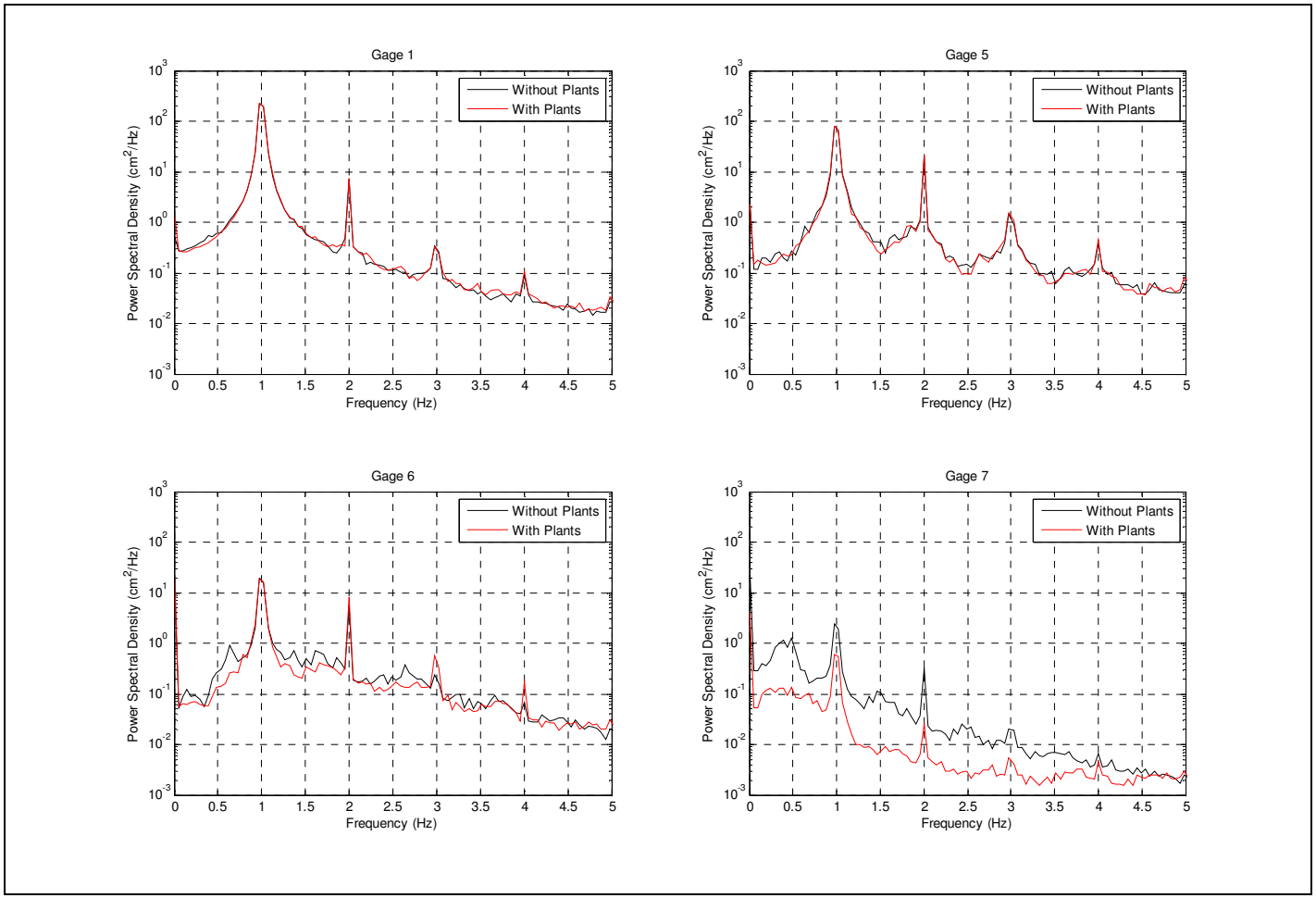

Figure 5.22 Case 1 Runs Power Spectral Density Comparisons

Case 2

As seen in Figure 5.23, similar to case 1, multiple harmonics of decreasing amplitude arise from the frequency transformation of each gage's output signal for both the without and with plants runs for case 2 (T_p = 1.5 s). These additional peaks, at intervals of 0.67 Hz, may be due to reflection resulting from allowing the regular wave condition 10 minutes to develop prior to data acquisition. These peaks are noticeably narrower than those of case 1. Figure 5.24 shows the magnitude of the 0.67 Hz peak decreases from approximately 100 cm^2/Hz at gage 1 to 60 cm^2/Hz at gage 6 for both the without and with plants runs indicating a decrease in energy as the waves approached the beach. The difference in peak magnitude between the 0.67 Hz and first harmonic (1.33 Hz) increases between gages 1 and 5 and then decreases between gages 5 and 7. A larger difference between these peaks indicates a smaller amount of reflection, or greater degree of energy absorption, at that gage. Figure 5.23 indicates a consistently weaker variance at gage 7 than gages 1 – 6 for both the without and with plants runs. Figure 5.24 also reveals a general slight energy reduction at gage 7 during the with plants run versus the without plants run for this case.

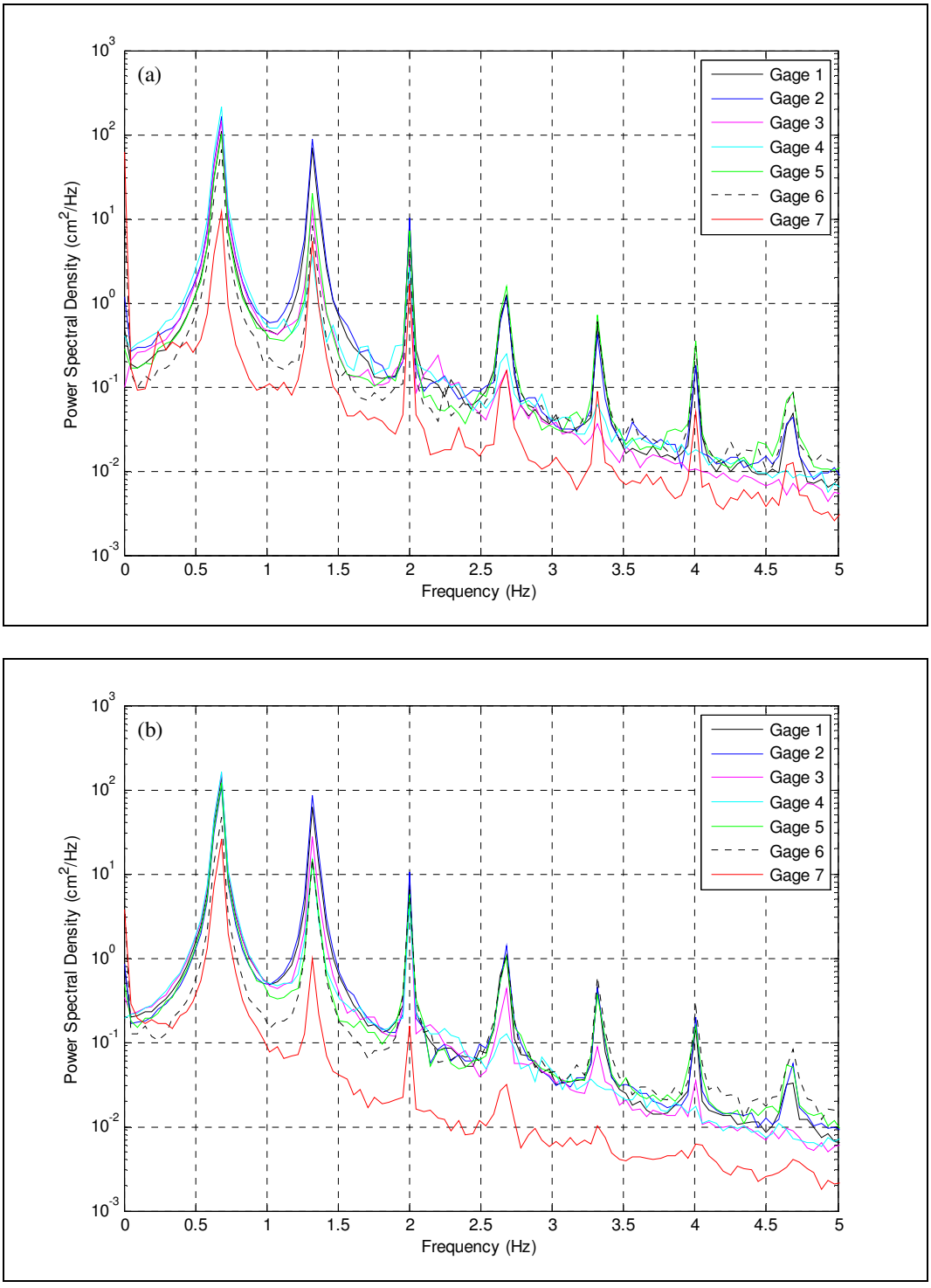

Figure 5.23 Case 2 Runs Power Spectral Density (a) Without Plants (b) With Plants

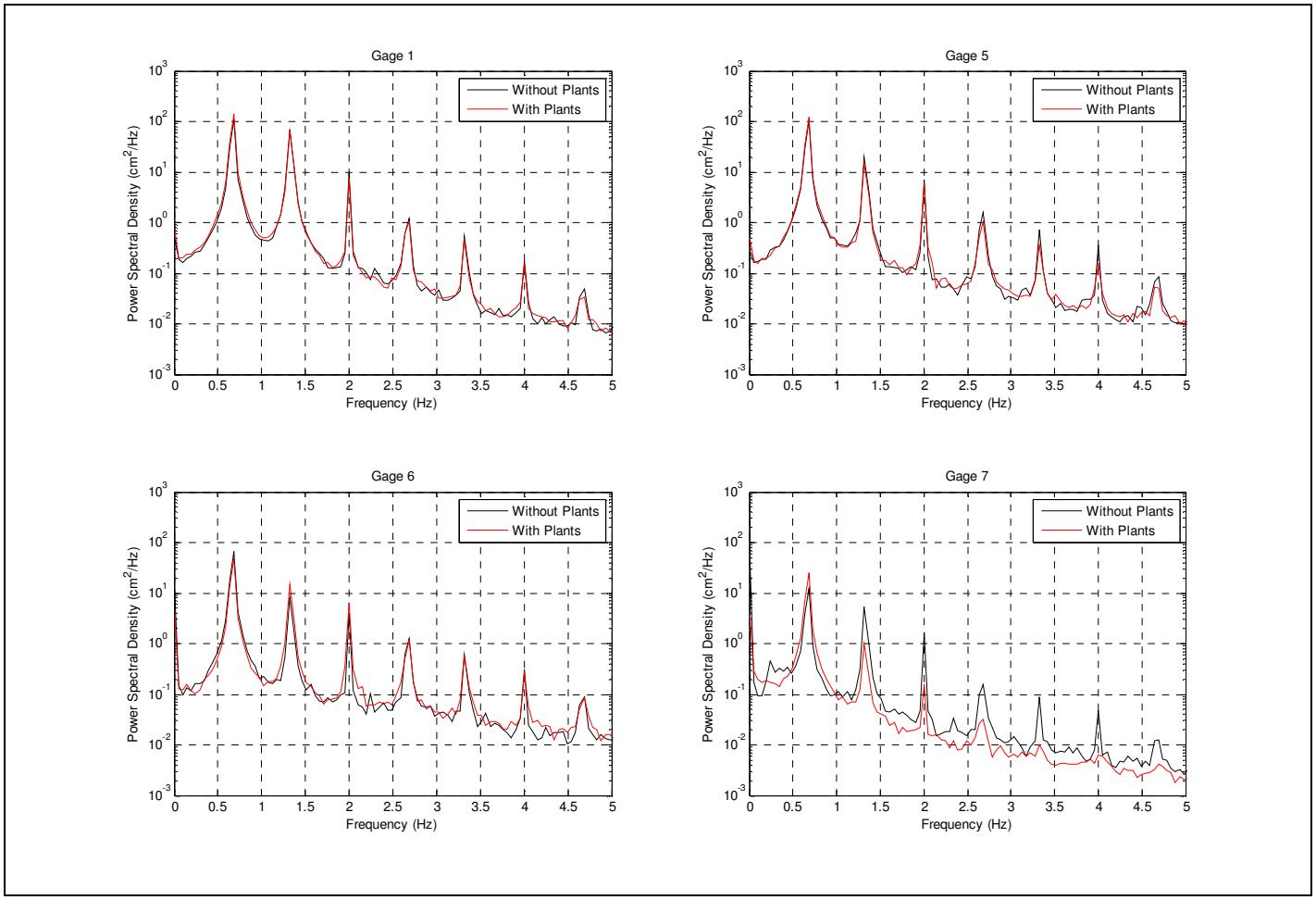

Figure 5.24 Case 2 Runs Power Spectral Density Comparisons

5.2.2 Irregular Wave Cases

Case 3

For case 3 (T_p = 1 s and γ = 3.3), the frequency transformation of each gage's output signal reveals a prominent wide peak centered about approximately 1 Hz for both the without and with plants runs (Figure 5.25). This peak generally retains its amplitude between the 7 gages. For both the without and with plants runs, the magnitude of the 1 Hz peak reaches approximately 2 cm^2/Hz at gage 1, 1 cm^2/Hz at gage 6, and 0.6 cm^2/Hz at gage 7. Notably, as compared to gages 1 – 6, a slight decrease in wave energy appears at gage 7 between 1 Hz and 2.5 Hz for the with plants run. Figure 5.25 reveals this pattern, to a lesser degree, in the spectra of the without plants run. Comparing the without and with plants runs over the frequency range, Figure 5.26 reveals a consistent variance between gages 1, 5, 6, and 7.

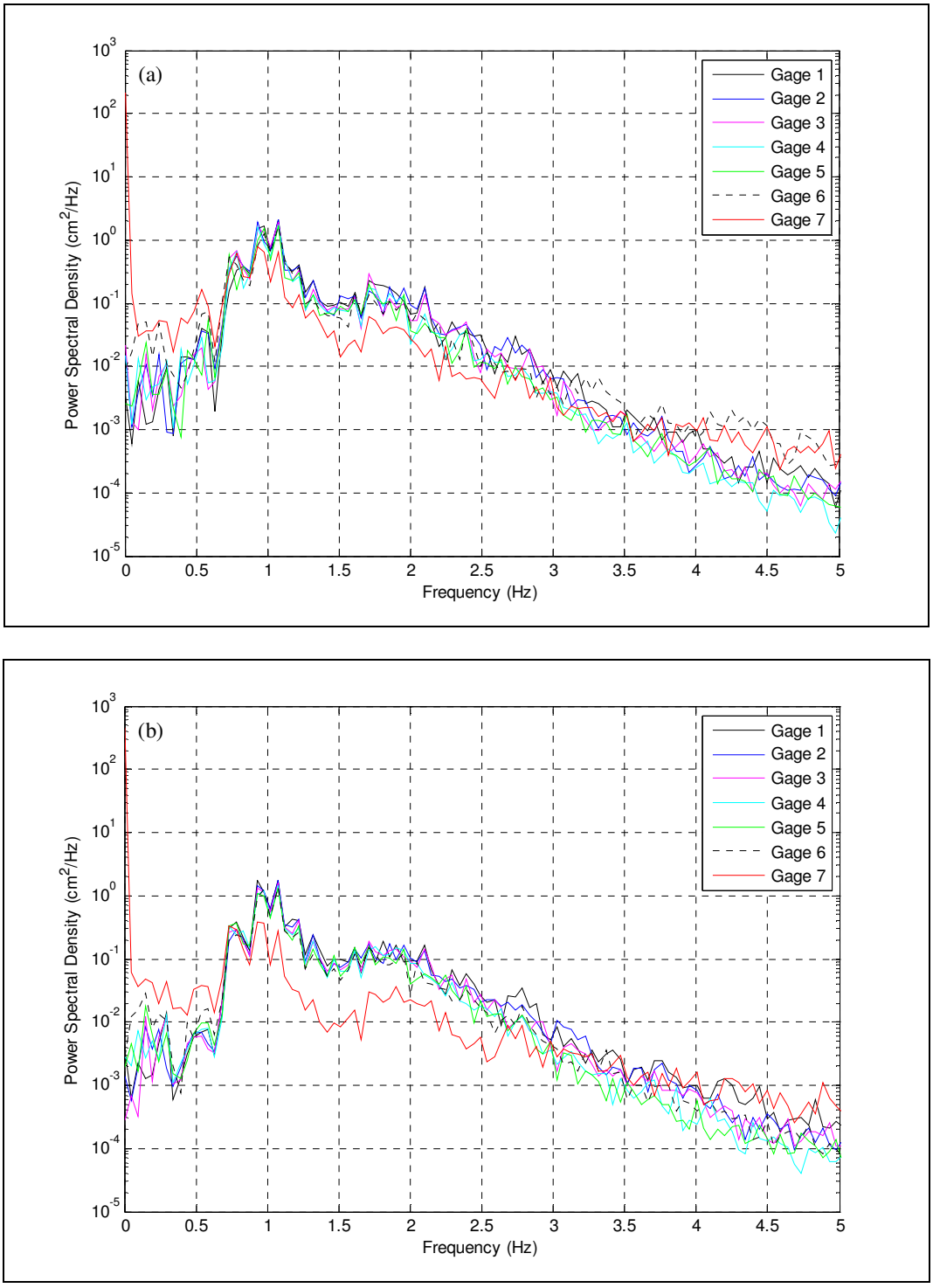

Figure 5.25 Case 3 Runs Power Spectral Density (a) Without Plants (b) With Plants

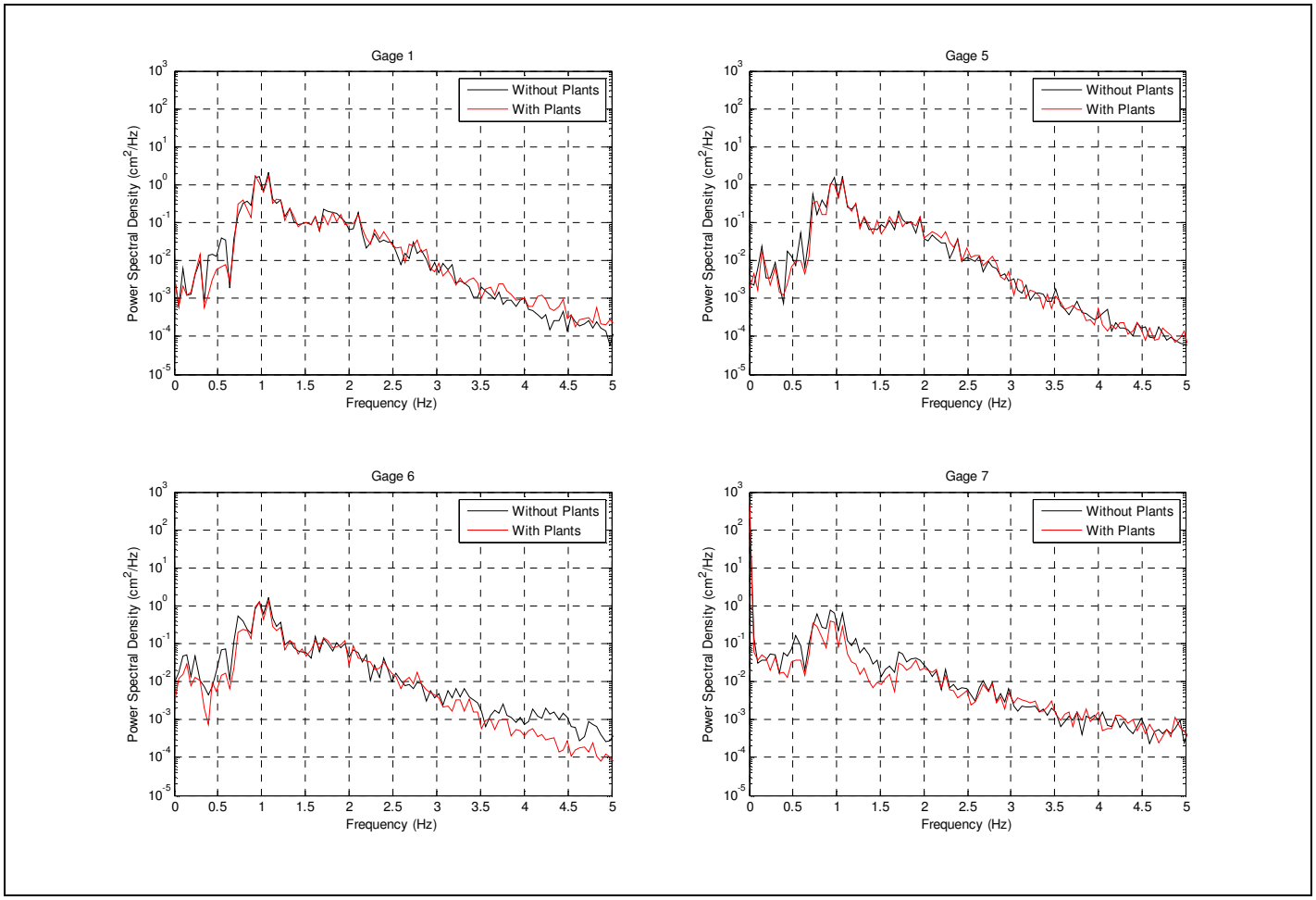

Figure 5.26 Case 3 Runs Power Spectral Density Comparisons

Case 4

The frequency spectrum of each gage's output signal for both the without and with plants runs of case 4 (T_p = 1.5 s and γ = 3.3) shows a wide peak centered about approximately 0.67 Hz (Figure 5.27). During both runs, the magnitude of the prominent frequency peak remains between approximately 2 cm^2/Hz and 10 cm^2/Hz. For both the without and with plants runs, the spectra show greater variance at gages 6 and 7, as compared to gages 1 – 5, at frequencies greater than 3.5 Hz. Figure 5.28 reveals the power spectral density remains generally less at gage 6 and consistently less at gage 7 during the with plants run as compared to the without plants run.

Case 5

For case 5 (T_p = 1.5 s and γ = 30), frequency transformation of each gage's output signal captures a sharper peak at 0.67 Hz with a slightly greater amplitude than the prominent peak seen in case 4 (Figure 5.29). Figure 5.30 shows the magnitude of this prominent peak reaches approximately 20 cm^2/Hz at gage 1 and decreases to approximately 9 cm^2/Hz at gage 7 for both the without and with plants runs. An additional peak centered about approximately 1.33 Hz arises in each gage's spectrum during both the without and with plants runs for this case. The magnitude of this first harmonic peak (1.33 Hz) remains approximately 1 cm^2/Hz at each of the gages during both runs. Similar to case 4, the spectra indicate greater variance at gages 6 and 7, as compared to gages 1 –5, at frequencies greater than 3.5 Hz during both runs. Figure 5.30 indicates the variance remains generally less at gage 6 and consistently less at gage 7 during the with plants run versus the without plants run.

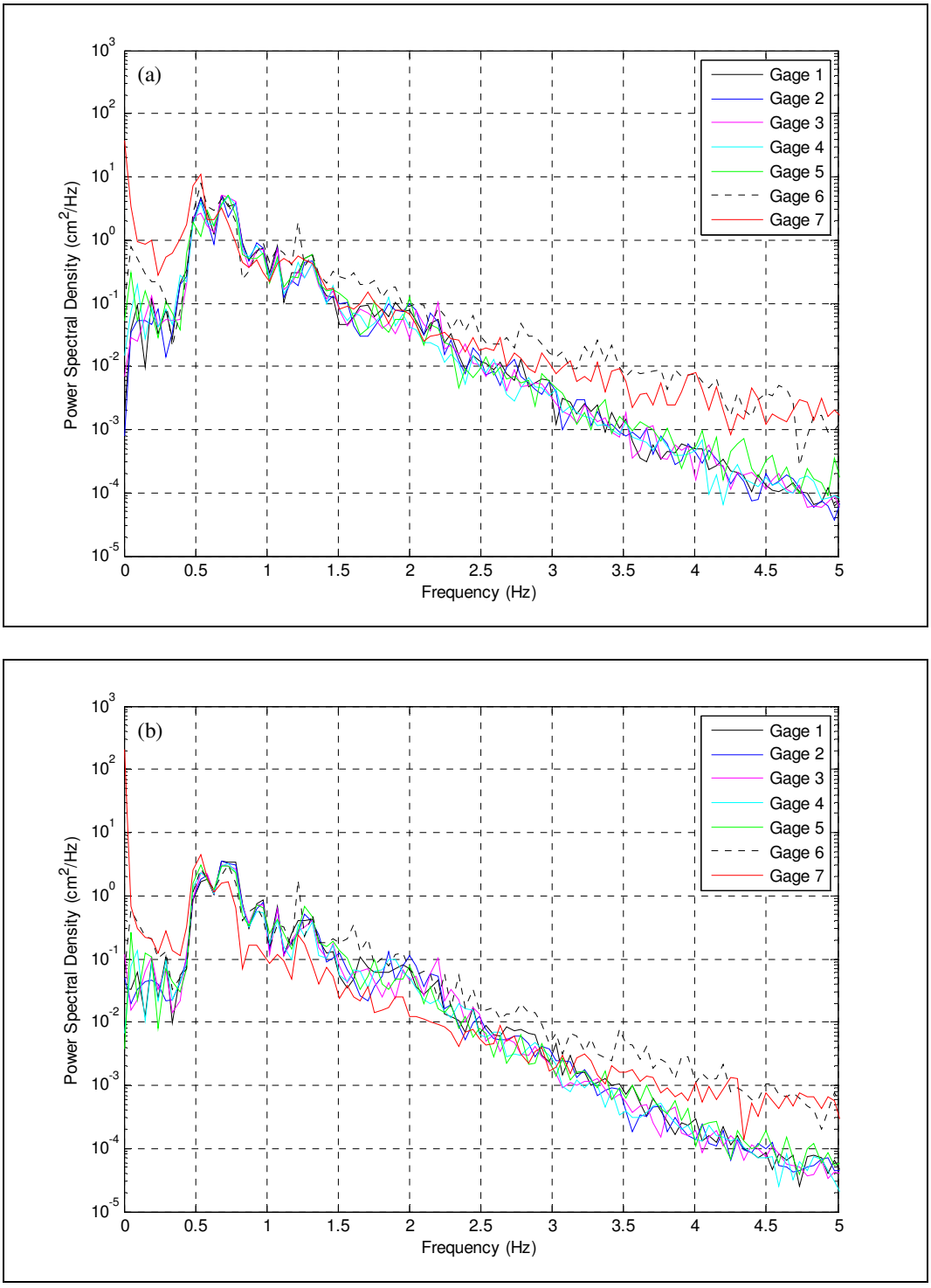

Figure 5.27 Case 4 Runs Power Spectral Density (a) Without Plants (b) With Plants

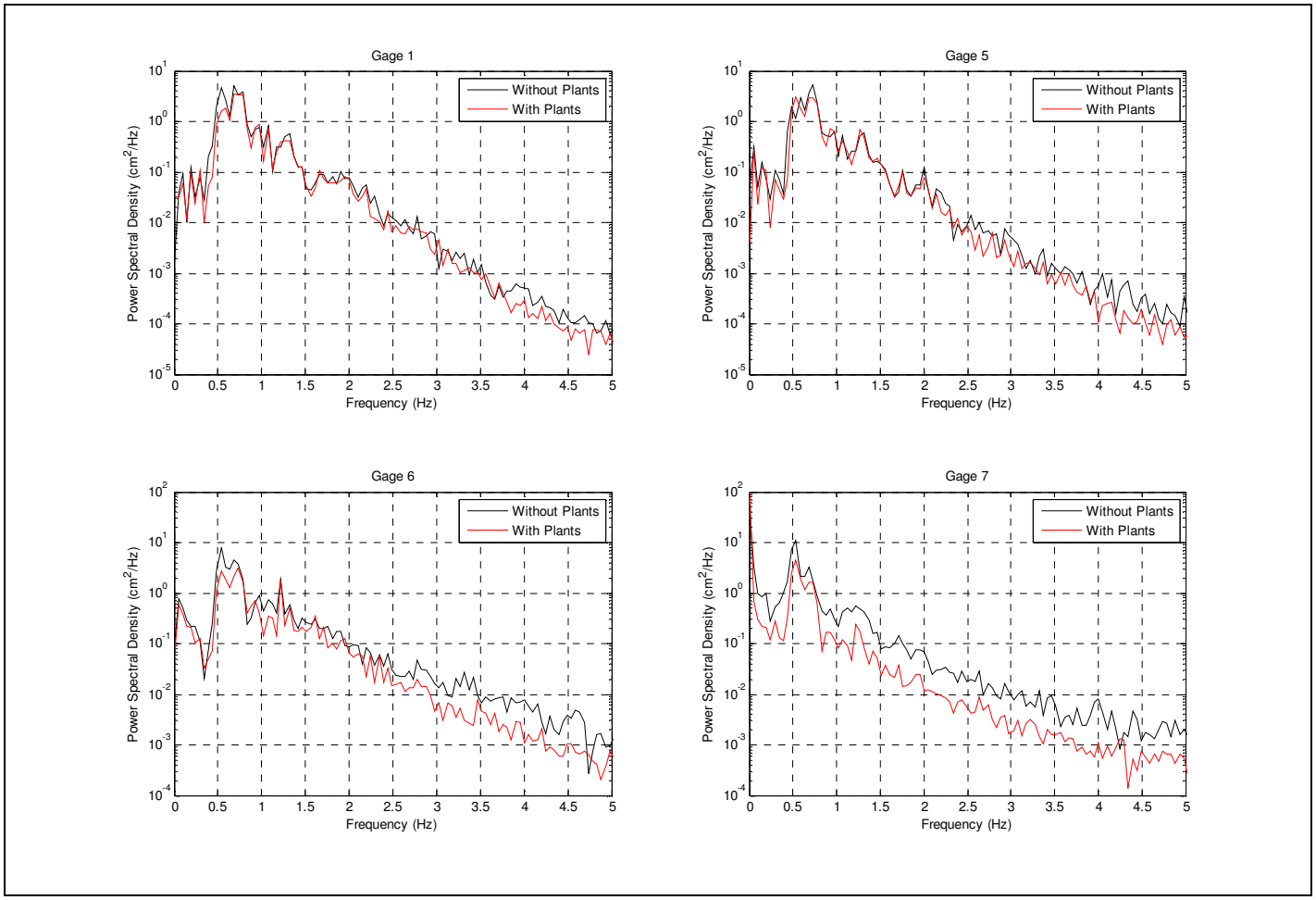

Figure 5.28 Case 4 Runs Power Spectral Density Comparisons

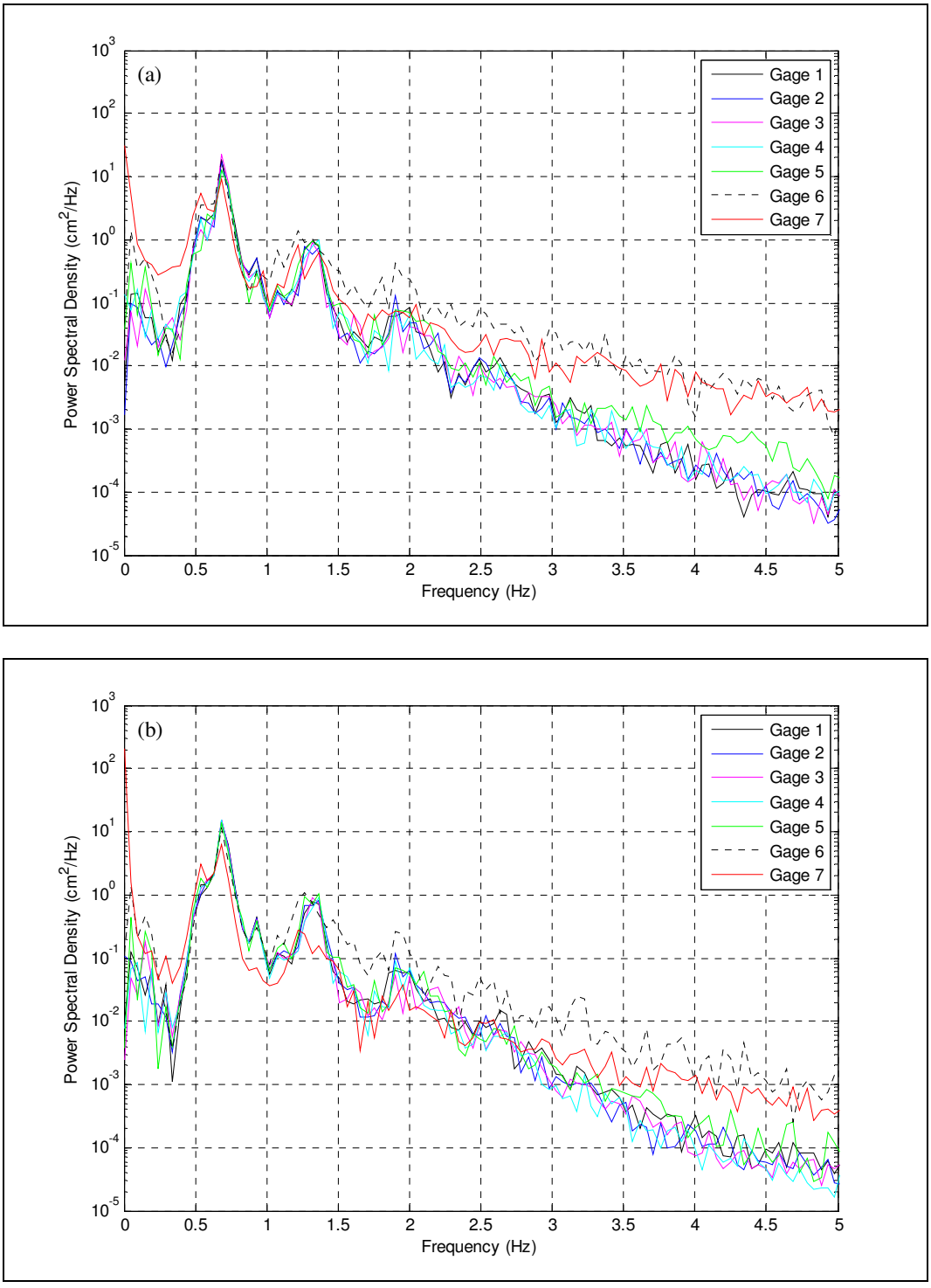

Figure 5.29 Case 5 Runs Power Spectral Density (a) Without Plants (b) With Plants

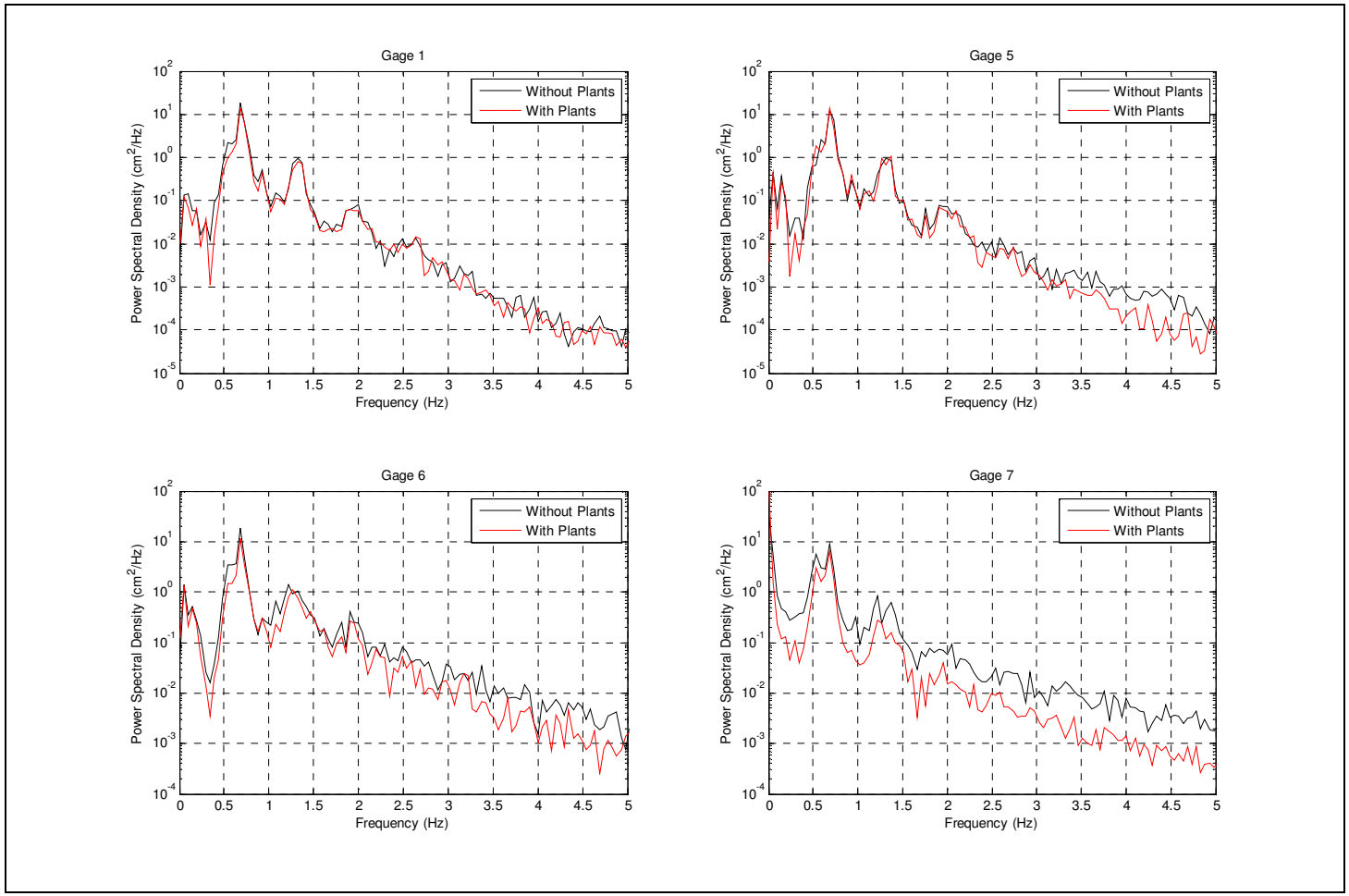

Figure 5.30 Case 5 Runs Power Spectral Density Comparisons

Case 6

The frequency transformation of each gage's output signal for both the without and with plants runs for case 6 (T_p = 2 s and γ = 3.3) produces a prominent peak at 0.5 Hz (Figure 5.31). The magnitude of this peak increases from approximately 10 cm^2/Hz between gages 1 and 6 to approximately 30 cm^2/Hz at gage 7 during the without plants run. To a lesser degree the with plants run shows a similar pattern (from approximately 2 cm^2/Hz between gages 1 and 6 to approximately 9 cm^2/Hz at gage 7). During the without plants run, gages 6 and 7 generally capture greater variance than gages 1 – 5 at frequencies greater than 3 Hz. Figure 5.32 indicates a consistently weaker variance at gages 6 and 7 occurred during the with plants run as compared to the without plants run.

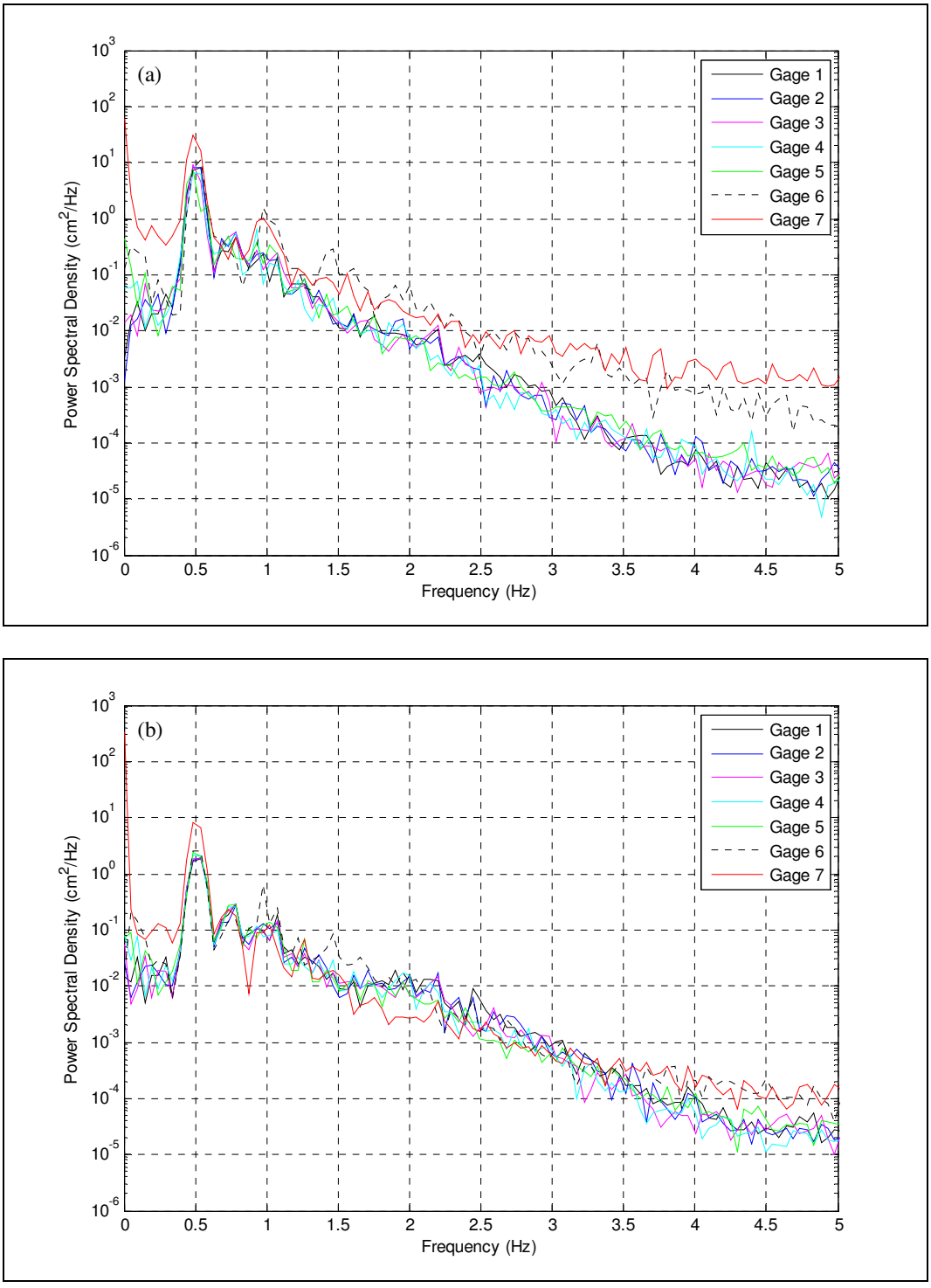

Figure 5.31 Case 6 Runs Power Spectral Density (a) Without Plants (b) With Plants

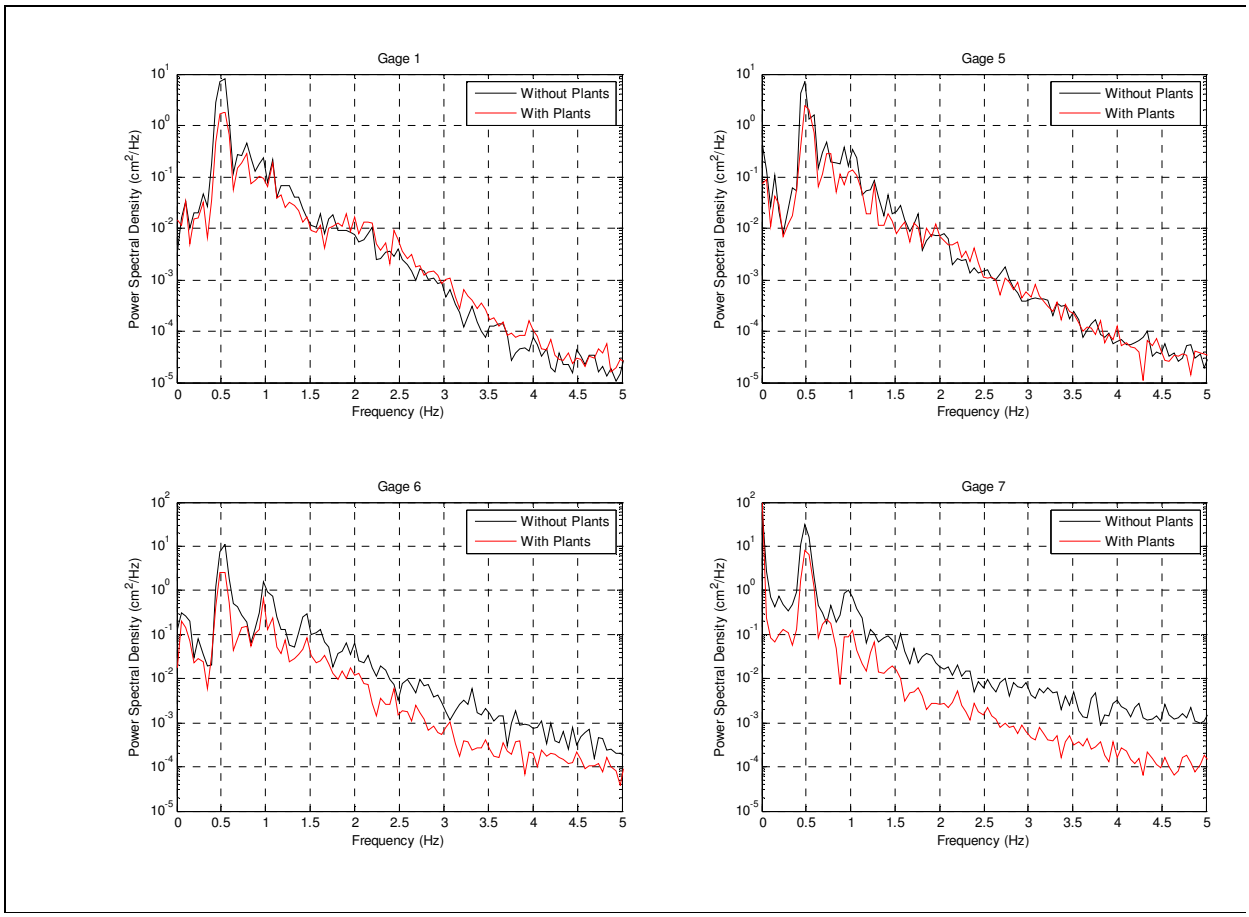

Figure 5.32 Case 6 Runs Power Spectral Density Comparisons

Chapter 6

CONCLUSIONS

6.1 Overview

Studies show wetland vegetation create lower energy environments by dampening wave energy. This study employed laboratory experiments to investigate the effect of a model eelgrass bed on wave runup. Time series analysis reveals insight into the behavior of the waveform as it shoaled up the ramp. Spectral analysis determines the distribution of wave energy over the frequency domain.

6.2 Regular Wave Cases

Case 1

Case 1 employed a regular wave train with a 1 s period. During both runs, at gage 1, the wave measured approximately 14 cm from crest to trough with an approximate 8 cm tall crest. The runup/rundown pattern generally retained the 1 s period but was quite muddled. The excursion remained between approximately 2.5 cm above and 3 cm below still water level during the without plants run and varied between approximately still water level and 2 cm below still water level with plants in the flume. Thus, the plants generally hindered runup above still water level. Notably, the plants oscillated with the passing waves but remained bent toward the wave maker.

The water surface elevation time series variance steadily decreased between gages 1 and 7. Transformation into the frequency domain also revealed a steady decrease in wave energy variance at the 1 Hz peak frequency as the waves approached the beach. Notably, the weakest variance occurred at gage 7 during both runs within the time and

frequency domains. Generally, a slight reduction in energy resulted at gage 7 during the with plants run as compared to the without plants run.

Case 2

Case 2 employed a regular wave train with a 1.5 s period. At gage 1, the wave height measured approximately 12 cm with a slightly taller crest than trough. The runup/rundown pattern generally retained the 1.5 s period. The excursion remained between approximately 3 cm above and 3 cm below still water level during the without plants run and varied between approximately 2 cm above and 2 cm below still water level with plants in the flume. Thus, the plants restricted the runup and rundown to within a more limited range. Notably, the plants oscillated with the oncoming waves becoming prone in both directions and the waves broke further offshore during the with plants run than during the without plants run.

The variance in water surface elevation increased and decreased between gages 1 and 5 without plants in the flume but steadily decreased between gages 1 and 7 during the with plants run. At the 0.67 Hz peak frequency, the power spectra generally match these patterns with the weakest variance occurring at gage 7 during both runs. Also, at this prominent peak, a slightly greater wave energy variance occurred at gage 7 during the with plants run as compared to the without plants run. Overall, a slight reduction in energy occurred at gage 7 with plants in the flume versus without.

Comparison of Regular Wave Cases

Water surface elevation time series and spectral analyses reveal similar patterns during both regular wave cases. During both cases, the plants hindered runup and

rundown to within a smaller range. The runup/rundown patterns also occurred slightly further offshore under the influence of the plants during both cases. The runup/rundown patterns generally retained the initial waveform period but the pattern was more regular during case 2 as compared to case 1.

Comparing each gage's energy spectrum reveals much narrower peaks during case 2 indicating a stronger periodicity as compared to case 1. A reduction in energy occurred at gage 7, as compared to gages 1 – 6, during both runs of each case with a greater reduction during both runs of case 1. Overall, during both runs, a weaker variance occurred at gage 7 with plants in the flume versus without.

6.3 Irregular Wave Cases

Case 3

Using the TMA spectrum Matlab program, case 3 incorporated a 1 s peak period and spectral width parameter of 3.3. Observation revealed minimal wave breaking occurred during both runs. The plants oscillated with the waves but remained positioned toward the wave maker. The mean water level remained slightly lower during the with plants run as compared to the without plants run (2.5 cm below still water level versus 1.6 cm below still water level). Notably, during both runs, the runup was generally proportional to and similar in extent to the wave height at gage 6.

The variance of the water surface elevation remained steady within the time and frequency domains between each of the gages during both runs. A wide peak centered about the 1 Hz peak frequency at each gage during both runs.

Case 4

Case 4 incorporated a 1.5 s peak period and gamma of 3.3. The plants oscillated with the passing waves becoming prone in both directions frequently. The mean water level remained slightly lower during the with plants run as compared to the without plants run (2 cm below still water level versus 0.7 cm below still water level). The runup/rundown pattern was generally smoother and within a smaller range under influence of the plants.

Without plants in the flume, the water surface elevation time series variance remained steady between gages 1 and 5 and increased at gages 6 and 7 while during the with plants run, the variance of each gage's time series remained steady. A prominent wide peak arises at 0.67 Hz within the frequency spectrum of each gage's output signal during both runs. Overall, the wave energy variance generally matches the time series variance with a slight increase at gages 6 and 7 during the without plants run. A general energy reduction at gage 6 and consistent reduction in energy at gage 7 occurred during the with plants run as compared to the without plants run.

Case 5

Case 5 incorporated a 1.5 s peak period and gamma of 30. Notably, a sharper breaking wave occurred without plants in the flume. The plants oscillated with the passing waves becoming prone in both directions frequently. The mean water level remained slightly further down the ramp during the with plants run as compared to the without plants run (2 cm below still water level versus 0.7 cm below still water level). Under the influence of the plants, the runup and rundown generally proceeded smoothly along the ramp while the rundown was returned more abruptly without plants in the flume.

The variance of each gage's output time series remained steady during both runs with exception of an increase at gages 6 and 7 during the without plants run. A prominent sharp peak at 0.67 Hz arises as well as the first harmonic with a smaller amplitude arise within the frequency spectrum of each gage's output signal. Overall, the time series and wave energy variances generally follow similar patterns, i.e. a slight increase at gages 6 and 7 during the with plants run. Wave energy variance remains generally less at gage 6 and consistently less at gage 7 during the with plants run versus the without plants run.

Case 6

Case 6 incorporated a 2 s peak period and gamma of 3.3. Notably, a plunging breaker occurred without plants in the flume while a smoother breaking occurred slightly further offshore under influence of the plants. The plants oscillated with the passing waves and became prone in both directions frequently. The mean water level remained slightly lower during the with plants run as compared to the without plants run (2.5 cm below still water level versus 1 cm below still water level). The runup and rundown generally proceeded smoothly along the ramp under influence of the plants. Without plants in the flume, a larger rundown was seen to return more abruptly up the ramp.

During the without plants run, the variance of each gage's output time series remained steady between gages 1 and 5 and increased at gages 6 and 7. A prominent sharp peak at 0.5 Hz arose within each gage's frequency spectrum with an apparent increase in variance at gages 6 and 7. These same patterns appear in the with plants run analyses but to a lesser degree. Wave energy variance is consistently weaker at gages 6 and 7 during the with plants run as compared to the without plants run.

Comparison of Irregular Wave Cases

Water surface elevation time series and spectral analyses reveal similar patterns between the irregular wave cases. Minimal wave breaking and steady water surface elevation and wave energy variances occurred during both runs of case 3 (T_p = 1 s and γ = 3.3). By increasing the peak period, for case 6 (T_p = 2 s and γ = 3.3), under influence of the plants, smoother breaking occurred slightly further offshore. Similar patterns in time series and wave energy variances occurred during both runs but to a lesser degree with plants in the flume. Unlike the two regular wave conditions, where the water surface elevation and wave energy variances steadily decreased, for case 6, the two variances increased at gages 6 and 7. Analysis of cases 4 and 5 (T_p = 1.5 s) reveal patterns which follow those of case 6 as opposed to those of case 3. In addition to a sharper peak at the prominent 0.67 Hz frequency, a peak at the first harmonic (1.33 Hz) appears with the larger spectral width (3.3 for case 4 and 30 for case 5).

References

Asano, T., Deguchi, H., and Kobayashi, N. (1992). Interaction between water waves and vegetation. *Proceedings of 23rd ICCE*, ASCE, 2710–2723.

Chesapeake Bay Program. (2000). "Chesapeake Bay Submerged Aquatic Vegetation Water Quality and Habitat-Based Requirements and Restoration Targets: A Second Technical Synthesis," Chesapeake Bay Program.

Dalrymple, R. A., Kirby, J. T., and Hwang, P. A. (1984). Wave Diffraction due to areas of energy dissipation. *Journal of Waterway, Port, Coastal, and Ocean Engineering*, **110** (1), 67–79.

Dean, R. G. (1978). "Effects of vegetation on shoreline erosional processes." Wetland Functions and Values: The State of Our Understanding, American Water Resources Association.

Denny, M. W., Gaylord, B. P., and Cowen, E. A. (1997). Flow and flexibility. II. The roles of size and shape in determining wave forces on the bull kelp Ne*reocystis luetkeana*. *Journal of Experimental Biology*, **200**, 3165–3183.

Dubi, A. and Torum, A. (1996). Wave energy dissipation in kelp vegetation. *Proceedings of 25th ICCE*, ASCE, 2626–2639.

Dubi, A. and Torum, A. (1994). Wave damping by kelp vegetation. *Proceedings of 24th ICCE*, ASCE, 142–156.

Elwany, M. H. S., O'Reilly, W. C., Guza, R. T., and Flick, R. E. (1995). Effects of southern California kelp beds on waves. *Journal of Waterway, Port, Coastal, and Ocean Engineering*, **121** (2), 143–150.

Fonseca, M. S., Fisher, J. S., Zieman, J. C., and Thayer, G. W. (1982). Influence of the seagrass, *Zostera marina L*., on current flow. *Estuarine, Coastal, and Shelf Science*, **15**, 351–364.

Fonseca, M, Kenworthy, W., and Thayer, G. (1998). "Guidelines for the Conservation and Restoration of Seagrasses in the United States and Adjacent Waters," NOAA, Silver Spring, MD.

Gambi, M. C., Nowell, A. R. M., and Jumars, P. A. (1990). Flume observations on flow dynamics in *Zostera marina* (eelgrass) beds. *Marine Ecology Progress Series*, **61**, 159–169.

Gaylord, B., Blanchette, C., and Denny, M. (1994). Mechanical consequences of size in wave-swept algae. *Ecological Monographs*, **64** (3), 287–313.

Gaylord, B. and Denny, M. W. (1997). Flow and flexibility. I. Effects of size, shape, and stiffness in determining wave forces on the stipitate kelps *Eisenia arborea* and *Pterygophora californica*. *Journal of Experimental Biology*, **200**, 3141–3164.

Ghisalberti, M. and Nepf, H. M. (2002). Mixing layers and coherent structures in vegetated aquatic flows. *Journal of Geophysical Research*, **107** (C2), 3-2–3-11.

Jackson, G. A. (1984). Internal wave attenuation by coastal kelp stands. *Journal of Physical Oceanography*, **14**, 1300–1306.

Kobayashi, N., Raichle, A., and Asano, T. (1993). Wave attenuation by vegetation. *Journal of Waterway, Port, Coastal, and Ocean Engineering*, **119** (1), 30–48.

Koch, E., Fonseca, M., Whifield, P., and Chiscano-Doyle, C. (2003). "Wave exposure or sediment characteristics: what is limiting the distribution of *Zostera marina* (eelgrass) in Chincoteague Bay, MD, USA?," UMCES, Cambridge, MD.

Kouwen, N. and Li, R. (1980). Biomechanics of vegetative channel linings. *Journal of the Hydraulics Division*, ASCE, **106** (HY6), 1085–1103.

Kouwen, N. and Unny, T. E. (1973). Flexible roughness in open channels. *Journal of the Hydraulics Division*, ASCE, **99** (HY5), 713–728.

Kouwen, N., Unny, T. E., and Hill, H. M. (1969). Flow retardance in vegetated channels. *Journal of the Irrigation and Drainage Division*, ASCE, **95** (IR2), 329–342.

Lovas, S. M. and Torum, A. (2000). Effect of submerged vegetation upon wave damping and run-up on beaches: A case study on *Laminaria Hyperborea*. *Proceedings of 27th ICCE*, ASCE, 851–864.

Nepf, H. M. (1999). Drag, turbulence, and diffusion in flow through emergent vegetation. *Water Resources Research*, **35** (2), 479–489.

Nepf, H. M. and Koch, E. W. (1999). Vertical secondary flows in submersed plant-like arrays. *Limnology and Oceanography*, **44** (4), 1072–1080.

Nepf, H. M. and Vivoni, E. R. (2000). Flow structure in depth-limited, vegetated flow. *Journal of Geophysical Research*, **105** (C12), 28,547–28,557.

Raupach, M. R. and Thom, A. S. (1981). Turbulence In and Above Plant Canopies. *Anuual Review of Fluid Mechanics*, **13**, 97–129.

Stewart, R., McFarland, D., Ward, D., Martin, S., and Barko, J. (1997). "Flume Study Investigation of the Direct Impacts of Navigation-Generated Waves on Submersed Aquatic Macrophytes in the Upper Mississippi River," ENV Report 1, USACE, Vicksburg, MS.

Wallace, S. and Cox, R. (2000). Effects of seagrass on nearshore current and wave dynamics. *Proceedings of 27th ICCE*, ASCE, 878–890.

Wallace, S., Luketina, D., and Cox, R. (1998). Large scale turbulence in seagrass cano-pies. *13th Australasian Fluid Mechanics Conference*, Melbourne, Australia.

Appendix A

FIELD VISIT PHOTOGRAPHS

Figure A1 Plan View of Flume at Gage 6 During Case 6 With Plants Run

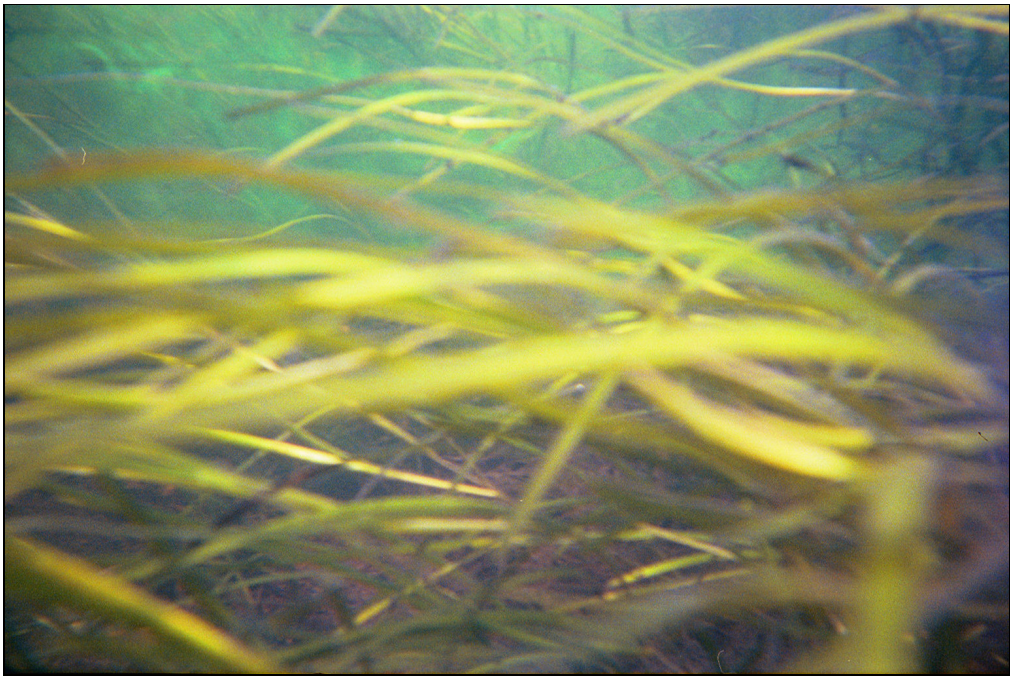

Figure A2 Plan View of Flume at Gage 6 During Case 6 With Plants Run

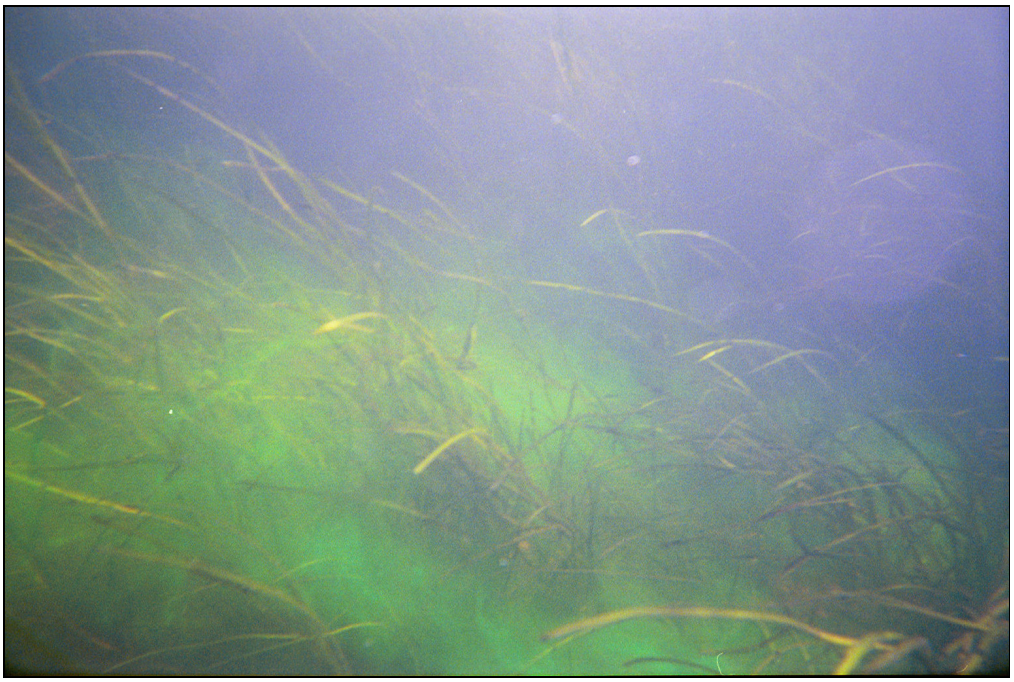

Figure A3 Plan View of Flume at Gage 6 During Case 6 With Plants Run

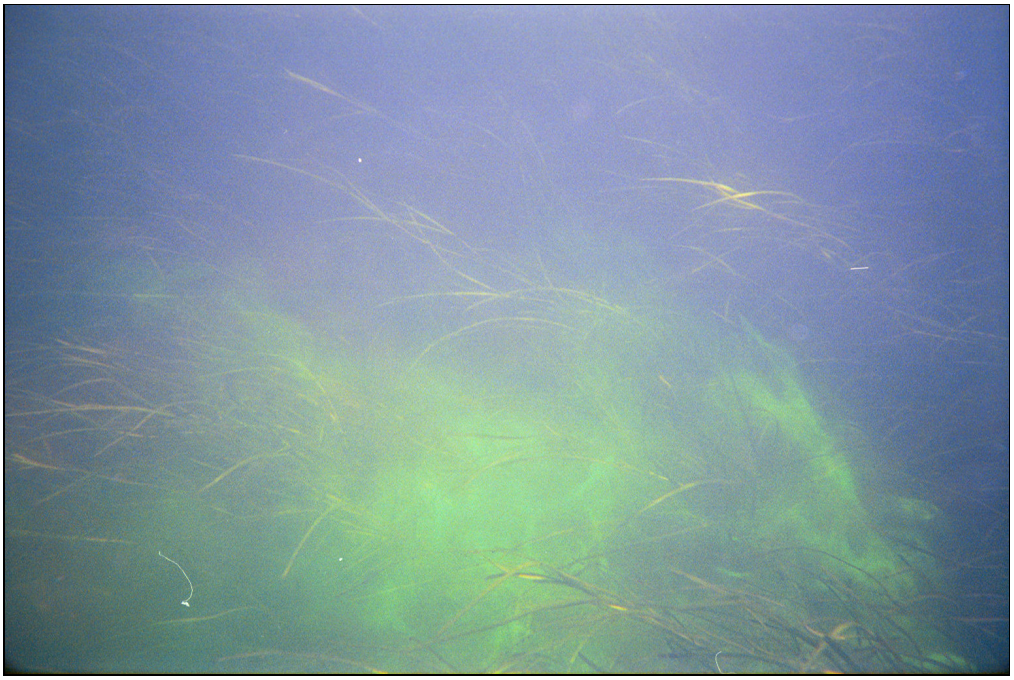

Figure A4 Plan View of Flume at Gage 6 During Case 6 With Plants Run

Appendix B

EXPERIMENT PHOTOGRAPHS

Figure B1 Picture of Gage Setup Facing Wave Maker from Above Ramp

Figure B2 Picture of Beach and Runup Wire Facing Wave Maker from Above Ramp

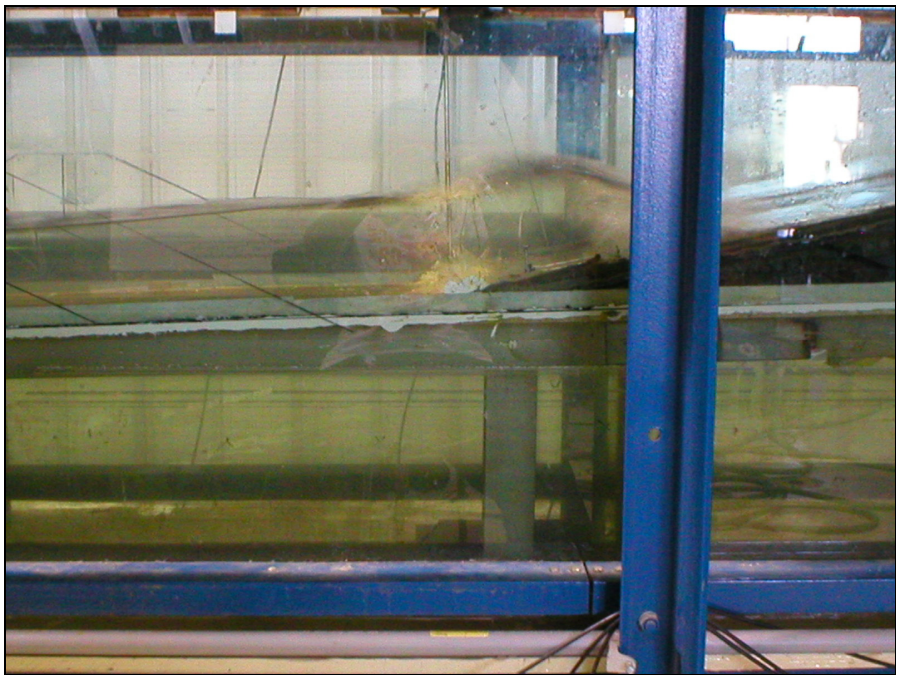

Figure B3 Plan View of Flume at Gage 6 During Case 3 Without Plants Run

Figure B4 Plan View of Flume at Gage 6 During Case 4 With Plants Run

Figure B5 Plan View of Flume at Gage 6 During Case 6 With Plants Run